Stony Brook University

Neural Underpinnings of Anxiety: Multi-modal Magnetic Resonance Imaging Approach

A Dissertation Presented

by

Jiook Cha

to

The Graduate School

in Partial Fulfillment of the

Requirements

for the Degree of

Doctor of Philosophy

in

Neuroscience

Stony Brook University

December 2013

Stony Brook University

The Graduate School

Jiook Cha

We, the dissertation committee for the above candidate for the

Doctor of Philosophy degree, hereby recommend

acceptance of this dissertation.

Dr. Lilianne Mujica-Parodi
Associate Professor, Department of Biomedical Engineering

Dr. Alfredo Fontanini
Assistant Professor, Department of Neurobiology and Behavior

Dr. Lorna Role
Professor, Department of Neurobiology and Behavior

Dr. Aprajita Mohanty
Assistant Professor, Department of Psychology

This dissertation is accepted by the Graduate School

Charles Taber

Dean of the Graduate School

Abstract of the Dissertation

Neural Underpinnings of Anxiety: Multi-modal Magnetic Resonance Imaging Approach

by

Jiook Cha

Doctor of Philosophy

in

Neuroscience

Stony Brook University

2013

Anxiety disorders affect about 40 million American adults yearly. Recent conceptualization suggests that abnormal brain connectivity of the corticolimbic network underlies anxiety-related maladaptive behaviors. However, it is still unclear which brain circuits mediate specific behaviors, as well as how such brain-behavior based mechanisms contribute to the pathophysiology of anxiety. In this dissertation, we used both neurobiology and behavior to investigate the etiology of generalized anxiety disorder. Specifically, we hypothesized that distinct neural mechanisms may exist in two different constructs of the negative valence system: reactivity to imminent threat (fear) and to distal and uncertain

threat (anxiety). We used behavioral paradigms targeted to elicit reactivity to either fear or anxiety, and identified brain circuitry that may underlie each state using multi-modal MRI and statistical modeling. First, we found that the amygdala–prefrontal connectivity explains individual differences of attentional bias towards threat (induced using affect-valence faces), and that BDNF Val66Met polymorphism, a genetic risk factor of anxiety, has an indirect impact on this behavior by modulating connectivity. Second, we identified circuit-wide neural features (grey and white matter structural and functional connectivity) that account for maladaptive ventromedial prefrontal cortical threat reactivity in clinical anxiety. Finally, we found novel evidence that abnormal dopaminergic signaling, from the midbrain ventral tegmental area to the corticolimbic system, may underlie patients' lack of specificity ('over-generalization') in threat-detection. Together, the studies presented in this dissertation provide a circuit-based model for the neural underpinnings of clinical anxiety.

Acknowledgements

Without great mentors I have met in Stony Brook, I could not have achieved any. I would, first, like to thank Lilianne Mujica-Parodi for teaching me human neuroscience and quantitative thinking and approaching in neuroimaging. Your encouragement and belief are most important ingredients in my doctoral training. I would like to thank Alfredo Fontanini for his warm support, thoughtful advice, and your recommendation of me to Lilly; that is how this dissertation started. I would like to thank Lorna Role for guidance throughout my training and insights into interpretation of data. I am also grateful to Aprajita Mohanty for your thoughtful feedback, which significantly enhances the dissertation work. I owe so much to my lab members, Joshua Carlson, Tsafrir Greenberg, Denis Rubin, Tomer Fekete, Sanja Nedic, Felix Beacher, and Shmoo. I particularly thank my good friend, the finest American, Dan Dedora.

Without great mentors I have met in Seoul, I could not have started any. I would like to thank Drs. In-Beom Kim and Myung-Hoon Chun at Catholic Medical College for their guidance and lessons to be a scientist. I am also grateful to Dr. Hojoung Lee for her wholehearted support and sincere advice.

Without my wife, Eana, none of this work would be meaningful to me. I appreciate your crucial contribution to this dissertation via getting married with

me, raising the two kids, and supporting me. It is impossible to fully express my love and gratitude here. My daughter, Grace 유라, and my son, Victor 유창, I cannot wait to hear your feedback on this dissertation. I thank you for saying good bye to me so cool on Sunday evenings when I had to quit playing with you and head to lab. I now have learned, partially, how to do science, but I am still figuring out how to love you or to let you know how much I love you. My parents, Dong-Jin Cha and Bok-Gi Sung, I now understand how much you have loved me and are proud of me.

Last, I thank Fyodor Dostoyevsky for his greatest insight into human mind and psychology, which made me endeavor to study human brain and behavior.

Table of Contents

List of Tables

List of Figures

VITA

EDUCATION:

The Catholic University of Korea M.S., Neurobiology	Seoul, Korea 2009
Korea University B.S., Environmental Life Science	Seoul, Korea 2007

HONORS AND AWARDS:

Distinguished Travel Award, Stony Brook University	2013
Sigma Xi Awards for Travel, Stony Brook University	2013
Travel Award, The Association for Research in Vision and Ophthalmology	2008
Korea Research Foundation Science Scholarship for undergraduates	2007
College Specialization Project Scholarship, Korea University	2005

TEACHING EXPERIENCE:

Curriculum development of control system modeling for K-12 students (as a part of the educational component in NSF Career award; PI, Dr. Mujica-Parodi)	2010-
Teaching assistant of undergraduate biology laboratory course	2009-2010

MENTORING EXPERIENCE:

Neural underpinnings of individual variability in pattern recognition. Provided mentorship to an undergraduate in neuroimaging data analysis and manuscript preparation.	2013
Impacts of temporal lobe epilepsy on functional/structural network. Provided mentorship to researchers in hypothesis development and fundamentals of neuroimaging methodology.	2013

PROFESSIONAL ACTIVITIES

Military service in Korean Army attached to US Army 2003-2005

TALKS:

1. “Neural underpinnings of anxiety: Dissecting the anxious brains”, NIMH, Bethesda, MD 2013
2. “Neural mechanisms of overgeneralization of threat in Generalized Anxiety Disorder, Duke University, Durham, NC 2013
3. "Maladaptive ventral tegmental area dopaminergic aversion circuit is pathological anxiety in humans", US-Korea Annual Conference, East Rutherford, NJ. 2013
4. "Impoverished prefrontal activity in Generalized Anxiety Disorder explained by morphometrics and connectivity", Stony Brook University, Stony Brook, NY 2012

PUBLICATIONS:

A. Human Neuroimaging: Biomarker of anxiety and anxiety disorder

1. JM Carlson*, **J Cha***, E Harmon-Jones, LR Mujica-Parodi, G Hajcak, "Influence of the BDNF genotype on amygdalo-prefrontal white matter microstructure is linked to nonconscious attention bias to threat.", *Cerebral Cortex* Epub (Feature article; *equally contributed). 2013
2. JM Carlson*, **J Cha***, LR Mujica-Parodi, "Functional and structural amygdala–anterior cingulate connectivity correlates with attentional bias to masked threat." Cortex Epub (*equally contributed). 2013
3. T Greenberg, JM Carlson**, J Cha,** G Hajcak, LR Mujica-Parodi, "Ventromedial prefrontal cortex reactivity is altered in generalized anxiety disorder during fear generalization.", *Depression and Anxiety*. 2013
4. F Beacher, T Fekete, **J Cha**, D Rubin, D Klein, LR Mujica-Parodi, "Small world network properties in prefrontal cortex relate to predictors of psychopathology risk in young children: a NIRS study", *Neuroimage* Epub (Special edition). 2013

5. T Greenberg, JM Carlson**, J Cha,** G Hajcak, LR Mujica-Parodi, "Neural reactivity tracks fear generalization gradients.", *Biological Psychology* (Special edition). 2013

B. Neuroanatomy: Retina research in animal models

6 **J Cha**, HL Kim, F Pan, MH Chun, SC Massey, IB Kim, "Variety of horizontal cell gap junctions in the rabbit retina.", *Neuroscience Letters*. 2012

7 SA Kim, JH Jeon, MJ Son, **J Cha**, MH Chun, IB Kim, "Changes in transcript and protein levels of calbindin D28k, calretinin and parvalbumin, and numbers of neuronal populations expressing these proteins in an ischemia model of rat retina.", *Anatomy & Cell biology*. 2010

8 SA Kim, CK Jung, TH Kang, JH Jeon, **J Cha**, IB Kim, MH Chun, "Synaptic connections of calbindin-immunoreactive cone bipolar cells in the inner plexiform layer of rabbit retina.", *Cell and Tissue Research* . 2010

9 CK Park, **J Cha**, SC Park, PY Lee, JH Kim, IB Kim, MH Chun, "Differential expression of two glutamate transporters, GLAST and GLT-1, in an experimental rat model of glaucoma.", *Experimental Brain Research*. 2009

MANUSCRIPTS UNDER REVIEW:

1. **J Cha**, JM Carlson, D Dedora, T Greenberg, G Hajcak, LR Mujica-Parodi, " Generalizing Fear: hyperactive ventral tegmental area and altered connectivity in human generalized anxiety." 2013
2. **J Cha**, T Greenberg, JM Carlson, D Dedora, G Hajcak, LR Mujica-Parodi, "Circuit-wide Structural and Functional Factors of Ventromedial Prefrontal Fear Response and Contribution to Anxiety Disorder" (In revision) 2013
3. JM Carlson, **J Cha**, LR Mujica-Parodi, "Human orbitofrontal cortex and euphoric experience" (In revision) 2013
4. LR Mujica-Parodi, JM Carlson, **J Cha**, D Rubin, "Amygdala Reactivity and Regulation Predict Resilience to Real-World Acute Stress" 2013

MANUSCRIPTS IN PROGRESS:

1. **J Cha**, LR Mujica-Parodi, "Hippocampal threat learning is attenuated in generalized anxiety disorder" (in preparation). 2013
2. D Dedora*, **J Cha***, D Rubin, L.R. Mujica-Parodi, "Quantifying prefrontal dysregulation in generalized anxiety disorder: power spectrum scale invariance, and its association with corticolimbic connectivity" (in preparation; *equally contributed). 2013

CHAPTER I

General Introduction

I divided this chapter into four sections. The first provides an overview of anxiety and anxiety disorder, general emotion and anxiety circuitry, and potential factors of anxiety. The second section introduces additional emerging potential factors that are likely to be implicated in anxiety disorder, but that have not yet been directly addressed in humans. Then, I describe the importance of macro-scale brain connectivity in brain (dys-)function research and a few methods that I used in the research for this dissertation. This is followed by an introduction of an approach for breaking down complex anxious behaviors for systematic and quantitative research, that is, Research Domain Criteria. All of these finally constitute a proposed brain connectivity model of the pathophysiology of anxiety, leading to a set of testable hypotheses. Finally, I will describe the main experimental objectives to be addressed in this dissertation.

Background

Anxiety and Anxiety Disorder

Anxiety is a future-oriented state related to preparation for potential negative events, and characterized by marked negative affect. It is distinct from fear, in that the latter is present-oriented alarm response to imminent danger, such as immediate fight or flight response (Barlow, 2002). Anxiety and fear are part of normal emotional states and responses, which allows an organism to prepare for and rapidly adapt to ever-changing life environments.

It is considered that psychological disorders onset, when state of anxiety and fear becomes excessive and uncontrollable, thus, pervasive and persistent. There exist various forms of anxiety disorders, which are collectively the most widespread psychiatric disorders experienced by Americans, with a lifetime prevalence of 28.8% (Kessler et al., 2005). They are often debilitating, because state of anxiety and fear requires significant amounts of psychological, physiological, and metabolic energy, which normally should return to a basal level quickly.

DSM-IV categorizes anxiety disorder into six: generalized anxiety disorder, post-traumatic stress disorder, obsessive-compulsive disorder, panic

attacks, phobias and social phobia (or social anxiety disorder). Of these, anxiety disorder is a broad category of disorders with potentially diverse etiology and symptomatology. In this dissertation, I will focus on the most general and basic form, that is, generalized anxiety disorder.

The lifetime prevalence of generalized anxiety disorder is estimated at 5%, and the female to male ratio at about 2:1 (American Psychiatric Association. and American Psychiatric Association. Task Force on DSM-IV., 2000). GAD has also been known as "chronic anxiety neurosis" and is often described as being characterized by chronic anxiety not attached to specific situations, or "free-floating anxiety" In terms of clinical features, patients with GAD complain of anxiety or bitterness, are easily startled, and may not be able to sleep well, spending restless hours. Patients with GAD typically engage in excessive avoidance and escapist tendencies in an effort to cope with their discomfort. At times, there may be discernible reasons for anxiety; however, at other times, the person's concerns are unjustified or the anxiety symptoms are out of proportion to the actual occasion for worry. GAD appears to be a chronic disorder, with symptoms waxing and waning over the years or decades.

Etiological considerations for GAD suggest a genetic role, as supported by family (Noyes et al., 1987; Newman and Bland, 2006; Coelho et al., 2007) and twin studies (Chantarujikapong et al., 2001; Hettema et al., 2001; Mackintosh et

al., 2006; Kendler et al., 2007; Kubarych et al., 2008; Hettema et al., 2012). However, it is not entirely clear "what" is inherited, although several findings suggest abnormalities in GABAergic and noradrenergic activity. The GABAergic dysfunction hypothesis, in particular, is supported by the effectiveness of benzodiazepines in this disorder (Lapierre et al., 1983; Rickels et al., 2000; Vasile et al., 2005). Common treatments include cognitive behavior therapy or medications, such as, benzodiazepines, antidepressants and buspirone (American Psychiatric Association. and American Psychiatric Association. Task Force on DSM-IV., 2000).

Brain Circuitry of Negative Affect Processing

An understanding of the brain circuitry pathological anxiety requires a conceptualization of the emotion processing circuit, with a particular focus on the processing of negative affect. Here, I introduce current understanding of the brain circuitry of negative affect processing that is closely related to onset and maintenance of anxiety.

Gray and McNaughton conceptualized a thorough and insightful framework for the pathophysiology of anxiety, including a theory of the septo-hippocampal network in the negative valence system (Gray and McNaughton, 2000b). The septo-hippocampal system detects conflicts when several stimuli or

features compete for attention. As competition produces the state of anxiety, in order to disambiguate the conflicts, the septo-hippocampus inhibits all prepotent goals and behaviors while gathers more information to make decisions that are more informed. This theory lends significant support to the neuropsychological model of anxiety and anxiety disorder proposed in this dissertation **(Figure 1.1A)**.

A neural model of emotion regulation is another important axis. In this model, the corticolimbic system consists of ventral and dorsal functional networks. Dysregulation between the ventral network, which involves perception of emotional stimuli and mediation of autonomic responses and includes the amygdala, insula, ventral anterior cingulate cortex (ACC) and ventral PFC, and the dorsal network, which involves cognitive processes such as selective attention or reappraisal and emotional perception and includes the hippocampus, dorsal ACC and PFC, may explain neural underpinnings of anxiety disorder **(Figure 1.1B)**.

Under this conceptualization, Etkin proposed a more detailed corticolimbic model of negative emotion processing (**Figure 1.1C**) (Deckersbach et al., 2006; Etkin, 2010). This model contains three major groups: the core limbic group (e.g., the amygdala and insula) registering emotional stimuli and mediating physiological response, the dorsal prefrontal group (e.g., the dorsal anterior cingulate and dorsomedial prefrontal cortex) evaluating extensive affective and

contextual information and communicating with other higher order cortical systems, and the emotion regulation group (e.g., the rostral, subgenual ACC, and vmPFC) regulating emotion.

In short, the dynamic interplay among distributed brain systems is essential in affect processing. This leads to the various circuitry models of anxiety disorder that are supported in numerous human neuroimaging research (Olesen et al., 2003; Adler et al., 2004; Cannistraro et al., 2007; Schlosser et al., 2008; Dima et al., 2010; Schlosser, 2010). Nevertheless, it is worth noting that there is critical a methodological limitation in the search for neural correlates of the patient–controls dichotomy that is essentially based on subjective symptom reports; that is, such research may not tell much about mechanisms of pathophysiology. Therefore, it is crucial to breakdown a complex construct (or a set of symptoms) into observable and objective dimensions. One can then apply complementary approaches to address underlying biological, neural, psychological, or behavioral substrates to a specific domain of anxiety or anxiety disorder; this will allow a more complete picture of the etiology of mental illnesses. I will introduce more about this in what follows.

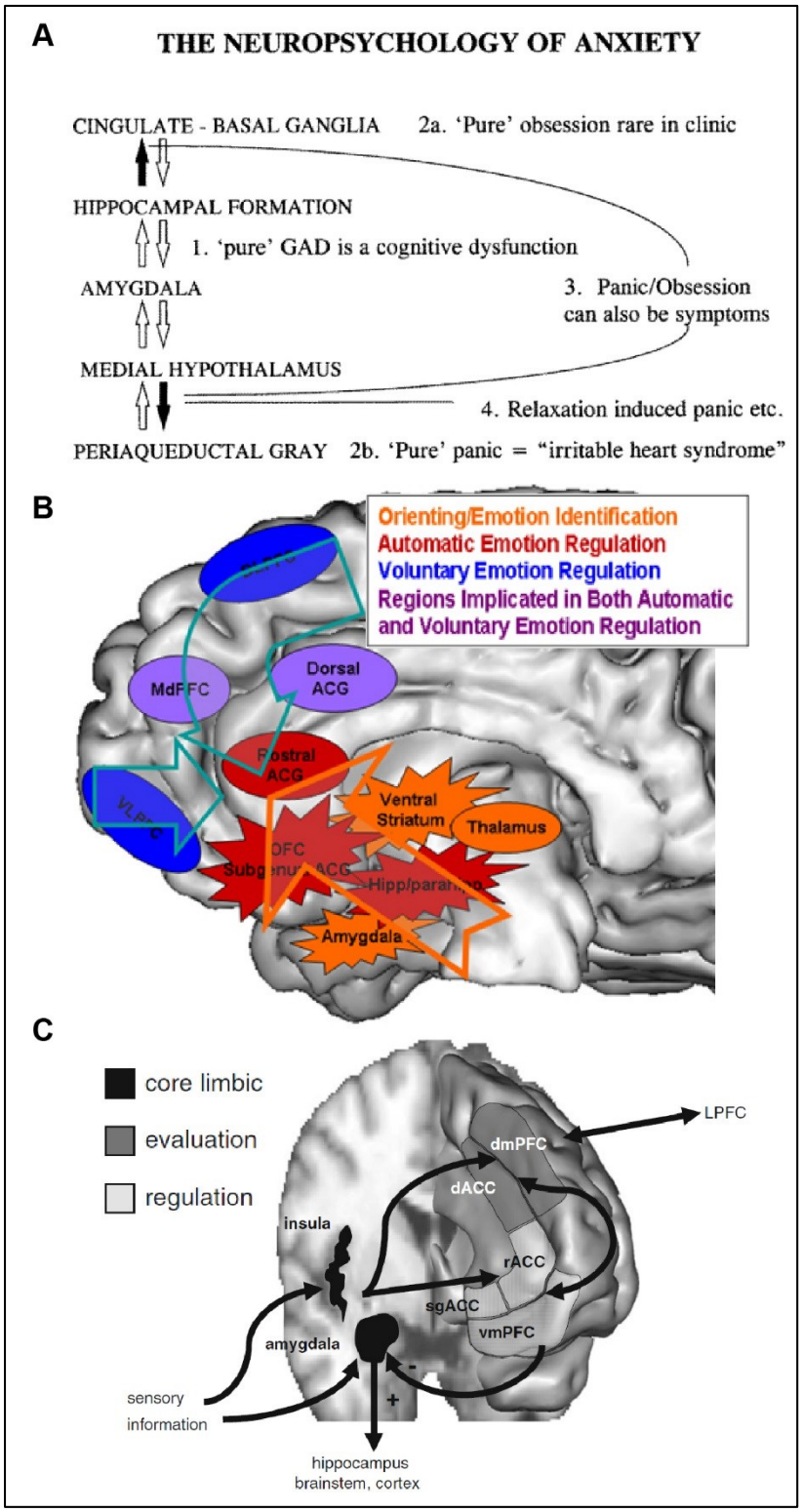
A
THE NEUROPSYCHOLOGY OF ANXIETY
CINGULATE - BASAL GANGLIA
2a. 'Pure' obsession rare in clinic
HIPPOCAMPAL FORMATION
1. 'pure' GAD is a cognitive dysfunction
AMYGDALA
3. Panic/Obsession can also be symptoms
MEDIAL HYPOTHALAMUS
4. Relaxation induced panic etc.
PERIAQUEDUCTAL GRAY
2b. 'Pure' panic = "irritable heart syndrome"
B
Orienting/Emotion Identification
Automatic Emotion Regulation
Voluntary Emotion Regulation
Regions Implicated in Both Automatic and Voluntary Emotion Regulation
MdPFC
Dorsal ACG
Rostral ACG
Ventral Striatum
Thalamus
Amygdala
C
core limbic
evaluation
regulation
LPFC
dmPFC
dACC
insula
rACC
sgACC
vmPFC
amygdala
sensory information
hippocampus
brainstem, cortex

Figure 1.1. Neural or neuropsychological models of anxiety. ***A,*** Gray and McNaughton's neuropsychological model. Here, different forms of anxiety disorder are linked to slightly different neural dysregulation. For example, panic is directly controlled by the lowest level, the midbrain periaqueductal grey; phobia by the medial hypothalamus and amygdala; and the primary cognitive aspects of anxiety by the septo-hippocampal system. Interestingly, the generalized anxiety disorder is viewed as a primarily cognitive dysfunction with secondary changes in arousal or avoidance consequent on connections between the hippocampal formation and amygdala (Adapted from Gray and McNaughton, 2000). ***B,*** emotion regulation model in anxiety disorder. This model links abnormalities of prefrontal regulatory brain regions to dysregulation of emotion, and onset and developement of anxiety disroder (Adapted from Phillips et al., 2008). ***C,*** corticolimbic circuit of negative emotion processing in anxiety. The circuit is categorized into three major groups: core limbic, evaluation, and regulation group (Adapted from Etkin 2010).

Emerging Factors of Anxiety

Mounting evidence suggests the involvement of novel factors in clinical anxiety and in the vulnerability to anxiety. A formal conceptualization of the pathophysiology of anxiety thus needs to account for recently discovered factors of anxiety. These factors have been examined in preclinical populations and animal models, yet remain to be directly tested either in clinical populations or in a more systematic way. In this section, I will introduce some of the factors in question, the relationships of which to anxiety behaviors constitute the primary motivation of this dissertation.

Human Genetic Variability and Anxiety

Several human genetic variances are implicated in the anxiety trait or anxiety-related behaviors. One example is Brain-derived neurotrophic factor (*BDNF*) Val66Met. *BDNF* regulates neural development, connectivity, and plasticity (Poo, 2001; Martinowich and Lu, 2008). It is a substitution of valine (Val) to methionine (Met) at codon 66 (Egan et al., 2003). *BDNF* Val66Met is associated with poorer episodic memory, abnormal hippocampal activation, and lower hippocampal n-acetyl aspartate (Egan et al., 2003). Furthermore, in animal models, where this polymorphism does not naturally occur, neurons transfected with Met-*BDNF* show lower depolarization-induced secretion and fail to localize

to secretory synapses (Egan et al., 2003). A more recent animal study confirmed that Met-*BDNF* transfection lowers BDNF secretion and increases fear-related behaviors such as freezing (Chen et al., 2006). In line with these rodent models, human homozygous Met+ carriers are reported to be at increased risk for mood disorders (Montag et al., 2010b), and both homozygous and heterozygous Met+ carriers display heightened rumination (Hilt et al., 2007; Beevers et al., 2009) and inefficient fear conditioning (Hajcak et al., 2009). Additionally, the Met-*BDNF* Val66Met has been linked to increased depression in women across ethnic backgrounds (Verhagen et al., 2010). In human functional neuroimaging research, Met+ carriers show a hyperactive amygdala response to emotional stimuli (Montag et al., 2008). Morphometric research using structural MRI indicates that Met+ carriers show smaller amygdala, hippocampus, caudate, and dorsolateral prefrontal volumes, compared with Val+ homozygous individuals (Pezawas et al., 2004). In terms of white matter, greater fiber integrity has been linked to the *BDNF* Val66Met in a number of the major fiber tracts (Chiang et al., 2011) and in particular the uncinate fasciculus (Tost et al., 2013).

Another example is the serotonin-transporter-linked polymorphic region (often called "5-HTTLPR"). The short variant of this polymorphism reduces the transcriptional efficiency of the 5-HTT gene promoter, resulting in decreased 5-HTT expression. 5-HTTLPR is a genetic susceptibility factor for general affective

disorders (Collier et al., 1996). In relation to anxiety, 5-HTTLPR is linked to trait anxiety (Lesch et al., 1996), which is also supported by more recent meta-analysis research (Schinka et al., 2004). In neuroimaging research, the short variant has been associated with reduced gray matter volumes in the ACC, hyperactive amygdala to negative (i.e., fearful) emotion stimuli and attenuated negative perigenual ACC - amygdala coupling with negative emotion processing (Pezawas et al., 2005).

Dopamine and Anxiety

Although dopamine has long been associated with various psychiatric disorders, such as schizophrenia, addiction, and depression, it has yet to be linked to anxiety disorder at least in human studies. However, mounting evidence indicates that abnormalities of the dopaminergic circuit may be related to anxiety or chronic stress induced psychiatric conditions. In this dissertation, I therefore hypothesize that the midbrain dopaminergic circuit plays an important role in the threat-related adaptive behavior in close relation with the existing Gray's septo-hippocampal system **(cf. Figure 1.1A)**.

Dopamine is plays a central role in negative motivation (Pezze and Feldon, 2004; Fairhurst et al., 2007; Joshua et al., 2008; Liu et al., 2008; Fadok et al., 2009; Matsumoto and Hikosaka, 2009; Baliki et al., 2010; Bromberg-Martin

et al., 2010; Zweifel et al., 2011; Cohen et al., 2012; Stamatakis and Stuber, 2012; Brooks and Berns, 2013). Recent research involving optogenic dissection indicates that the midbrain ventral tegmental area (VTA) receives glutamatergic inputs from the lateral habenular and projects to the dopaminoreceptive medial prefrontal cortex. This constitutes the dopaminergic aversion circuit that is anatomically distinct from the mesolimbic reward circuit **(Figure 1.2.)** (Lammel et al., 2012).

The midbrain VTA critically interacts with the hippocampal memory system, and this hippocampal–VTA loop plays an essential role in controlling the entry of information and memory **(Figure 1.3.)** (Lisman and Grace, 2005; Lodge and Grace, 2006). In this model, external inputs come through the entorhinal cortex to the dentate gyrus/CA3 areas, which provide input to CA1. CA1 functions as a comparator in relation to the VTA and passes novelty signals to the subiculum and then to the basal forebrain and to the midbrain dopamine cells. Of note, the VTA mesocortical projection is likely to interact with this functional loop.

It is worth noting that the hippocampal-VTA loop is essentially embedded on the Gray and McNaughton's septo-hippocampal system. Nonetheless, the VTA has yet to be conceptualized as part of the negative valence system or its abnormalities linked to pathophysiology of anxiety (although a recent article

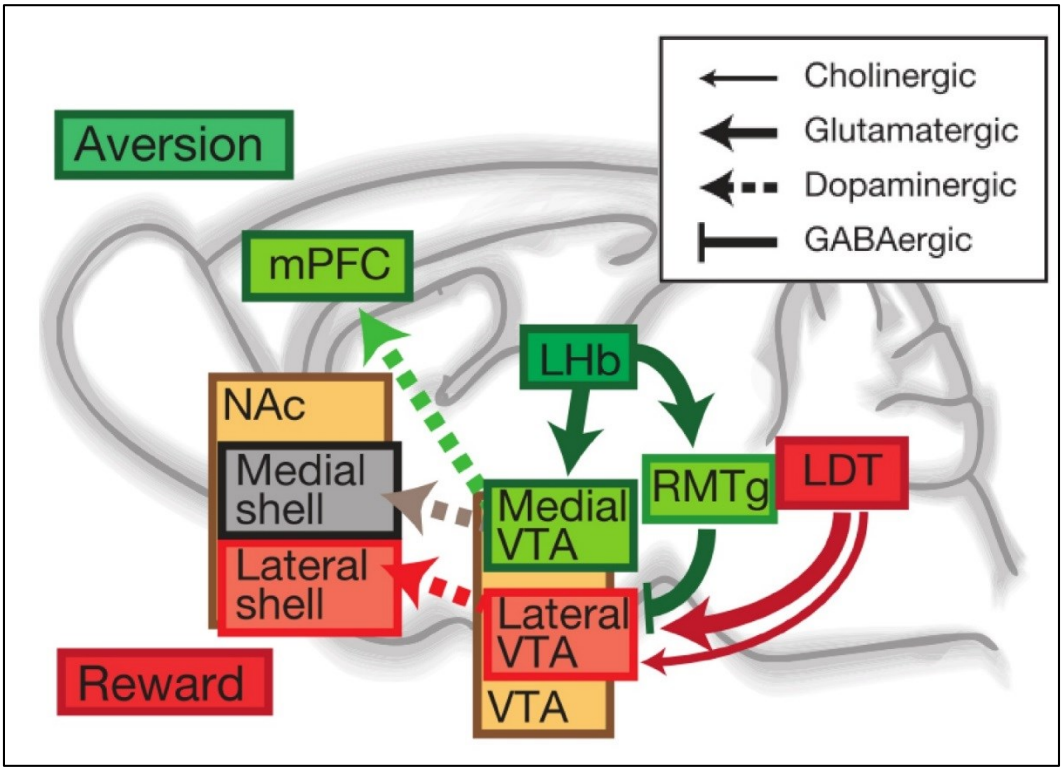

Figure 1.2. Proposed motivation circuits driven by distinct inputs (i.e., LHb and LDT) into the VTA. This dissertation will examine abnormal threat (or aversion) processing in this the dopaminergic aversion circuit is implicated in human clinical anxiety. Green shading represents negative and red/pink indicates positive motivation circuit. mPFC, medial prefrontal cortex; LDT, laterodorsal tegmentum; LHb, lateral habenula; NAc, nucleus accumbens; RMTg, rostromedial tegmental nucleus. (Modified from Lammel et al., 2013).

reviews the involvement of mesocorticolimbic dopamine system in negative affect (Brooks and Berns, 2013), it does not focus on a formal circuit). In this dissertation, I therefore propose that the dopaminergic VTA is central to threat processing and that abnormal reactivity and connectivity of this pathway is implicated in clinical anxiety.

Furthermore, recent studies report that an alteration in the dopaminergic circuit is likely to underlie the pathophysiology of certain mental disorders, particularly the ones closely related to chronic stress. Social defeat stress alters VTA dopamine transmission (Anstrom et al., 2009) and that the long-term impact of the social defeat stress is critically dependent on the neurotrophic factor BDNF that is expressed in the VTA (Berton et al., 2006). Dopaminoreceptive neurons are likely target site of disturbance under chronic stress, critically via glucocorticoid release **(Figure 1.4.)** (Barik *et al*, 2013) and epigenetic control (i.e., DNA hyper-methylation of the tyrosine hydroxylase gene) (Niwa et al., 2013). Furthermore, an increase in dopaminergic neuronal activity and morphological alterations in the VTA appear to underlie anxiety-related behaviors in a mouse model of bipolar disorder, which are, notably, rescued by and lithium treatment, a common medication for mood disorder (Coque et al., 2011a).

However, to my best knowledge, no single human study has linked abnormalities of the dopaminergic circuit to pathological anxiety. If abnormal dopaminergic circuit is indeed implicated in human anxiety disorder or trait anxiety, this will add significant information about basic dopaminergic function and the consequence of its malfunction, and will motivate future research for treatment strategies targeting the normalization of dopaminergic neuronal activity.

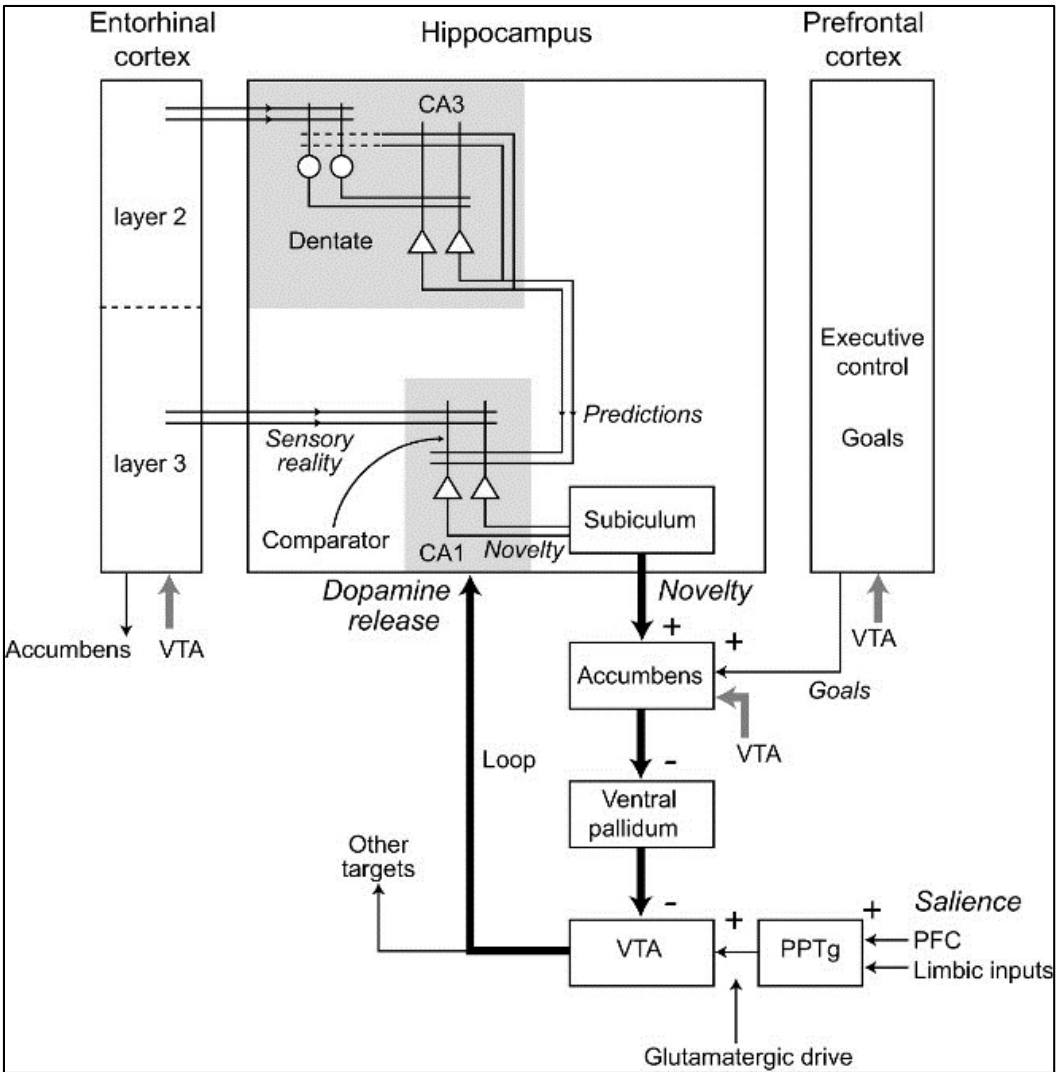

Figure 1.3. Hippocampus-VTA loop: controlling the entry of information into memory. This model describes rather complex information flow within the hippocampus–VTA loop that is essentially embedded on the Gray and McNaughton's septo-hippocampal system. External inputs come through the entorhinal cortex to the dentate gyrus/CA3 areas, which provide input to CA1. CA1 functions as a comparator in relation to the VTA and passes novelty signals to the subiculum and then to basal forebrains and to the midbrain dopamine cells. Of note, the VTA projection to the prefrontal cortex is likely to be related to this functional loop. PPTg, pedunculopontine tegmentum (Adapted from Lisman and Greace, 2005).

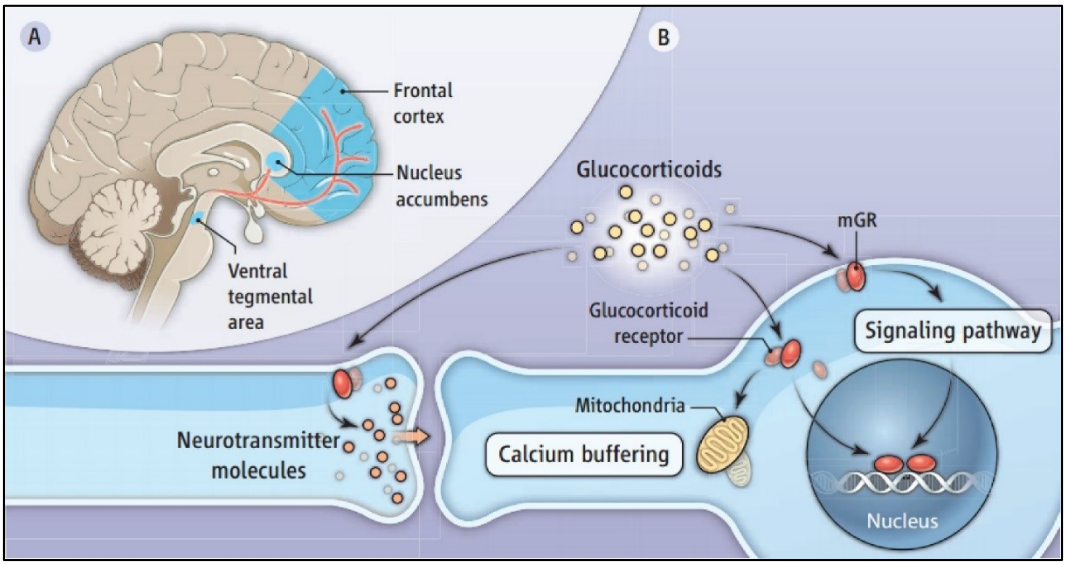

Figure 1.4. Chronic stress reactivity via glucocorticoids and brain circuitry. ***A,*** Chronic stress stimulates glucocorticoid signaling, impacts of which are targeted on dopamine circuit, that is, mesolimbic and mesocortical pathways. ***B,*** Genomic and non-genomic processes mediate stress-induced glucocorticoid actions. Barik et al. and Niwa et al. recently report that this mechanism is most likely to act on specific dopamine projections (Barik et al., 2013; Niwa et al., 2013). I propose that brain circuitry of anxiety should consider these recent findings. (Adapted from (McEwen, 2013).

Neuroimaging Technology for Brain Connectivity

Macro-Scale Brain Connectivity

How neurons (or brain systems) interact with each other to produce a behavior is central to neuroscience. In animal research, various anatomical and functional assays exist to examine connection properties of neurons, primarily at micro-scale. Recent developments in technologies using MRI are now enabling the systematic and quantitative investigation on brain connectivity at the macro-scale. For example, diffusion weighted imaging combined with computational estimation of probable white matter tracts (i.e., tractography) can demonstrate anatomical connections of the living brain. Although numerous technical issues remain to be resolved, such MRI-based connectivity technology has rapidly been becoming the primary tool of human neuroscience and connectome research because of its relatively simple and generalizable methodology and because there are no alternatives for studying living brains.

Such an access to the macro-scale connectivity has greatly advanced our knowledge of brain function and structure. For example, Honey et al. used fMRI to examine the dynamics of interregional functional connections in the absence of external input – so called, 'resting-state connectivity'– and report significant overlap with the structural connectivity matrix, based on previous anatomical

tracing data **(Figure 1.5.)** (Honey et al., 2007). This seminal report has promoted similar approaches in the study of human whole brain networks, which could have been not possible without MRI (Bassett and Bullmore, 2009; Meunier et al., 2009; Van Dijk et al., 2010).

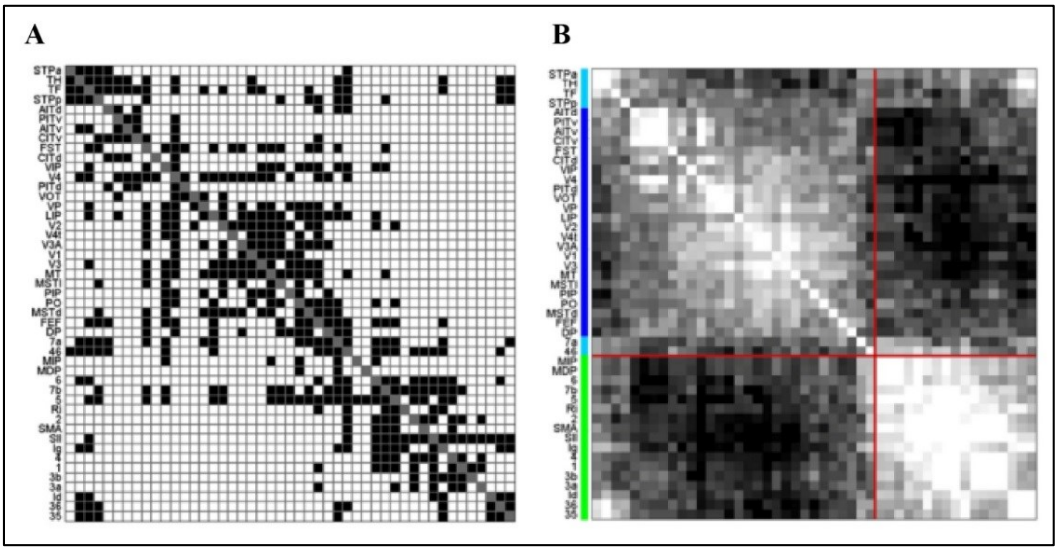

Figure 1.5. Macro-scale functional and structural connectivity using MRI. **(A)** Structural connection matrix of macaque neocortex based on anatomical tracing data. **(B)** Functional connection matrix generated from resting-state fMRI connectivity, which shows overlap with the underlying structural network. (Modified from Honey et al., 2007).

Methods For Investigating Brain Connectivity

Intrinsic functional connectivity (often called fcMRI) has rapidly gained attention as a general brain mapping tool to examine, primarily, large-scale functional networks, because of the simplicity of this technique (e.g., short data acquisition –several minutes, no need for an experimental design –resting state– and generalizable and unifiable data analytic strategies). FcMRI is based on the slow (usually < 1Hz) intrinsic fluctuations in hemodynamics measurable with fMRI and the coupling of these ultra-slow fluctuations that are observed in many brain systems known to have synaptic connections (Buckner et al., 2013). FcMRI results partitally correlate with anatomical estimates of structural connectivity by diffusion tractography (Honey et al., 2007; Damoiseaux and Greicius, 2009; Greicius, 2009) and by tract tracing in non-human primates (Vincent et al., 2007; Margulies et al., 2009; Mars et al., 2011). Thus, a major application of intrinsic functional connectivity is to define coupled networks of distributed brain regions.

For all of its usefulness, it should also be noted that functional connectivity is nevertheless an ambiguous mapping tool. Despite a general correspondence with anatomical connectivity, there are observations of functional correlations between brain regions that are not anatomically connected. This could be due to indirect relationships via a third region, which the functional connectivity technique cannot disambiguate. Furthermore, fcMRI is known to be

more sensitive to confounding influences from conditions such as motion and physiological modulations than are other task-based parametric mapping approaches. Interestingly, some known statistical methods to control these issues are reported to cause spurious negative correlations (or anti-correlations), which in turn has led to the development of novel algorithms (such as the component-based noise correction method), which minimize motion confounding and do not cause secondary artifacts (Behzadi et al., 2007).

In addition, because of its task-free nature, the interpretation of results may sometimes be limited. For example, different subdivisions of the ACC are known to have distinct connection properties with the amygdala depending on contexts or tasks (Mohanty, 2007). However, a resting-state fcMRI differentiating the ACC shows positive correlation with the amygdala and other limbic regions alike (Margulies et al., 2007). This shows that correlation and anti-correlation in fcMRI may not interpreted as an excitatory or inhibitory nature of a given connection.

Another method for investigating brain connectivity in anxiety is diffusion tractography. Magnetic resonance diffusion tractography is a method to identify and characterize anatomical substrates of connectivity in the living brain. In diffusion weighted imaging, the intensity of voxels indicates the estimate of the water diffusion rate. Using a mathematical model (e.g., a diffusion tensor model),

one can calculate several diffusion parameters, such as anisotropy and diffusivity. These parameters have been widely used in human neuroimaging, particularly in the characterization of white matter microstructure in disease conditions. Neurobiological interpretations of the parameters are heavily dependent on correlation studies. For example, fractional anisotropy is known to positively correlate with axonal density or diameter and degrees of fasciculation. However, similar to the fMRI, the exact mechanism underlying the diffusion signal or parameter in the brain is yet to be known.

Tractography is a computational estimation of a likely connection across diffusion voxels **(Figure 1.6.)**. Therefore, the reliability of the tractography solutions is bound by the quality of diffusion imaging. Of note, the quality varies across brain regions and depends on multiples factors, such as imaging sequence, existence of crossing fibers and general confounding factors of MR (motion or physiological modulations). Despite such limitations, diffusion tensor tractography reliably reconstructs white matter bundles observable in post-mortem human dissection (Stieltjes et al., 2001; Catani et al., 2002) and from ex vivo tracer studies in non-human primates (Behrens et al., 2003). I will describe details of diffusion tractography and algorithms in the methods section of each relevant chapter.

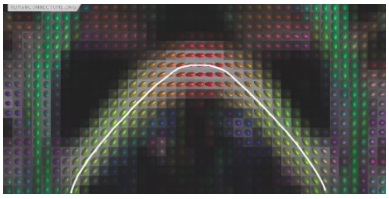

Figure 1.6. Diffusion tensor image of the corpus callosum. Diffusion directions are shown as a long axis. Directions are color-coded: red, left-right; green, back-front; blue, up-down. Tractography is estimation of a connection (Human Connectome Project website).

Novel Classification of Psychopathology: Research Domain Criteria

The National Institutes of Mental Health (NIMH) has initiated a strategic plan for "new ways of classifying psychopathology based on dimensions of observable behavior and neurobiological measures" (http://www.nimh.nid.gov/research-priorities/rdoc). Implementation of this strategy launched the Research Domain Criteria (RDoC) project (Insel and Cuthbert, 2009; Cuthbert and Insel, 2010a; Cuthbert and Insel, 2010b; Insel et al., 2010; Sanislow et al., 2010; Morris and Cuthbert, 2012; Cuthbert and Kozak, 2013; Morris et al., 2013). The current diagnosis of mental disorders is based on clinical observation and phenomenological symptom reports. However, the clinical syndromes based on subjective symptoms are not unitary disorders. It is therefore critical to map each observable dimension of complex behaviors onto a specific set of neurobiological substrates, such as genetic factors or brain circuits. This will allow a more complete account of pathophysiology and the development of more specific treatment strategies for mental disorders.

In relation to fear and anxiety, a relevant domain construct in RDoC is *negative valence system*, which has several subconstructs, including acute threat (fear) and potential threat (anxiety). An acute threat evokes a phasic fear response, which is an active coping mechanism characterized by fight or flight, while a more remote or uncertain threat generates a more persistent state of anxious apprehension and hypervigilance.

While abnormally increased sensitivity to either type of threat is closely related to clinical anxiety, the underlying neural circuitry is thought to be different, as I mentioned above. A critical contribution to the neuropsychiatry of anxiety would be the identification of a specific circuit and a set of factors that drive a distinct dimension of these negative valence systems. In this dissertation, I will therefore map these two particular constructs onto genes, brain regions, and circuits using complementary approaches combining cognitive paradigms and multi-modal MRI. I will describe this in more detail in what follows.

Table 1.1. Research domain criteria matrix of negative valence systems.

Domain Construct *Subconstruct*	Units of Analysis							
	Genes	Molecules	Cells	Circuits	Physiology	Behavior	Self-Reports	Paradigms
Negative Valence Systems								
Acute threat ("fear")								
Potential threat ("anxiety")								

Proposal for a Connectivity Model of Anxiety

In this dissertation, I propose the existence of two brain networks, each of which involves reactivity to distinct types of threat, that is, imminent and remote threats. Such a distinction is critical for a systematic and integrative investigation on brain circuitry and other factors of a specific pathophysiology of anxiety.

Amygdala–Prefrontal "Fear" Network

In response to imminent threat, the nervous system in human and animal models alike produces a set of phasic fear responses to adapt to the environment (Ohman et al., 2001). Central to a fear response is a rapid allocation of attentional resources to threat, which serves to prioritize visual cortical processing within the

retinotopic location (Carlson et al., 2011b). It has been suggested that excessive attention bias to threat is closely related to greater vulnerability to clinical anxiety (Fox, 2002; Mogg and Bradley, 2002).

In a recent study, the negative attention bias indexed by facilitation of reaction time towards a threat (e.g., fearful facial expression) was found to predict physiological reactivity (e.g., cortical release) to real-life stress more significantly than widely used self-reported psychological questionnaires (Fox et al., 2010). Neuroimaging studies using this behavioral paradigm reveal that the amygdala and the rostral ACC are essential brain regions involved in negative attention bias. The existence of multiple stimuli compete for attention, and the ACC monitors and resolves conflicts while the amygdala detects threat and signals in a bottom-up fashion to the prefrontal systems (Mathews and Mackintosh, 1998; Mathews and MacLeod, 2002). Within the prefrontal system, the ACC is most densely and reciprocally connected with the amygdala (Porrino et al., 1981; Amaral and Price, 1984). Dynamic interaction of the amygdala–ACC network is critical to emotion related attention modulation (Mohanty, 2007). Based on this I propose that that the connectivity between the threat detecting function of the amygdala and the conflict monitoring function of the ACC plays a critical role in the onset and maintenance of anxiety in relation to hypersensitivity to imminent threat or fear. Although this proposal may not be a novel contribution of this dissertation to the

neuroscience field, systematic approaches to explain brain (connectivity)–behavior mechanism are sparse. Based on the aforementioned complementary connectivity tools available, the present study aims to investigate functional and anatomical substrates of the amygdala–ACC network that are critical in negative attentional bias and the contribution of other factors (e.g., genetic risk factor of anxiety, BDNF Val66Met polymorphism) to this relationship. This constitutes the first major question of this dissertation.

Mesocorticolimbic "Anxiety" Network

The vmPFC is the key structure in the anxiety circuitry. In response to remote and uncertain threat, the vmPFC receives inputs from various distributed systems to mediate precise appraisal and subsequent decision making to adaptive the volatile environments, including limbic regions and even the midbrain neuromodulatory regions. Here I propose that the entire mesocorticolimbic circuit with the vmPFC being central involves reactivity to distal and uncertain threat.

Numerous studies report the vmPFC's involvement in various cognitive and affective domains, such as autonomic control (Gianaros et al., 2004; Nagai et al., 2004; Ohira et al., 2009; Critchley et al., 2011; Thayer et al., 2012), threat processing (Milad et al., 2007b; Wager et al., 2009; Diekhof et al., 2011) and valuation (McClure et al., 2004; Valentin et al., 2007; Boorman et al., 2009; Chib

et al., 2009; Hare et al., 2009; Kumaran et al., 2009).The vmPFC integrates information from cortical and subcortical areas to generate affective meaning and to make a decision about a value-based choice or threat appraisal (e.g., whether a stimulus represents a threat or safety) (Roy et al., 2012).

Of note, central to such versatile and integral roles of the vmPFC is its extensive connectivity with the corticolimbic regions. In threat processing, it interacts with the dorsal prefrontal attentional network (Bishop et al., 2004; Hare et al., 2009), the hippocampus/parahippocampal gyrus (Kalisch et al., 2006; Milad et al., 2007a; Sierra-Mercado et al., 2011) and the thalamus for fear conditioning (Mitchell and Gaffan, 2008; Cross et al., 2012; Parnaudeau et al., 2013), and with the amygdala for fear regulation (Phelps et al., 2004; Sierra-Mercado et al., 2011). It is thus central to affective neuroscience to demonstrate how the vmPFC's integral functions are linked to its extensive connectivity. Furthermore, a quantitative and systematic account, ideally via complementary multi-modal MRI technology to account for structural and functional features, may provide much needed information about the pathophysiology of anxiety disorder, frequently characterized by the attenuation of vmPFC function (Drevets et al., 1997; Drevets et al., 1998; Etkin and Wager, 2007; Milad et al., 2009; Greenberg et al., 2013a).

Furthermore, the midbrain dopaminergic system plays an important role in negative affect processing. This system appears to closely interact with the

vmPFC, particularly in adaptive learning of unexpected outcomes (Takahashi et al., 2009). Based on the literature mentioned above, I propose to include the dopaminergic mesocorticolimbic system into the circuitry of uncertain threat ("anxiety"). This constitutes the second major question in this dissertation.

Questions Addressed in this Dissertation

As outlined above, the first goal of this dissertation is to investigate the amygdala–prefrontal "fear" circuit in response to imminent threat. To that end, the first two chapters of this dissertation will use the negative attention bias paradigm to probe the phasic fear response in healthy individuals. As this negative attention bias is related to the development of clinical anxiety, this paradigm stood out as a good framework to investigate the role of the amygdala–prefrontal circuit in this behavior. To examine connection properties, in Chapter 1 and 2, I will use non-invasive neuroimaging techniques to account for both anatomical and functional aspects. Specifically, diffusion MR and probabilistic tractography and voxel-wise examination will be used to measure the microstructure of the white matter tracts connecting the amygdala and the ACC. In addition to this, intrinsic functional connectivity will be measured in the amygdala–ACC network using resting-state fMRI. Such complementary

neuroimaging investigation on the role of the amygdala–ACC connectivity in attentional orientation to fearful stimuli would provide a novel mechanistic account on the brain-behavior relationship and a useful account on the pathophysiology of anxiety.

In addition to this, I will investigate potential impacts of genetic variability of a well-known risk factor of anxiety, that is, BDNF Val66Met. As mentioned above, a number of studies document the impacts of this genetic variance in humans on brain structure and anxious behaviors. I hypothesize that this genetic factor, specifically, the Met allele in the BDNF Val6Met, may have effects on the amygdala–prefrontal circuitry, which then contribute to individual differences in negative attention bias. This would provide unprecedented information about gene-brain connectivity-behavior relationship and novel insights on the mechanism of this genetic risk factor of clinical anxiety.

The second goal of this dissertation is to investigate brain circuitry of negative affect processing under uncertainty, that is, response to potential threats. Based on a previous report from our group – attenuated vmPFC threat processing in clinical anxiety– I first hypothesize that circuit-wide factors, including vmPFC grey matter structure and corticolimbic connectivity, are associated with vmPFC functioning during threat/safety assessment in ambiguity. To that end, in Chapter 4, I will first index individuals' vmPFC functioning based on fMRI during a fear

generalization task. Then, I will use multi-modal neuroimaging to characterize circuit-wide neural features of the vmPFC–mediated corticolimbic circuit.

In Chapter 5, I will hypothesize that the midbrain neuromodulatory structures are critically involved in threat generalization. More specifically, mesocorticolimbic network that has been primarily linked to positive motivation may play an important role in negative motivation as well. Aberrant behaviors of this putative dopaminergic aversion circuit may be associated with clinical anxiety. To test this, based on the same data from Chapter 4, in Chapter 5, I will examine, first, BOLD reactivity and functional connectivity of the midbrain structure with the corticolimbic systems and, second, group differences in them. Altogether, the studies presented in this dissertation will provide a circuit-based model anxiety in a different dimension of anxious behavior, hence will provide a more complete picture.

CHAPTER II

(Modified from Carlson, Cha, Harmon-Jones, Mujica-Parodi and Hajcak, *Cerebral Cortex,* 2013)

Title: Influence of the BDNF genotype on amygdalo-prefrontal white matter microstructure is linked to nonconscious attention bias to threat

Authors: Joshua M. Carlson[1*], Jiook Cha[2*], Eddie Harmon-Jones[3], Lilianne R. Mujica-Parodi[1], and Greg Hajcak[4]

Author Affiliations: 1. Department of Biomedical Engineering; 2. Program in Neuroscience, State University of New York at Stony Brook, Stony Brook, NY; 3. School of Psychology, University of New South Wales, Sydney, NSW, Australia; 4. Department of Psychology, State University of New York at Stony Brook, Stony Brook, NY

*JMC & JC contributed equally to this work

Abstract

Cognitive processing biases, such as increased attention to threat, are gaining recognition as causal factors in anxiety. Yet, little is known about the anatomical pathway by which threat biases cognition and how genetic factors might influence the integrity of this pathway, and thus, behavior. For 40 normative adults, we reconstructed the entire amygdalo-prefrontal white matter tract (uncinate fasciculus) using diffusion tensor weighted MRI and probabilistic tractography to test the hypothesis that greater fiber integrity correlates with greater nonconscious attention bias to threat as measured by a backward masked dot-probe task. We used path analysis to investigate the relationship between brain-derived nerve growth factor genotype, uncinate fasciculus integrity, and attention bias behavior. Greater structural integrity of the amygdalo-prefrontal tract correlates with facilitated attention bias to nonconscious threat. Genetic variability associated with brain-derived nerve growth factor appears to influence the microstructure of this pathway and, in turn, attention bias to nonconscious threat. These results suggest that the integrity of amygdalo-prefrontal projections underlie nonconscious attention bias to threat and mediate genetic influence on attention bias behavior. Prefrontal cognition and attentional processing in high bias individuals appear to be heavily influenced by nonconscious threat signals relayed via the uncinate fasciculus.

Introduction

Humans have evolved to rapidly respond to signals of potential threat (Ohman et al., 2001), even when these signals are nonconsciously processed (Beaver et al., 2005; Carlson et al., 2009a). This response includes an automatic allocation of attentional resources to the location of potential threat, which serves to prioritize visual cortical processing within this retinotopic location (Carlson et al., 2011b). Although affective processing biases are an adaptive aspect of the human fear response (Ohman et al., 2001), vulnerability to anxiety is linked to excessive attention bias to nonconscious threat (Fox, 2002; Mogg and Bradley, 2002). Furthermore, individual differences in nonconscious attention bias to threat prospectively predict cortisol release during laboratory-based and real-world stress (Fox et al., 2010). Critically, attention bias to threat is not only correlated with anxiety, but appears to play a casual role in its development (MacLeod et al., 2002). Given that attention bias is strongly and causally associated with stress reactivity and anxiety vulnerability, it is important to understand the anatomical pathway by which threat biases cognition and how structural variability in this pathway may relate to variability in attention bias behavior.

Models of cognitive processing biases claim that such biases only occur when multiple stimulus representations compete for attention (Mathews and Mackintosh, 1998; Mathews and MacLeod, 2002). Under this model, the ACC is

thought to serve as a conflict monitor and resolver, while the amygdala is thought to nonconsciously evaluate threat and "bias" the monitoring system (i.e., ACC) in favor of threat. Similarly, Gray and McNaughton's (2000a) model states that fear-related or "active avoidance" type behaviors such as increased attention to threat are mediated by the amygdala-ACC system, while during states of uncertainty and anxiety septo-hippocampal activity accompanies the amygdala response to threat. Consistent with these models, accumulating evidence suggests that the amygdala detects and evaluates nonconscious representations of visual threat (Morris et al., 1998; Whalen et al., 1998; Liddell et al., 2005), which are likely relayed via the pulvinar nucleus of the thalamus and the superior colliculus (Morris et al., 1999; Morris et al., 2001; Liddell et al., 2005). Furthermore, amygdala reactivity to nonconscious threat is elevated in a variety of negative affect-related dispositions such as anxiety (Etkin et al., 2004), depression (Sheline et al., 2001), anger (Carlson et al., 2010), and post-traumatic stress disorder (Rauch et al., 2000; Armony et al., 2005). More recent research has linked the facilitation of spatial attention by nonconscious threats to an amygdala-ACC network (Carlson et al., 2009b), in which amygdala reactivity is positively coupled with ACC activity. Additionally, amygdala activation during nonconscious attention bias to threat is elevated among anxious individuals (Monk et al., 2008). Anatomically, attention bias to threat is correlated with greater ACC gray matter volumes (Carlson et al., 2012b). Within the prefrontal cortex, the ACC is one of the most densely and

reciprocally connected with the amygdala (Porrino et al., 1981; Amaral and Price, 1984) and the uncinate fasciculus is the primary white matter tract connecting these structures. Thus, the uncinate fasciculus directly connects the "threat evaluating" amygdala to the "conflict resolving" ACC and we therefore expect that the integrity of this tract be positively correlated with attention bias behavior. Yet, this relationship has not been tested.

The extent to which genetic factors influence the integrity of the uncinate fasciculus pathway, and in turn, attention bias behavior is currently unknown. Growth factors such as brain-derived neurotrophic factor (*BDNF*) are critical in regulating neural development, connectivity, and plasticity (Poo, 2001; Martinowich and Lu, 2008) and for precisely this reason, genetic variability affecting these growth factors may contribute to variability in white matter integrity across individuals. Here we turn our attention to a single nucleotide polymorphism in the *BDNF* gene, which results in the substitution of valine (Val) to methionine (Met) at codon 66—the *BDNF* Val66Met polymorphism (Egan et al., 2003). The frequency of the Met/Met (4.5%, 15.9%), Met/Val (27.1%, 50.3%), and Val/Val (68.4%, 33.%) genotypes has been shown to differ across ethnic backgrounds (United States (a primarily Caucasian sample) & Japan, respectively; Shimizu et al., 2004). The substitution of Met for Val reduces a number of factors associated with synaptic plasticity and memory such as

memory performance, hippocampal activity, synaptic activity, BDNF dendritic expression, and activity dependent secretion of BDNF (Egan et al., 2003). Additionally, Met/Met mice manifest less neuronal BDNF secretion and display increased fear-related behaviors such as freezing (Chen et al., 2006). Similar to the mouse model, Met/Met humans are at increased risk for mood disorders (Montag et al., 2010b) and Met+ (i.e., Met/Met & Met/Val) adults display heightened rumination (Hilt et al., 2007; Beevers et al., 2009) and disrupted fear conditioning (Hajcak et al., 2009). Additionally, the Met-*BDNF* genetic has been linked to increased depression in women across ethnic backgrounds (Verhagen et al., 2010). In human functional neuroimaging research Met+ individuals show a hyperactive amygdala response to emotional stimuli (Montag et al., 2008)—an effect exaggerated in anxious individuals (Lau et al., 2010). Human structural neuroimaging research indicates that Met allele carriers show smaller amygdala, hippocampus, caudate, and dorsolateral prefrontal volumes, compared to Val/Val individuals (Pezawas et al., 2004). However, in terms of white matter, greater fiber integrity has been linked to the Met-*BDNF* genetic variant in a number of the major fiber tracts (Chiang et al., 2011) and in particular the uncinate fasciculus (Tost et al., 2013). Given the prevalent impacts of *BDNF* Val66Met on neural structure including white matter (Chiang et al., 2011; Tost et al., 2013) and fear-related behavior (Chen et al., 2006), we hypothesized that Met+ individuals

would display greater uncinate fasciculus fiber integrity and increased attentional bias to nonconscious threat.

The primary goal of this study was to test the relationship between amygdalo-prefrontal tract integrity and attention bias behavior. Based on the models (Mathews and Mackintosh, 1998; Gray and McNaughton, 2000b; McNaughton and Gray, 2000; Mathews and MacLeod, 2002) and research (Carlson et al., 2009b; Carlson et al., 2012b) outlined above, we hypothesized that greater amygdalo-prefrontal tract integrity predicts greater levels of nonconscious attention bias to threat. To test this hypothesis we used a recently designed global tractography method (Yendiki et al., 2011b) to reconstruct the entire uncinate fasciculus tract and measured nonconscious attention bias to threat with a backward masked fearful face dot-probe task. Further, we examined the role of the *BDNF* Val66Met polymorphism on this brain-behavior relationship (Martinowich and Lu, 2008; Montag et al., 2008; Montag et al., 2010b; Tost et al., 2013). Specifically, we used structural equation modeling to test the hypothesis that differences in *BDNF* genotype would influence fiber integrity and in turn attention bias behavior.

Methods

Participants

Forty (16 female) consenting adults 19-25 years old participated. Our sample contained 18 Caucasians, 3 African Americans, 15 Asians, 0 Hispanic, and 4 individuals of other ethnicities[1]. Thirty-five reported being right handed. Potential participants were screened for metal in their bodies. The Institutional Review Board of Stony Brook University approved this study. Participants were compensated for their time.

Dot-probe Task

The task was performed in a small testing room outside the scanner. Stimuli were presented on a 60Hz PC monitor and stimulus presentation was controlled by E-Prime (Psychology Software Tools, Pittsburg, PA). Facial stimuli were from a standardized database (Gur et al., 2002). Four individual identities (two male) of fearful and neutral grayscale faces were used for the initial (i.e.,

---

[1] Ethnicity was neither associated with attention bias to threat ($F_{3,36} = 1.82$, $P = 0.16$) nor uncinate fasciculus integrity, $F_{3,36} = 1.27$, $P = 0.3$.

masked) faces and a different female identity with an open-mouthed happy facial expression was used as a mask. As depicted in **Figure** 2.1a, trials started with a white fixation cue (+) centered on a black background for 1000 ms. Afterwards, two faces were then simultaneously presented to the left and right of fixation (33 ms). Each face subtended approximately 5 × 7° of visual angle. Faces were separated by 14°. To limit the potential influence of perceptual inconsistencies, these initial faces were instantly masked with an open mouth happy face (100 ms) offset by 1° on the vertical axis (Carlson and Reinke, 2008). A target dot immediately followed in either the location of the left or the right face and remained on the screen until a response was made. Participants responded to the location of the dot using the numeric pad on a keyboard: pressing the "1" key with their right index finger for left-sided targets and the "2" key with their right middle finger for right-sided targets. The fixation cue remained in the center of the screen throughout the entirety of each trial. Participants were instructed to always fixate on this cue.

Trials used to calculate attention bias scores contained one fearful and one neutral face. For half of these trials, the target dot was presented in a spatially congruent location to the fearful face, while for the other half the target dot was spatially incongruent (i.e., appeared behind the neutral face). The facilitation of spatial attention by backward masked fearful faces is marked by faster reaction

times on congruent compared to incongruent trials. Thus, attention bias scores were calculated as the mean difference between congruent and incongruent reaction times. Values that are more negative are indicative of an attention-related reduction of reaction time on congruent compared to incongruent trials. The task contained 40 congruent and 40 incongruent trials equally presented in each visual field plus 40 neutral-neutral trials.

Participants also completed a task designed to assess awareness of the backward masked faces. Participants were instructed that each trial would contain two sets of faces presented in rapid succession and that they should identify the facial expressions of the first set of faces. Stimulus presentation for this task was identical to the dot-probe task with the exception that following the masked faces participants were prompted to use a keyboard to indicate whether they saw a fearful face on the left, a fearful face on the right, or two neutral faces. The task included 60 trials: 20 of each type.

Genotyping Procedure

Participants were genotyped for Val66Met BNDF polymorphism. The genotyping procedures for BDNF have previously been described (Hajcak et al., 2009). Briefly, we used the QuickExtract DNA Extraction Solution (Epicentre Technologies, Madison, WI, USA) to extract DNA from buccal cells, and a high-

resolution melt analysis for genotype analysis. Our sample contained 18 Met carriers (Met/Met = six & Met/Val = 12) and 22 homozygous Val/Val individuals. Using the Hardy–Weinberg equilibrium calculator (Rodriguez et al., 2009) our BDNF genotype distribution did not deviate from the expected distribution (χ^2 (1) = 3.27, $p > 0.05$).

Image Acquisition

Participants were scanned at the Stony Brook University Social, Cognitive, and Affective Neuroscience (SCAN) center with a 3 Tesla Siemens Trio whole body magnetic resonance image scanner. DTIs were collected using the following parameters: TR = 5500 ms, TE = 93 ms, FOV = 220 × 220 mm, Matrix = 120 × 220 × 220, Voxel size = 1.7 × 1.7 × 3.0 mm, EPI factor = 128, slices = 40, slice thickness = 3 mm, Bandwidth = 1396 Hz/pixel, GRAPPA acceleration factor = 2. The series included two initial images acquired without diffusion weighting and with diffusion weighting along 40 non-collinear directions ($b = 800$ sm^{-2}). T_1-weighted images were acquired in the same session with the following parameters: TR = 1900 ms, TE = 2.53, Flip angle = 9°, FOV = 176 × 250 × 250 mm, Matrix = 176 × 256 × 256, and Voxel size = 1 × 0.98 × 0.98 mm.

Image Processing

We corrected eddy current distortions for each subject, and registered individual images without diffusion weighting to T_1 images. We used FDT (FMRIB software library's Diffusion Toolbox 2.0) for DTI preprocessing. We performed cortical parcellation and subcortical segmentation from individual's T_1-weighted image employing an automated cortical reconstruction and volumetric segmentation tool, Freesurfer 5.1 (http://surfer.nmr.mgh.harvard.edu/).

Global Tractography: TRACULA

We performed a recently developed global tractography method, TRACULA (TRActs Constrained bv UnderLying Anatomy; (Yendiki et al., 2011b), to reconstruct our a priori white matter tract of interest, the uncinate fasciculus. Global tractography parameterizes a connection between two regions at a global level, instead of tracking through a local orientation field. This global approach has several advantages over local tractography in that it eschews local uncertainty issues due to noise or partial volume effects, and it can increase the sensitivity and robustness of the tractography solutions by informing tractography process of a known connection between two regions (Jbabdi et al., 2007). Furthermore, TRACULA minimizes bias due to the need of manual intervention, for example to set arbitrary angle or length for tractography or to draw anatomical

boundaries for tracts, which potentially lead to spurious results. TRACULA uses a Bayesian framework for global tractography with anatomical priors (Yendiki et al., 2011a) Prior information on the surrounding anatomy of the pathway are derived from training data sets of 33 healthy adults, of which major pathways including the uncinate fasciculus are identified by a neuroanatomist (see Yendiki A et al., 2011 for detailed manual labeling procedures). Notably in TRACULA, two end regions for the tractography algorithm are obtained by intersection of the pre-labeled tract atlas and the brain areas of a test subject, parcellated and segmented in Freesurfer. Based on this prior knowledge, posterior distributions of tracts are estimated via a Markov Chain Monte Carlo (MCMC) algorithm (see individual tracts in **Figure** 2.2). Statistics on standard diffusion measures (i.e., fractional anisotropy, axial diffusivity, radial diffusivity, and mean diffusivity) are then extracted from the estimated posterior pathway distribution.

DTI Metrics and Statistical Analysis

Based on earlier work (Carlson et al., 2009b; Carlson et al., 2012b), we tested the directional hypothesis that greater attention bias would be associated with greater uncinate fasciculus fiber integrity. Based on the reports that the Met-BDNF variant of Val66Met SNP is associated with greater white matter integrity (Chiang et al., 2011) and increased fear-related behaviors (Chen et al., 2006) we

tested the directional hypotheses that Met allele carriers would show greater fiber integrity in the uncinate fasciculus and greater attention to threat. Our primary measure of interest was fractional anisotropy, which is an indicator of fiber integrity and degree of myelination (Le Bihan, 2003). Radial and axial diffusivity, which respectively measure the degree of myelination and axonal integrity (Song et al., 2003), were also assessed. Fractional anisotropy was positively correlated with axial diffusivity (left: $r = 0.62$, $P = 0.00004$ right: $r = 0.52$, $P = 0.0003$), but negatively with radial diffusivity (left: $r = -0.90$, $P < 0.00001$; right: $r = -0.90$, $P < 0.00001$). Thus, we tested an inverse relationship with radial diffusivity. Given our directional tests, we used one-tailed p-values.

We diagnosed potential outliers for every test at a threshold of Cook's distance of 4/n (i.e., 0.1). When potential outliers were detected, robust linear regression was used. Robust regression in Stata 12 used a stepwise weighting estimation (i.e., Huber weighting and bi-weights) and a bi-weight tuning constant of 6 was used (Goodall, 1983).

Path Analysis

We combined path analysis and a model comparison method in AMOS 18 (SPSS Inc.) to test the serial relationship of BDNF SNP, FA of the left uncinate fasciculus, and attention bias. We chose path analysis because it can effectively

differentiate direct and indirect effects, and with aid of structural equation model functionality (e.g., bootstrap model comparison method), it provides a useful approach for hypothesis testing. We first built the most intuitive model (Model 1), which assumed serial effects of BDNF genotype onto FA and FA onto attention bias. We then constructed five variations and compared model fit to choose the best one. Confounding variables in the model included age, sex, and ethnicity for the effects of BDNF on the FA in addition to awareness level and information processing speed for attention bias.

Given our sample size of forty and the numbers of parameters included in the model, our degrees of freedom were only eight for the intuitive model. Thus, a goodness of model fit could be driven by only a few outliers. Our data indeed contained one potential outlier whose attention bias index is more than 2 SD + average (**Figure** 2.1c), and this outlier significantly decreased goodness of model fit: in case of the intuitive model (Model 1), $\chi 2/df$ dropped from 0.914 (without the outlier) to 0.793 (with the outlier). We thus excluded this outlier from the path analyses. No outliers were found in FA. For model comparison, we employed a bootstrapping method following the Linhart and Zucchini's approach (Linhart and Zucchini, 1986) in addition to comparison of standard goodness of fit statistics. The bootstrapping approach involves four steps. First, we generated bootstrap samples considering the original data as the population for sampling. Second, the

five models were fitted to every 10,000 bootstrap samples using the maximum likelihood function. For each iteration, the discrepancy between each bootstrap sample and the bootstrap population was calculated. Third, the average discrepancy across bootstrap samples for each model was calculated. Fourth, the best model among the five was selected based on the mean discrepancy. We additionally considered standard goodness of fit measures, such as AIC (Akaike's Information Criterion), the root mean square error of approximation (RMSEA) and the comparative fit index (CFI). Cutoff criteria for RMSEA (<0.06) and CFI (0.95) were considered (Hu and Bentler, 1999).

Results

Behavior

Reaction time data was restricted to correct responses occurring within 150-750ms (Carlson and Reinke, 2008), which resulted in 2.5% of the data being discarded for incorrect responses and another 2% discarded for premature or delayed responses. Thus, 95.5% of the reaction time data was used for analysis. Overall, participants responded faster on congruent compared to incongruent trials (mean congruent-incongruent difference = -6.20ms, s.d. =17.50, t_{39} = -2.24, P = 0.02) suggesting that at the group-level attention was captured by backward

masked fearful faces[2]. For correlation analyses, *Attention Bias* scores were calculated as the congruent-incongruent difference, where values that are more negative indicate faster responses on congruent trials and thus, greater attentional bias to threat. Participants' performance on a post-task assessment of awareness was at chance ($t_{39} = 0.82$, $P = 0.21$).

Reconstructed Uncinate Fasciculus

We reconstructed the uncinate fasciculus in each subject (Supplementary **Figure** 2.1). In order to quantify variability of the reconstructed tracts, we examined voxel-wise coefficients of variance (**Figure** 2.2). The tracts showed shared configuration in the inmost region (i.e., low coefficients of variance) and highly variable configuration in the outmost region (i.e., high coefficients of variance). Each posterior distribution of the uncinate fasciculus had on average

[2] It should be noted that age ($r = -.16$, $P = 0.34$), gender ($t_{38} = 0.07$), handedness ($t_{38} = 0.97$), and ethnicity ($F_{3,36} = 1.82$, $P = 0.16$) were not associated with attention bias scores.

13,715 voxels (± 495; sem), and an average of 38.6% (± 1.3; sem) of them were non-overlapping with the probabilistic atlas of the uncinate fasciculus (JHU

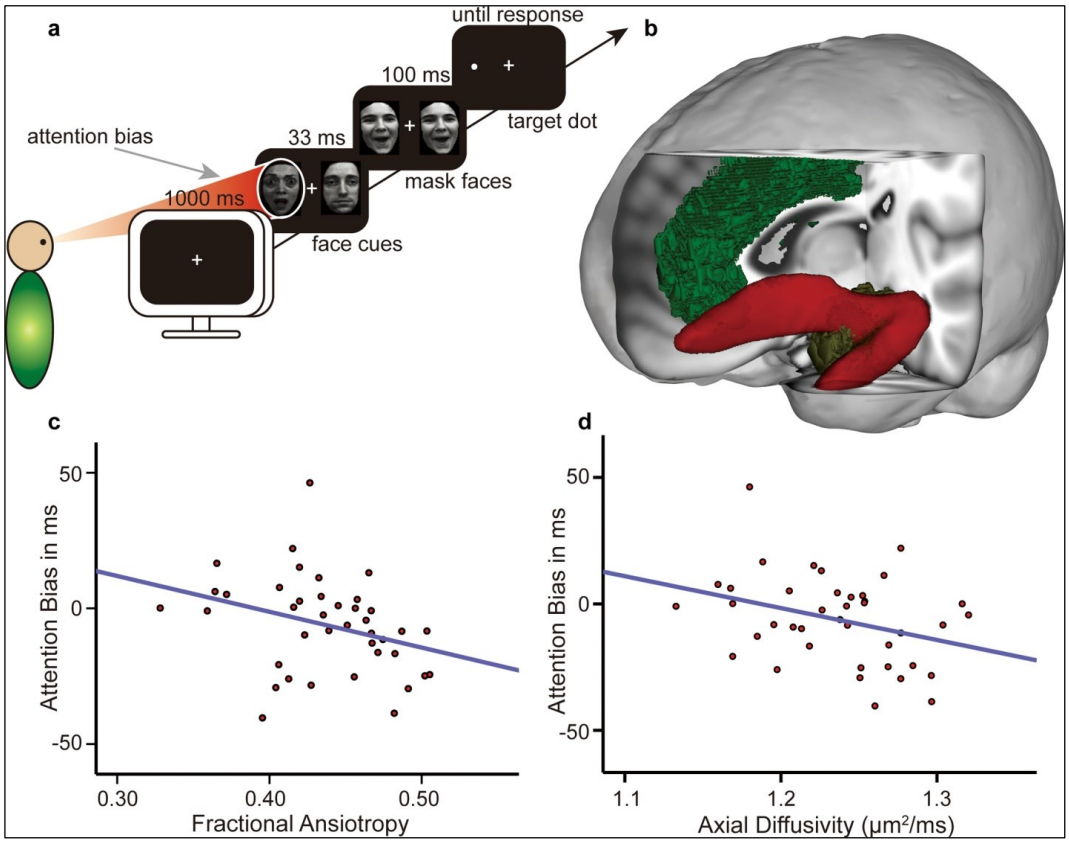

Figure 2.1. Negative attention bias paradigm, amygdala-prefrontal white matter reconstruction, and attention bias-connectivity correlation. (**a**) An example of a congruent trial. Attention bias is calculated as the difference between masked fear congruent and incongruent dot-probes, where greater attention to threat is reflected by a more negative value. (**b**) Posterior distribution of the reconstructed uncinate fasciculus averaged across 40 subjects and thresholded at 20% maximum. The uncinate fasciculus (red) connects the amygdala (brown) to ventral prefrontal and anterior cingulate (green) cortices. (**c**) Scatter plots depicting correlations between attention bias and left uncinate fasciculus fractional anisotropy and (**d**) axial diffusivity.

White-Matter Tractography Atlas; http://fsl.fmrib.ox.ac.uk/fsl/fslview/; Supplementary Table). An average of 79.9% (± 0.7; sem) of the atlas was non-overlapped with the posterior distribution map. These results indicate a high degree of uncinate fasciculus variability across individuals and highlight the problem of solely using a standardized atlas for DTI analysis without consideration of this large degree of individual variability.

Correlations with Attention Bias

As predicted, greater left uncinate fasciculus fractional anisotropy (FA: $r_{partial}$ = -0.36, P = 0.01; **Figure** 2.1c) and axial diffusivity (AD: $r_{partial}$ = -0.35, P = 0.02; Fig1d) were correlated with greater attention bias to threat with a trend observed for the right uncinate fasciculus (FA: $r_{partial}$ = -0.20, P = .11; AD: $r_{partial}$ = -0.25, P = .07). We controlled for participants' level of awareness and speed of information processing (Wiens, 2006; Turken et al., 2008). These effects were robust to potential outliers (FA: t_{36} = -2.33, P = 0.01; AD: t_{36} = -1.67, P = 0.053, robust linear regression; see Materials and Methods for outlier diagnosis). The overall effect was in an uncinate-fasciculus specific manner as we did not observe a correlation with the mean fractional anisotropy of the entire brain (r = -0.07, P = 0.32).

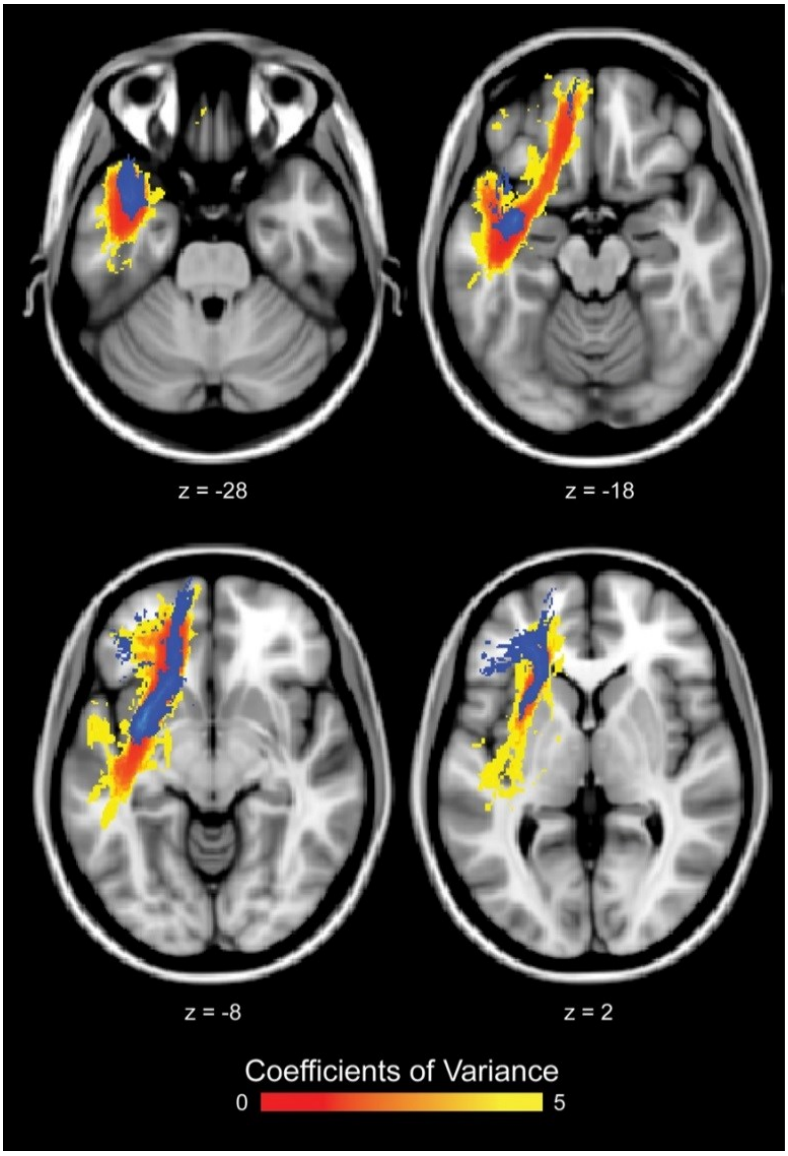

Figure 2.2. Variability map of the reconstructed amygdala-prefrontal white matter tract. The voxel-wise coefficients of variance map (shown in red-yellow) of the reconstructed uncinate fasciculus showed shared inmost region and highly variable outmost region. A probabilistic uncinate fasciculus atlas (shown in blue; JHU White-Matter Tractography Atlas; http://fsl.fmrib.ox.ac.uk/fsl/fslview/) was overlapped. The voxel-wise CV map was derived from posterior distribution map in each subject.

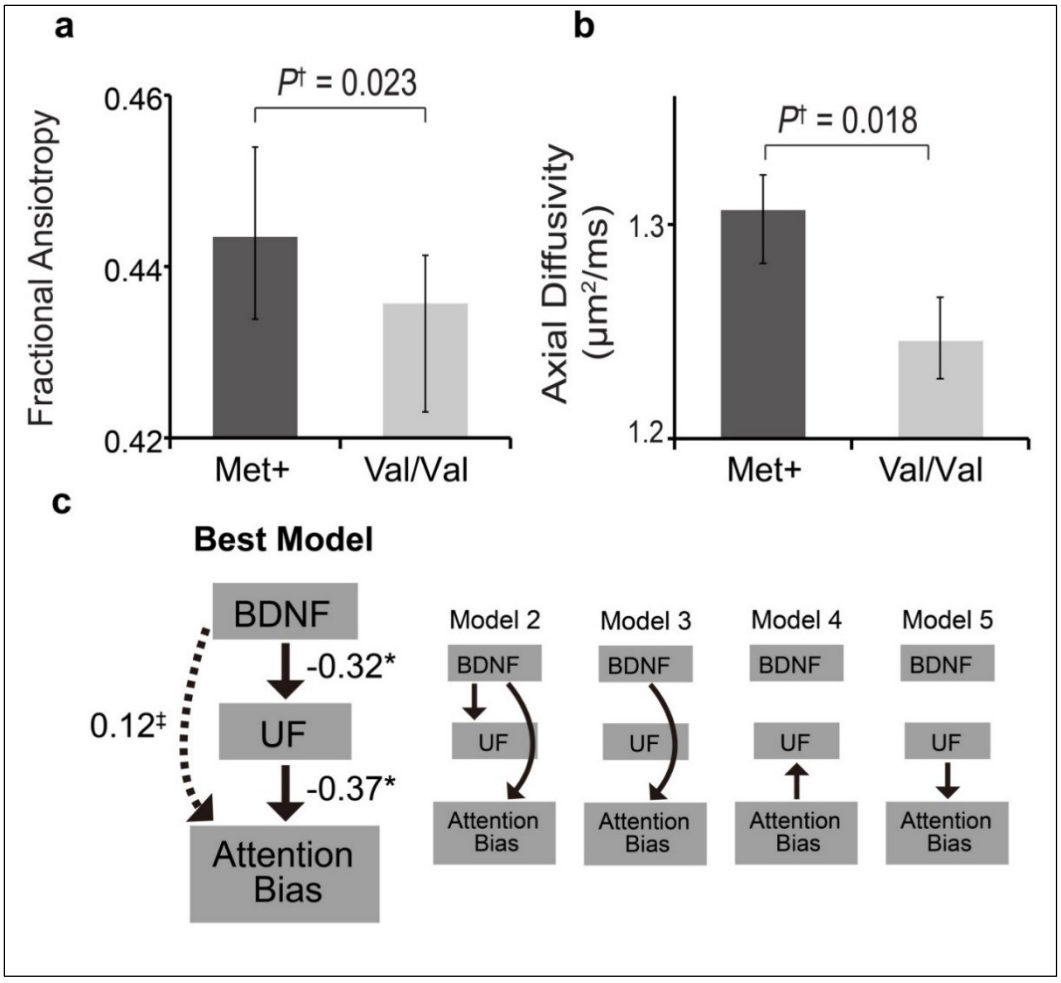

Figure 2.3. Impacts of BDNF met66val genetic variance on the amygdala-prefrontal fiber integrity and negative attention bias. The Met+ BDNF variant (Met/Met and Met/Val) as compared to Val/Val, resulted in greater fractional anisotropy (a) and axial diffusivity (b) in the left uncinate fasciculus. Effects controlled for age, sex, and ethnicity. (c) Five regression models containing BNDF Val66Met, FA of uncinate fasciculus, and attention bias were compared. The best model selected based on multiple model fit criteria suggests that BDNF Val66Met influences uncinate fasciculus integrity, which in turn influences attention bias to threat. Bold arrows denote estimated direct effects. A dotted arrow in the best model indicates an indirect effect. BDNF = BDNF Val66Met polymorphism; UF = fractional anisotropy of the left uncinate fasciculus. † Significance of coefficients in robust linear regression. * $P < 0.05$, ‡ $P = 0.066$.

Impacts of BDNF SNP Variant on Fiber Integrity and Attention Bias

We then explored a link between uncinate fasciculus fiber integrity and genetic factors. As predicted, we found a significant effect of the Met allele (both Met/Val and Met/Met) on fractional anisotropy (t_{35} = -2.08, P = 0.02, robust linear regression) and axial diffusivity (t_{35} = -2.18, P = 0.02) in the left uncinate fasciculus (Fig3a and b). These effects controlled for ethnicity, sex, and age. We observed a trend-level effect of Met-*BDNF* variant on attention bias (P = 0.13, robust linear regression) when controlling for awareness and speed of information processing. Thus, the results suggest that the Met-*BDNF* variant is associated with greater uncinate fasciculus integrity, which is associated with attention bias to threat. This may suggest a serial impact of the genetic variant to white matter structure to attention bias behavior. To test such a relationship directly, we performed a path analysis between the *BDNF* SNP, fractional anisotropy of the uncinate fasciculus and attention bias. We built a model accounting for the serial relationship and four alternatives, and compared them. Confounding variables were included (see Methods and Materials). As predicted, the model of the serial influences showed the best goodness of model fit: lowest AIC (55.9) and mean discrepancy of bootstrap samples vs. population (49.3), highest Comparative Fit Index (0.93) and root mean square error of approximation (0.053) (Fig3c, Table1). In this model, the total effect of *BDNF* SNP on FA was β = -0.32, P =

0.043 (Bias-corrected using Bootstrap estimation) and the total effect of FA on attention bias was $\beta = -0.37$, $P = 0.03$. The indirect effect of the *BDNF* SNP on attention bias via FA was $\beta = 0.12$, $P = 0.066$). Overall, the model accounted for 35.3 % of variance in the FA and 20.6 % of AI variance (squared multiple correlations). These results strongly support the serial relationship of gene to white matter structure to behavior.

Table 2.1. **Comparison of path analyses of gene-brain-behavior relationship.**

Model	*df*	χ^2/df	Discrepancy of bootstrap samples and population	AIC	CFI	RMSEA	Squared Multiple Correlations
Model 1	18	1.11*	49.3*	55.9*	0.93*	0.053*	UF, 0.353; AI, 0.206
Model 2	18	1.32	53.0	59.8	0.79	0.092	UF, 0.353; AI, 0.101
Model 3	19	1.49	55.4	62.3	0.67	0.113	UF, 0.216; AI, 0.101
Model 4	19	1.18	50.6	56.3	0.88	0.068	UF, 0.383; AI, 0.060
Model 5	19	1.28	51.7	58.4	0.81	0.086	UF, 0.216; AI, 0.198
Independent Model	28	2.00	-	72.2		0.163	

*Indicating best goodness of model fit in each criterion. AI, attention bias; UF, FA of the uncinate fasciculus.

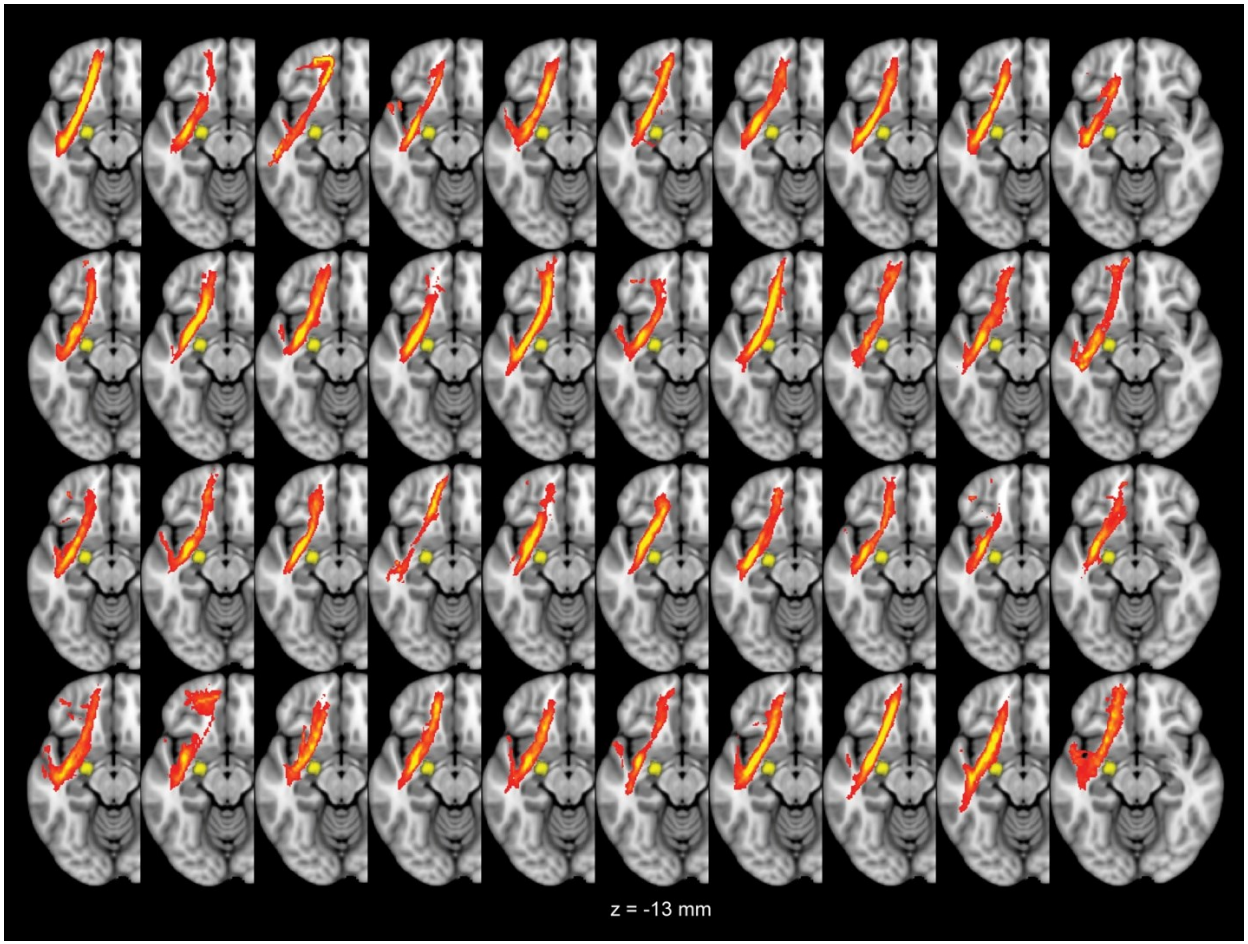

Figure 2.4. Posterior distribution of the reconstructed left uncinate fasciculus for 40 subjects. Individual tracts were thresholded at 20% maximum and registered to a MNI152 structural space for a presentational purpose. Note that the reconstructed fibers show a similar configuration as a whole, while they also show individual variability. Left amygdala is a Harvard-Oxford Cortical atlas and shown in yellow.

Table 2.2. Overlap between posterior distribution maps and an atlas of the left uncinate fasciculus. Only average 21% of the atlas was overlapped with the posterior distribution maps, and 61% of the posterior distribution was overlapped with the atlas. We normalized the posterior distribution maps to standard MNI space in order to compare with the atlas.

Subject	PD overlapped with atlas (%)	Atlas overlapped with PD (%)
1	65.9	20.5
2	71.0	21.3
3	65.9	20.9
4	69.3	22.1
5	59.2	20.8
6	67.3	20.9
7	75.7	23.1
8	58.0	22.9
9	64.8	25.4
10	56.2	12.9
11	54.3	26.1
12	60.0	24.7
13	61.4	20.2
14	51.3	15.1
15	63.0	24.9
16	57.7	18.4
17	70.7	22.3
18	62.0	20.9
19	70.5	18.8
20	65.6	27.7
21	63.8	23.6
22	57.7	19.5
23	70.4	21.7
24	71.4	20.2
25	53.7	15.9
26	65.2	22.1
27	36.9	14.3
28	62.0	15.6
29	71.7	24.0
30	57.5	21.6
31	46.6	31.5
32	44.9	14.7
33	55.7	11.9
34	62.8	18.6
35	72.0	25.5
36	60.0	19.3
37	49.3	16.4
38	51.8	18.3
39	63.7	30.7
40	51.4	28.0
Average	61.0 ± 1.3	21.1 ± 0.7

Discussion

We provide evidence linking uncinate fasciculus microstructure to elevated attention bias to nonconscious threat. The direction of this correlation suggests that for hyper-threat attentive individuals, the anterior cingulate (ACC) and amygdala together play a role in potentiating the nonconscious threat response. Our results further suggest that the Met allele of the *BDNF* Val66Met polymorphism elevates attention bias to threat through its influence on amygdalo-prefrontal connectivity.

Amygdala – Prefrontal Integrity and Attention Bias to Threat

Similar to the amygdala (Morris et al., 1998; Whalen et al., 1998; Liddell et al., 2005), the ACC is activated in response to nonconscious threat signals (Liddell et al., 2005; Williams et al., 2006b). Both the amygdala and ACC are hyperactive in response to nonconscious threats in anxiety disorders such as post-traumatic stress disorder (Bryant et al., 2008; Kemp et al., 2009) and are positively coupled during nonconscious threat processing (Williams et al., 2006a). Given evidence that the amygdala receives representations of nonconscious threat through a subcortical route (Morris et al., 1999; Morris et al., 2001; Liddell et al., 2005), the logical flow of information processing would be that the amygdala first detects these nonconscious fear representations and then relays this threat signal

to the ACC via the uncinate fasciculus. The existence of such forward projections is supported by anatomical studies in monkeys (Porrino et al., 1981; Amaral and Price, 1984). The ACC is thought to contain cognitive (dorsal) and affective (ventral) subdivisions (Bush et al., 2000), both of which appear to play a role in conflict monitoring and resolution (Botvinick et al., 1999; Etkin et al., 2006). We recently identified attention bias-related morphological variability in an ACC region at the conjunction of the traditional cognitive and emotion subdivisions (Carlson et al., 2012b). Greater attentional bias to threat was correlated with greater gray matter volume. Taken together, the data support the model purported by Mathews and Mackintosh (1998). Consistent with this model, we speculate that nonconscious threat-related information, detected in the amygdala, is relayed via the uncinate fasciculus to the ACC and during conditions of conflict (i.e., two facial expressions competing for attention), this threat signal "biases" the ACC to resolve conflict by favoring threat (at least for high bias individuals). Furthermore, it appears that for high bias individuals, the integrity of the fibers connecting the amygdala to the ACC are strengthened, which presumably results in a greater amygdala-driven threat bias.

There is increasing focus on cognitive processing biases, such as increased attention to threat, as causal factors in the development and maintenance of anxiety disorders (MacLeod et al., 2002). As such, attention bias modification

(ABM) was conceived as a treatment option where anxiety is alleviated through a training regimen that reduces an individual's attention bias to negative information. After a decade of ABM research, it appears that this treatment option has an efficacy comparable to selective serotonin reuptake inhibitors and cognitive behavioral therapy (Hakamata et al., 2010). Additional research suggests that training, on the order of hours to weeks, in both motor and cognitive domains leads to structural changes in gray and white matter observable in MRI (Scholz et al., 2009). Given the current results and earlier reports linking gray matter volume to attention bias behavior (Carlson et al., 2012b), one direction for future research would be to assess the impact of ABM treatment in reorganizing the amygdalo-prefrontal system. We hypothesize that greater treatment efficacy should coincide with a "reprogramming" of the underlying brain mechanisms. If this is true, structural biomarkers such as amygdala-prefrontal integrity may provide a definitive and stable measurement to tract the recovery of anxiety following ABM treatment. Although our initial evidence that neuroanatomical white matter structure correlates with attention bias to threat shows promise for measuring the efficacy of ABM treatment, further research is needed. As we did not screen participants for mental health status, it is particularly important that the relationship between attentional bias and amygdala-prefrontal integrity be studied in clinically anxious samples.

Attentional bias to threat is an important fear-related behavior that has been linked to increased anxiety (Fox, 2002; Mathews and MacLeod, 2002; Mogg and Bradley, 2002). However, fear and anxiety are not synonymous. Anxiety refers to a prolonged state of worry characterized by uncertainty in the risk assessment of potential (future) danger, while fear refers to a brief "fight or flight" response to a specific threat (Gray and McNaughton, 2000b; Sylvers et al., 2011). In Gray and McNaughton's (2000) model, anxiety arises from the activation of the septo-hippocampal "Behavioral Inhibition System" in conjunction with the amygdala threat response (**Figure 1.3**). With this distinction in mind, it is worth noting that previous DTI studies on trait or group level anxiety have produced mixed results in terms of the direction of the relationship (for review see Ayling et al., 2012b). Although a recent study with a large sample found that high trait anxious males have greater structural integrity of the left hemisphere uncinate fasciculus (Montag et al., 2012), a majority of studies (Kim and Whalen, 2009a; Pacheco et al., 2009b, a; Phan et al., 2009c; Phan et al., 2009b; McIntosh et al., 2012; Tromp et al., 2012b) have reported lower fiber integrity (e.g., fractional anisotropy) of the uncinate fasciculus for high anxious individuals (or those at genetic risk for anxiety; *5-HTTLPR* short allele). Given that anxiety is associated with the apprehension or worry about a potentially threatening future event, we would expect this response to be initiated by a top-down mechanism (i.e., prefrontal to amygdala). Alternatively, fear-responses such as increases in

attention to threat are immediate bottom-up stimulus driven events (i.e., amygdala to prefrontal). Thus, given that amygdalo-prefrontal communication is reciprocal (Porrino et al., 1981; Amaral and Price, 1984), it is likely that fear-related behaviors are linked to heightened "bottom-up" cognitive bias, whereas anxiety is linked to deficits in "top-down" signals. Additionally, question-answer type measures of anxiety, which are used in trait anxiety questionnaires and the structured clinical interview, are more likely to tap into reflective higher-order top down mechanisms. Regardless, it is likely that different aspects of fear and anxiety are differentially influenced by amygdala-prefrontal communication and it may therefore be more meaningful to relate variation in brain structure to specific symptom-relevant behavioral measures, rather than broadly defined traits or disorders. Thus, further DTI research on a variety of fear- and anxiety-related behaviors is needed to understand better how fiber integrity relates to different aspects of fear and anxiety.

Amygdala – Prefrontal Integrity and the BDNF Polymorphism

BDNF is associated with synaptic plasticity and Met/Met individuals are at increased risk for mood disorders (Martinowich and Lu, 2008; Montag et al., 2010b). Here, we extend these effects to attention bias to threat via uncinate fasciculus tract integrity. Our results complement earlier research suggesting that

Met+ individuals have a hyperactive amygdala response to emotional stimuli (Montag et al., 2008), especially in anxious individuals (Lau et al., 2010), and are more likely to display anxiety- and fear-related behaviors such as rumination (Hilt et al., 2007; Beevers et al., 2009) and the generalization of fear conditioning (Hajcak et al., 2009). Furthermore, our results add to a growing body of research linking variability in attentional bias to threat to an underlying genetic component (Beevers et al., 2007; Osinsky et al., 2008; Fox et al., 2009; Elam et al., 2010; Kwang et al., 2010; Perez-Edgar et al., 2010; Carlson et al., 2012a). Our results are particularly informative in that they suggest that the *BDNF* gene first influences the integrity of the uncinate fasciculus and this influence contributes to variability in one's allocation of attentional resources towards potential threats. Specifically we found the Met allele carriers have greater levels of uncinate fasciculus fractional anisotropy and axial diffusivity. In animal models, fractional anisotropy is an indicator of fiber integrity and degree of myelination (Le Bihan, 2003), while axial diffusivity is thought to measure axonal integrity (Song et al., 2003). Thus, if these models apply to the human brain, our results may suggest that the *BDNF* gene influences the mechanisms regulating the degree of myelination, axonal integrity, and general fiber integrity of the uncinate fasciculus, which ultimately contributes to variability in nonconscious attention bias across individuals.

Although BDNF is known to affect synaptic plasticity, it is still unclear how the *BDNF* Val66Met polymorphism influences white matter integrity in the human brain; neuroimaging literatures in this area have produced conflicting results. For example, in one study there was no association between the *BDNF* Val66Met polymorphism and white matter integrity (Montag et al., 2010a), while in other research the Met-*BDNF* genetic variant was linked to greater fiber integrity (e.g., increase fractional anisotropy or decreased radial diffusivity) in various major fibers, such as the cingulum bundle, inferior longitudinal fasciculus, inferior fronto-occipital fasciculus and uncinate fasciculus (Chiang et al., 2011; Voineskos et al., 2011; Tost et al., 2013). It should be noted that the majority of the fiber integrity research on the *BDNF* Val66Met polymorphism used voxel-wise approaches (except for Voineskos AN et al. 2011). While statistically stringent and suitable for exploratory analyses, this method may over look smaller, yet meaningful, effects. On the other hand, the present study focused on the global integrity of an *a priori* white matter pathway and revealed a localized effect of the *BDNF* Val66Met polymorphism on uncinate fasciculus fractional anisotropy and axial diffusivity. Thus, future hypothesis-driven research may benefit from similarly focused analyses. However, we should note that our sample was of mixed ethnicity (see Methods and Materials for details). Although ethnicity was not associated with attentional bias to threat or uncinate fasciculus integrity in our sample and prior work has shown that ethnicity does not influence

the relationship between BDNF and depression (Verhagen et al., 2010), future research should directly assess the effects of ethnicity on uncinate fasciculus integrity in a larger sample. Nevertheless, our results suggest that the *BDNF* genotype influences uncinate fasciculus fiber integrity, which is in turn linked to facilitated attention to nonconscious threat.

In conclusion, our results link individual differences in amygdalo-prefrontal white matter integrity to nonconscious attention bias to threat and the *BDNF* genotype. These results provide evidence for the notion that some individuals may be "hard-wired" to focus on the negative side of life.

CHAPTER III

(Modified from Carlson, Cha and Mujica-Parodi, *Cortex*, 2013)

Title: Functional and Structural Amygdala – Anterior Cingulate Connectivity Correlates with Attentional Bias to Masked Fearful faces

Authors: Joshua M. Carlson[1]*, Jiook Cha[2]*, and Lilianne R. Mujica-Parodi[1, 2]

Author Affiliations: 1. Department of Biomedical Engineering; 2. Program in Neuroscience, State University of New York at Stony Brook, Stony Brook, NY

*JMC & JC contributed equally to this work

Abstract

An attentional bias to threat is causally related to anxiety. Recent research links nonconscious attentional bias to threat with variability in the integrity of the amygdala – anterior cingulate pathway, which sheds light on the neuroanatomical basis for a behavioral precursor to anxiety. However, the extent to which structural variability in amygdala – anterior cingulate integrity relates to the *functional* connectivity within this pathway and how such functional connectivity may relate to attention bias behavior, remain critical missing pieces of the puzzle. In 15 individuals we measured the structural integrity of the amygdala – prefrontal pathway with diffusion tensor-weighted MRI, amygdala-seeded intrinsic functional connectivity to the anterior cingulate, and attentional bias toward backward masked fearful faces with a dot-probe task. We found that greater biases in attention to threat predicted greater levels of uncinate fasciculus integrity, greater positive amygdala – anterior cingulate functional connectivity, and greater amygdala coupling with a broader social perception network including the superior temporal sulcus, tempoparietal junction, and somatosensory cortex. Additionally, greater levels of uncinate fasciculus integrity correlated with greater levels of amygdala – anterior cingulate intrinsic functional connectivity. Thus, high bias individuals displayed a heightened degree of amygdala – anterior cingulate connectivity during basal conditions, which we believe predisposes

these individuals to focus their attention on signals of threat within their environment.

Introduction

Stimuli that signal the existence of potential threat are afforded greater attentional resources (Ohman et al., 2001). This attentional bias to threat is exaggerated in individuals with heightened anxiety (MacLeod and Mathews, 1988), even when awareness is restricted by backward masking and threat is preattentively processed (Fox, 2002; Mogg and Bradley, 2002). Furthermore, individual differences in preattentive attentional bias to threat predict cortisol reactivity to stress (Fox et al., 2010). Critically, an attentional bias to threat is not only correlated with anxiety, but appears to play a causal role in the development of anxious symptoms (Mathews and MacLeod, 2002). Thus, understanding the underlying neural correlates of individual variability in attentional bias to threat has important implications for the understanding of stress and anxiety.

Neuroimaging research has linked the facilitation of spatial attention by backward masked threats to elevated BOLD activity in an amygdala, ACC, posterior superior temporal sulcus (pSTS), and visual cortex network (Carlson et al., 2009b). Within this network, the amygdala appears to automatically detect crude preattentive representations of threat vs. non-threat information (Morris et al., 1998; Whalen et al., 1998; Morris et al., 2001), while the ACC appears to be involved in monitoring and resolving potential emotional conflicts (Etkin et al., 2006). The end product is a rapid prioritization of visual cortical processing

within the retinotopic location of potential threat (Carlson and Reinke, 2010; Carlson et al., 2011a). Anatomically, attentional bias to preattentive threat is predictive of greater ACC gray matter volume (Carlson et al., 2012b) and greater fiber integrity within the uncinate fasciculus amygdala – ACC white matter pathway(Carlson et al., 2013b). Given these anatomical associations, high bias individuals should display a heightened degree of amygdala – ACC intrinsic functional connectivity, which ultimately predisposes these individuals to focus their attention on signals of environmental threat. However, the extent to which variability in amygdala – ACC structural integrity relates to variability in the functional integrity of this network as it relates to attentional bias to masked threat is unclear.

Here, we measured the structural integrity of the uncinate fasciculus with diffusion tensor-weighted MRI, amygdala-seeded intrinsic or resting-state functional connectivity with the ACC, and measured attentional bias with a backward masked fearful face dot-probe task. We hypothesized that greater biases in attention to backward masked threats would predict (1) greater levels of uncinate fasciculus fiber integrity, (2) greater positive amygdala – ACC intrinsic functional connectivity, and (3) greater levels of uncinate fasciculus integrity would correlate with greater levels of amygdala – ACC intrinsic functional connectivity.

Methods

Participants

Fifteen consenting young adults (6 male) between the ages of 19 and 23 (M = 20.80, SD = 1.21) participated in this study. All individuals reported being right handed. The Institutional Review Board of Stony Brook University approved this study and participants were compensated for their time ($70.00).

Task

The task used here has been described in detail in earlier publications (Carlson and Reinke, 2008; Carlson et al., 2012b; Carlson et al., 2012a). Behavioral data were collected outside of the scanner. Briefly, trials started with a central fixation cue (+; 1000 msec) followed by face stimuli (5 × 7° of visual angle) simultaneously presented to the left and right of fixation (separated by 14°). Initial faces were displayed for 33 msec and then were masked (100 msec). A target dot appeared either on the left or on the right and remained until the participant responded. Trials used to calculate attention bias scores contained one fearful and one neutral face. There were 40 congruent (target dot presented on the same side as the fearful face) and 40 incongruent (target dot presented on the same side as the neutral face) trials. Attention bias scores are calculated as

congruent – incongruent reaction times (on correct trials with reaction times between 150-750ms). Participants used an E-Prime response box with their right hand to indicate the location of the dot. The task also contained 40 neutral-neutral trials.

Participants then completed a task to assess awareness of the masked faces. This task was identical to the dot-probe task in all aspects through the backward masking procedure. After the masking procedure, participants were asked to indicate with the response box whether they saw: a fearful face on the left, a fearful face on the right, or two neutral faces. There were 60 randomly presented trials.

Functional Magnetic Resonance Imaging

After completing the behavioral task, five minutes long "resting-state" (eyes closed) fMRI data was collected. A 3-T Siemens Trio whole body scanner was used to acquire 150 T2*-weighted whole-brain volumes with an EPI sequence sensitive to BOLD signal using the following parameters: TR = 2000 msec, TE = 23 msec, Flip Angle = 83°, Matrix Dimensions = 96 × 96, FOV = 224 × 224 mm, Slices = 35, Slice Thickness = 4 mm, Gap = 0. Standard preprocessing procedures were performed in SPM8, including image realignment, slice timing correction, normalization to standard MNI space, and spatial smoothing with a

Gaussian full-width-at-half-maximum 6 mm filter. Preprocessed images were filtered between 0.01 Hz and 0.1 Hz in the Functional Connectivity Toolbox v13 (Whitfield-Gabrieli et al., 2011), and entered in a first-level General Linear Model regressing out time courses from principle components associated with white matter and cerebrospinal fluid. Based on earlier work implicating the left amygdala in attentional bias to threat, a left amygdala seed mask for the functional connectivity analyses was derived from the Harvard-Oxford subcortical structural atlas (www.fmrib.ox.ac.uk/fsl/fslview/). This 1st-level analysis yielded a left amygdala seeded intrinsic functional connectivity map for each individual. We constructed a second-level model in SPM with attention bias scores as a regressor of interest. For our *a priori* target region, we derived ACC masks for each hemisphere. Our ROI analyses were family-wise error (FWE) small volume corrected (SVC) for 6 mm radius-spheres at ±4, 46, -4 (coordinates from which ACC BOLD activity showed significant association with attention-related amygdala activity in an earlier study; Carlson et al., 2009). For the completeness, we did the same analysis on right amygdala-seeded connectivity maps.

Diffusion Tensor Imaging

Diffusion Tensor Images were collected after fMRI acquisition using the following parameters: TR = 5500 ms, TE = 93 ms, FOV = 220 × 220 mm, Matrix

= 120 × 220 × 220, Voxel size = 1.7 × 1.7 × 3.0 mm, EPI factor = 128, slices = 40, slice thickness 3 mm, Bandwidth 1396 Hz/pixel, GRAPPA acceleration factor = 2. The series contained two initial images without diffusion weighting and with diffusion weighting along 40 non-collinear directions (b = 800 sm^{-2}).

We employed standard DTI preprocessing steps in FSL 4.1.9 (FMRIB Software Library; www.fmrib.ox.ac.uk/fsl) to correct for eddy current distortions and head motion. We then fitted a diffusion tensor model at each voxel by running the DTIFIT function in FSL. This yielded individual fractional anisotropy images, which we used for voxel-wise statistical analysis using Tract-Based Spatial Statistics (TBSS), part of FSL (Smith et al., 2006). TBSS projects all subjects' FA data onto a mean FA tract skeleton, before applying voxel-wise cross-subject statistics. We conducted a correlation test between FA voxels and attention bias scores, using Randomise 2.9 in FSL, which, unlike the earlier version, corrects for inflated significance in small samples. We focused our analysis on the uncinate fasciculus, based on our previous work (Carlson et al., 2013b); the mean FA skeleton within the JHU white matter pathway atlas (http://fsl.fmrib.ox.ac.uk/fsl/fslview/) was assessed in each hemisphere separately. Results were FWE corrected, applying TFCE (Threshold-Free Cluster Enhancement) option in Randomise. For better visibility, significant skeletonized FA voxels were flattened using 'tbss_fill' in FSL. We extracted mean FA values

from the significant clusters, and correlated with significant clusters of amygdala – ACC functional connectivity.

Results

Overall, participants displayed an attentional bias to threat (mean difference = –10.31 msec, *SD* =12.99, $t_{14} = -3.08$, $p_{one\text{-}tailed} = .004$). However, participants' performance on the post-task assessment of awareness was above chance ($t_{14} = 2.54$, $p_{one\text{-}tailed} = .01$). Therefore, as suggested in the literature (Wiens, 2006), participants' level of awareness was controlled for in subsequent analyses. Level of awareness did not significantly correlate with task performance ($r = .30$, $p = .28$), but the direction of this correlation would suggest that as awareness of threat increases attentional bias to threat decreases (i.e., our results cannot be attributed to an attentional bias to consciously detected threat). Nevertheless, in the current study, we do not claim that backward masking resulted in nonconscious processing per se, but rather a restricted level of automatic preattentive processing that may be at a peri-threshold level of conscious processing in some individuals.

We first tested whether the fiber integrity of the uncinate fasciculus was correlated with attentional bias to masked threat. Within the uncinate fasciculus, we found a correlated cluster within the left hemisphere tract proximal to the

ACC (MNI -25, 25, 14; **Figure 3.1**) at corrected $p_{roi} < 0.05$ (Tract Based Spatial Statistics; TBSS). In the right hemisphere tract this association was weaker and not significant at a corrected level ($p_{roi} > 0.16$; TBSS, $p_{uncorrected} = 0.02$). This association was specific to the left uncinate fasciculus as whole brain white matter (i.e., average FA values) did not correlate with attention bias scores ($p > 0.44$). We performed a follow-up analysis using average values extracted from the significant cluster in the left uncinate fasciculus. This revealed the effect remained significant when controlling for age (Pfefferbaum et al., 2000) and awareness (Wiens, 2006), $r_{partial} = -.84$, $p < .001$.

We then assessed the degree to which intrinsic functional coupling between the amygdala and ACC was correlated with attentional bias to threat. As displayed in **Figure 3.1b**, left amygdala – ACC intrinsic functional connectivity from resting-state fMRI was correlated with attentional bias to masked threat, maximum voxel (MNI 8, 46, 4,): $t_{14} = 5.16$, $p_{svc} < .05$, $r = -.69$, $p_{one\text{-}tailed} = .002$ and $r_{partial} = -.72$; $p_{one\text{-}tailed} = .003$ when controlling for age (Pfefferbaum et al., 2000) and awareness (Wiens, 2006). Of note, the mean coupling coefficient of this ACC cluster was not significantly different from zero (t = -0.54, $P = 0.60$; minimum, -0.44; maximum, 0.24). As presented in **Table 3.1**, additional whole brain targets of intrinsic left amygdala connectivity correlating with attention bias scores included areas of the occipital cortex, posterior insula, posterior superior temporal sulcus (pSTS),

tempoparietal junction (TPJ), and somatosensory cortex (SS). Correlations with attention bias on right amygdala – ACC connectivity maps were not significant at a corrected level (Peak $p_{svc} > 0.38$, $p_{uncorrected} = 0.01$). Finally, we explored the relationship between structural and functional measures of amygdala – ACC connectivity. As can be seen in **Figure 3.1**, the mean FA values of the uncinate fasciculus cluster was significantly correlated with the mean value of the functional connectivity cluster, $r = 0.47$, $p_{one\text{-}tailed} = 0.039$.

Table 3.1. Amygdala seeded connectivity correlations with attention bias scores

		MNI Coordinates				
Region	**Hemi**	**x**	**y**	**z**	**Voxels**	***t***
Ventral Anterior Cingulate	R	8	46	4	30 *	5.16
Dorsal Anterior Cingulate	L	-10	24	38	11	5.00
	R	2	28	18	11	4.75
Posterior Insula	L	-48	-14	-4	30	5.23
	R	40	-22	0	38	8.31
Postcentral Gyrus/Somatosensory Cortex	L	-48	-30	58	33	5.21
	R	34	-32	52	62	6.81
	R	20	-42	42	22	6.14
	R	38	-46	66	22	4.98
Tempoparietal Junction	L	-66	-26	10	11	5.01
	R	54	-14	2	10	4.59
	R	66	-16	6	15	4.49
Posterior Superior Temporal Sulcus	R	66	-40	4	13	4.18
Occipito-Temporal Cortex	R	58	-58	-6	18	4.98
Cuneus/Lingual Gyrus	R	2	-66	20	12	5.14

Reported activations were significant at $p < 0.001$ uncorrected, Cluster extent 10 voxels; *$p < 0.01$, result significant at $p_{svc} < 0.01$ (6mm sphere radius applied)

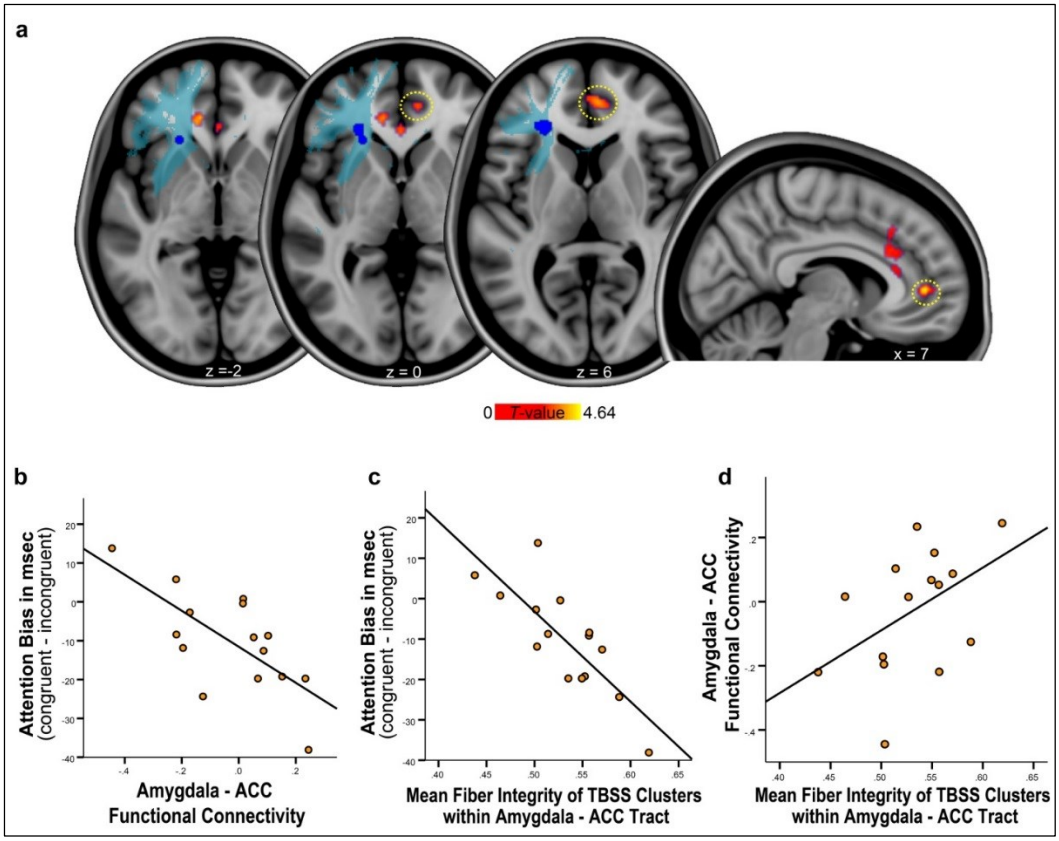

Figure 3.1. Functional and structural amygdala-prefrontal connectivity and 3-way relationship with negative attention bias. For visualization purposes, activation within the ACC is displayed at $p < .05$. **(a)** Areas within ACC (yellow-red) in which intrinsic functional connectivity with the left amygdala correlated with attentional bias to threat. These areas bordered the clusters (dark blue) within the uncinate fasciculus (light blue; JHU white matter atlas), whose FA values predicted attention bias. The FA results were flattened for better visibility. Scatter plots of correlations between attentional bias to masked threat and amygdala – perigenual ACC **(b)** structural integrity and **(c)** intrinsic functional connectivity (from cluster circled in yellow) in addition to the relationship between **(d)** amygdala –ACC structural and functional connectivity.

Discussion

In this study, we linked individual differences in attentional bias to threat to intrinsic connectivity of the amygdala – ACC. High bias individuals displayed greater intrinsic functional coupling, while low bias individuals displayed diminished coupling. Additionally, we confirmed earlier work showing that the structural integrity of this pathway is correlated with greater biases in attention to nonconscious threat (Carlson et al., 2013b). Furthermore, consistent with prior work on the relation between brain structure and function (e.g., the default mode network; Greicius et al., 2009), we demonstrate that variability in intrinsic functional coupling of the amygdala – ACC accounts for the structural integrity of the uncinate fasciculus, more specifically, the prefrontal vicinity.

The current results add to a growing body of work implicating the amygdala – ACC system in attention bias behavior (Armony and Dolan, 2002; Carlson et al., 2009b; Carlson et al., 2012b; Carlson et al., 2013b). Cognitive processing biases are thought to manifest when multiple stimulus representations compete for attention (Mathews and MacLeod, 2002). Within this framework, the ACC monitors and resolves potential conflicts (Botvinick et al., 1999; Etkin et al., 2006), while the amygdala appraises environmental stimuli for their threat potential (Adolphs et al., 1999) and "biases" the monitoring system to favor stimuli with a high potential for threat. On the other hand, negative affect (e.g.,

negative word in a Stroop task) is known to elicit an increase in the amygdala – rACC correlation in an fMRI study (Mohanty et al., 2007). Of note, in the same study, Mohanty et al. report functional differentiation of dorsal and rostral ACC in cognitive and emotion processing (Mohanty et al., 2007); however, we did not find such a differentiation in our functional coupling measures along the dorsal/rostral ACC. It is probably because our measure is from task-free resting-state fMRI. A robust paradigm may be thus required to show different connection properties, that is, positive or negative correlation elicited by a given condition. Our results therefore provide evidence that greater amygdala – ACC functional connectivity under basal conditions correlates with attentional bias to masked threat, which may predispose high bias individuals to focus on threat.

Beyond amygdala – ACC intrinsic coupling, we found that high bias individuals also display heightened intrinsic functional connectivity between the amygdala and social perception/cognition-related areas such as the TPJ, pSTS, and SS cortex. Respectively, these regions have been shown to be involved in processing others' intentions/thoughts (Saxe and Kanwisher, 2003), dynamic aspects of face perception, such as eye gaze direction and expression (Puce et al., 1998; Haxby et al., 2000; Hoffman and Haxby, 2000), in addition to the recognition of others' affective states (presumabley through simulation; Adolphs et al., 2000). Amygdala – pSTS coupling has previously been linked to

nonconscious fearful face processing (Jiang and He, 2006) and attentional responses to such faces (Carlson et al., 2009b). Other visual areas such as the cuneus/lingual gyrus and occipitotemporal cortex displayed heightened intrinsic connectivity with the amygdala in high bias individuals. Thus, the amygdala appears to be broadly connected with visual processing cortical regions including those associated with social perception, which may be linked to preattentive perceptions of others' affective states and intentions, in high bias individuals. It is unclear if this facilitation of social perceptual regions is specific to the social stimuli used in this task (i.e., fearful faces) or if this network is more broadly engaged in threat- or salience-elicited attention. Further research will be needed to address the specificity of this network and to further dissect the attentional response to threat in order to identify the specific roles that each structure plays in mediating this behavior. In particular, it is unclear exactly how activity in the amygdala – ACC system translates into facilitated visual perceptual processing in the context of attentional bias to threat. Previous research suggests that the amygdala has direct projections back to areas of visual cortex (Adolphs, 2004). Additional research suggests that the amygdala projects to the diffuse modulatory centers including the acetylcholine producing cells in the nucleus basalis, which has been implicated in animal models of emotional attention (Holland and Gallagher, 1999) and the gray matter near this region correlates with attention bias to threat (Carlson et al., 2012b). Prior research has shown that the attentional

response to visual threat facilitates visual cortical activity (Pourtois et al., 2004; Pourtois et al., 2006; Carlson and Reinke, 2010; Carlson et al., 2011a) and the preferential processing of emotional stimuli in visual cortex has been shown to be amygdala-dependent (Vuilleumier et al., 2004). Yet, the exact route in which the amygdala – ACC system facilitates visual cortical processing remains unclear. Of note, it is methodologically challenging to map a functional organization of the paralimbic system modulating visual system; fMRI does not have a fine temporal resolution disambiguate the mili-second scale processes and EEG/MEG may not have an access to amygdala reactivity.

It is worth noting that the group mean value of the amygdala – ACC functional coupling did not significantly deviate from zero. However, this may not lead to a null effect of this coupling. Rather, given the correlation results that this measure indeed accounts for individual variability of fiber integrity and the negative attention behavior alike, we interpret that our subject samples may display a significant cross-subject variance. Future research on larger samples may disambiguate this and provide a more accurate account on the amygdala – ACC connectivity.

CHAPTER IV

(in revision in the Journal of Neuroscience)

Title: Circuit-wide structural and functional measures predict ventromedial prefrontal fear generalization: implications for generalized anxiety disorder

Author: Jiook Cha[1], Tsafrir Greenberg[2], Joshua M. Carlson[3,4], Daniel J. DeDora[3], Greg Hajcak[2], Lilianne R. Mujica-Parodi[1,3]*

Author Affiliations: 1. Program in Neuroscience; 2. Department of Psychology; 3. Department of Biomedical Engineering, Stony Brook University, Stony Brook, NY, 11794; 4. Department of Psychology, Northern Michigan University, Marquette, MI 49855.

*Corresponding author

Abstract

The ventromedial prefrontal cortex (vmPFC) plays a critical role in a number of evaluative processes, including risk assessment. Impaired discrimination between threat and safety is considered a hallmark of clinical anxiety. Here, we investigated the circuit-wide structural and functional mechanisms underlying faulty vmPFC threat assessment in humans. Patients with generalized anxiety disorder (n=32, female) and healthy individuals (n=25, age-matched female) were tested on a task that assessed the generalization of conditioned threat during fMRI scanning. Using structural, functional (i.e., resting-state) and diffusion MRI, we assayed vmPFC thickness as well as structural and functional connectivity with corticolimbic systems. We first demonstrate that all three factors predict individual variability of vmPFC threat assessment. Then, using structural equation modeling, we show that vmPFC fear generalization mediates the impact of these factors onto generalized anxiety disorder. Together, our findings support a multivariate—and therefore "multi-hit"—etiological model of psychopathology.

Introduction

Anxiety disorders are the most widespread class of psychiatric disorders, with a lifetime prevalence of 28.8% (Kessler et al., 2005)., Previous research has linked various fear learning processes to anxiety, including fear generalization (Kheirbek et al., 2012; Lissek, 2012) and impaired regulation of conditioned fear, extinction learning and learning recall (for review, see (Milad and Quirk, 2012). The ventromedial prefrontal cortex (vmPFC) is frequently implicated in impaired fear learning in anxiety disorder (Milad and Rauch, 2007). Indeed, an indiscriminating vmPFC response to a continuum of threat and safety signals appears to be associated with pathological anxiety (Greenberg et al., 2013a).

A recent conceptualization emphasizes that the vmPFC integrates cognitive and affective processes via an extensive convergence of cortical and subcortical afferents in computing affective value and mediating adaptive behavior (Roy et al., 2012). During threat processing, in particular, the vmPFC interacts with the corticolimbic system to mediate a number of coordinated responses including the prefrontal attentional network (Bishop et al., 2004; Hare et al., 2009), the hippocampus/parahippocampal gyrus (Kalisch et al., 2006; Milad et al., 2007a; Sierra-Mercado et al., 2011) and the thalamus for fear learning (Mitchell and Gaffan, 2008; Cross et al., 2012; Parnaudeau et al., 2013), and the amygdala for regulating the fear response (Phelps et al., 2004; Sierra-Mercado et al.,

2011). VmPFC function thus appears to depend upon the dynamics of a larger circuit.

Anatomical studies provide further support for the integrative role of the vmPFC (Price, 2007; Lehman et al., 2011). VmPFC morphometric variability, measured via thickness appears to contribute to vmPFC function. Previous research reports that individuals with a thicker vmPFC show a better fear extinction performance indexed by physiological responses (Milad et al., 2005; Hartley et al., 2011); however, a direct link between vmPFC thickness and threat-processing function has yet to be investigated.

Based on this literature, we hypothesize that an individual's efficiency of vmPFC threat processing is explained by the size of the vmPFC and the vmPFC circuit-wide connectivity pattern between the vmPFC and the corticolimbic system. To that end, we tested patients with Generalized Anxiety Disorder (GAD) and healthy controls on a task that assessed fear generalization in response to cues, which varied in perceptual similarity to an electric shock conditioned stimulus during fMRI scanning. We investigated vmPFC thickness, structural and functional connectivity with corticolimbic systems, using structural MRI, diffusion weighted imaging–tractography and resting-state functional connectivity mapping. We found, first, that individual differences of vmPFC threat assessment that distinguishes patients with clinical anxiety and healthy controls are associated

with the circuit-wide neural features and, second, that this effect mediates the influence of the neural factors onto generalization anxiety disorder. Our results may support a multivariate etiological model of psychopathology.

Methods

Participants.

Fifty-seven participants [all female, age-matched (mean = 22.3 ± 4.5 years)] were recruited from Stony Brook, NY, USA. This study was approved by the Stony Brook University IRB; all subjects provided written informed consent. To reflect the higher prevalence of anxiety disorders in females and to minimize sample heterogeneity, we included only females in the study. Psychiatric diagnoses were based on DSM-IV, through both an informal clinical interview and structured clinical interview for DSM-IV Axis I Disorders; this procedure confirmed the diagnoses of generalized anxiety disorder (GAD) in the patient group (n=32) and absence of Axis I diagnoses in the control group (n = 25). Of the 32 patients, 17 had comorbid major depressive disorder (MDD). All controls were free of any current or past psychiatric conditions. To avoid medication-related confounds, patients were free from psychiatric medication for at least six months before the time of the experiment. All 57 participations underwent four

MR scans: fMRI during the fear generalization task, resting-state, diffusion, and structural MRI.

Study Design.

The fear generalization task consisted of (i) pre-scan fear conditioning with electric shock, followed by (ii) the fear generalization fMRI phase (Greenberg et al., 2013b). Prior to the fear conditioning phase, we adjusted amplitudes of the electric shock (mA) to a level that was "uncomfortable but not painful" for each subject. We then instructed participants that only one of the visual stimuli (i.e., a mid-sized red rectangle) would be paired with the shock at 50% chance during the generalization task. We administered the conditioning phase when the participants were positioned in a scanner. Cues were presented for 2000ms. A mid-sized red rectangle paired with 500ms-long electric shock (CS, conditioned stimulus; delivered 1500ms after the cue onset) was presented five times, and six rectangles with varying widths (GS, generalization stimuli: ± 20%, ± 40%, and ± 60%) were each presented, without shock, once in a pseudo-random order (**Figure 4.1A**). Trials were separated by jittered fixation screens. The generalization fMRI phase was initiated immediately following the conditioning.

The generalization task was composed of three blocks. Each block consisted of 40 trials (5 trials x 8 conditions; 6 GS, CS paired with shock, CS

unpaired with shock) for 120 trials. We pseudo-randomly presented seven red rectangles with an identical height (56 pixels) and varying widths (280 pixels for CS; ± 20%, ± 40%, and ± 60% for GS) for 2000ms on a black background. Stimuli were flanked with inter-stimulus intervals ranging from 4 to 10s with a white fixation crosshair on a black background. In addition, we collected post-task ratings of shock-likelihood for each rectangle, rated on a Likert-type scale of one (certainly not shocked) to five (certainly shocked). The duration of the task was 15 minutes and 12s.

Resting state fMRI was collected in a separate session. Participants were instructed to view a white fixation crosshair centrally presented on black background for 5 minutes.

MRI Data Acquisition.

Participants were scanned with a 3T Siemens Trio scanner at the Stony Brook University Social, Cognitive and Affective Neuroscience center. We acquired 440 T_2*-weighted echo planar images, for the fear generalization task, and 143 T_2*-weighted echo planar images for the resting-state task. These were acquired with an oblique coronal angle and TR = 2100ms, TE = 23ms, flip angle = 83º, matrix = 96 × 96, FOV = 224 × 224mm, slices = 37, and slice thickness = 3.5mm. For structural scans, T_1-weighted images were acquired with the

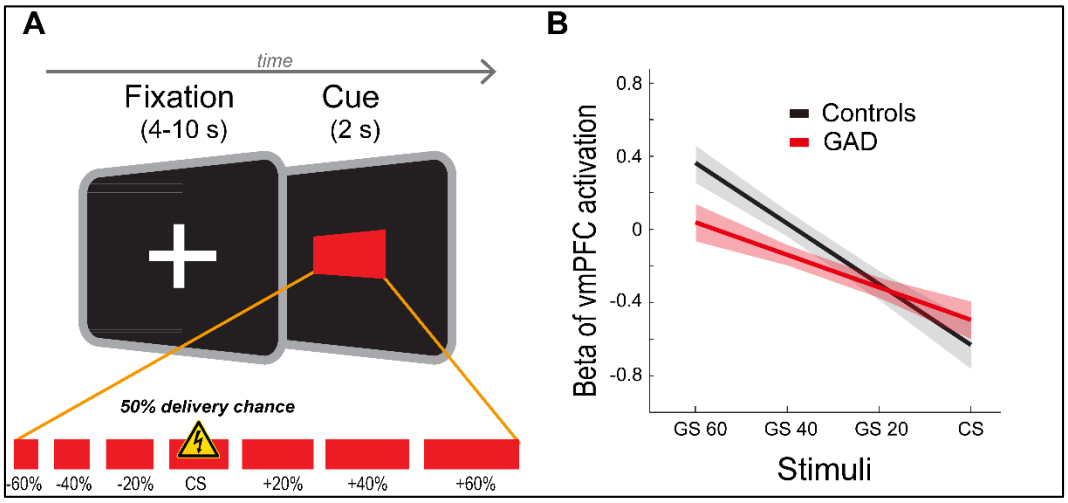

Figure 4.1. Fear generalization paradigm and threat overgeneralization of the ventromedial prefrontal cortex in anxiety disorder. ***A,*** Fear generalization paradigm. Red rectangle stimuli with systematic length variation of ±60, ±40, ±20% from conditioned stimulus (CS) were used as generalization stimuli (GS). ***B,*** Group differences in the vmPFC activity gradient across stimuli. Patients showed less discriminating vmPFC activity revealed by a decrease in the slope of the linear fit. This data has been previously reported (Greenberg et al., 2013a) and the slope of the linear fit was used to index vmPFC functioning during the fear generalization task in this study. Shaded areas represent a SE. GAD, Generalized Anxiety Disorder.

following parameters: TR = 1900 ms, TE = 2.53, flip angle = 9°, FOV = 176 × 250 × 250 mm, matrix = 176 × 256 × 256, and voxel size = 1 × 0.98 × 0.98 mm. Diffusion and resting-state fMRI were collected in separate sessions. We collected dMRI using the following parameters: TR = 5500 ms, TE = 93 ms, FOV = 220 × 220 mm, matrix = 120 × 220 × 220, voxel size = 1.7 × 1.7 × 3.0 mm, EPI factor = 128, slices = 40, slice thickness = 3 mm, bandwidth = 1396 Hz/pixel, GRAPPA acceleration factor = 2. The series included two initial images acquired without diffusion weighting and with diffusion weighting along 40 non-collinear directions (b = 800 sm^{-2}). Five minutes resting-state fMRI, consisting of 143 volumes, was collected using the same scanning parameters as the fear generalization task.

Functional MRI analyses: Generalization Task.

The fear generalization data used in this work were identical to that of our previous report (Greenberg et al., 2013a). Specifically, we used the same measure as Greenberg et al. to index vmPFC function - the slope of linear fit of the vmPFC BOLD activity gradient across each stimuli (**Figure 4.1B**). This provides an easily interpretable index on the generalization effect, and best predicts clinical anxiety (**Table 4.1**).

We performed standard preprocessing procedures, including motion correction, normalization, and smoothing with a 6-mm Gaussian kernel in SPM 8 (www.fil.ion.ucl.ac.uk/spm). For the first level model, we entered five regressors, i.e., onsets of GS ±60%, GS ±40%, GS ±20%, CS with shocks, CS without shocks and six motion parameters. Serial autocorrelations were modeled using an AR (1) process, and canonical HRF was used for the basis function in model estimation. For the fear generalization gradient in the vmPFC, we first tested if the vmPFC showed significant activation across the stimuli, by conducting a region of interest (ROI) analysis for effects of interest at corrected $P < 0.05$. We then extracted the first eigenvariate within a 6 mm-radius sphere centered on the local maxima ($P < 0.05$, FWE corrected) for each of the "CS (unpaired with shock) - Baseline", "GS 20% - Baseline", "GS 40% - Baseline" and "GS 60% - Baseline" contrasts across all participants. Mean values for each of the four contrasts were plotted as a 4-point gradient. We calculated a slope of a linear fit of these values in each participant.

Functional MRI: Resting-State Intrinsic Functional Connectivity.

We conducted resting-state functional connectivity analyses using the Functional Connectivity Toolbox (http://www.nitrc.org/projects/conn/). This approach utilizes a robust correction method for non-neural noise correlations to

minimize spurious negative correlations often resulting from regressing out a global signal (Behzadi et al., 2007). We applied standard preprocessing procedures in SPM 8, including realignment, smoothing with a 6-mm FWHM, and normalization. Preprocessed images were filtered between 0.01 Hz and 0.1 Hz. After preprocessing, correlation analyses were performed between mean time-series of the vmPFC mask and voxel-wise time-series across the whole brain, in a subject level (i.e., 1st level analysis). The vmPFC mask was derived from the fear generalization result - a 6 mm-radius sphere centered on the group maxima in effects of interest. The vmPFC-seeded correlation maps (i.e., Fisher-transformed Pearson's correlation coefficients) were entered into a second level random effect model. To examine the association between functional coupling and the vmPFC fear generalization gradient, we entered mean-centered (by each group) vmPFC fear generalization gradients, that is, slopes of linear fit, as a covariate, and group as a between-subject factor.

We investigated correlational effects in several ROIs. Bilateral ROI masks were derived from the AAL atlas (http://www.sph.sc.edu/comd/rorden/template.html). Based on the well-established corticolimbic fear circuit, we chose the following subcortical ROIs: the amygdala (Phelps et al., 2004; Sierra-Mercado et al., 2011), hippocampus/parahippocampal gyrus (Kalisch et al., 2006; Milad et al., 2007a;

Sierra-Mercado et al., 2011), thalamus (Mitchell and Gaffan, 2008; Cross et al., 2012; Parnaudeau et al., 2013) and the following cortical ROIs: the PFC (Bishop et al., 2004; Hare et al., 2009). For exploratory purposes, we examined the pallidal and striatal regions, in which no significant associations were found. We divided the PFC mask into two subregions - dorsal (middle frontal gyrus), and ventral (inferior frontal gyrus). In each ROI, we identified significant clusters at corrected alpha of 0.05 using AFNI's 3dClustSim (http://afni.nimh.nih.gov/pub/dist/doc/program_help/3dClustSim.html); we estimated ROI-specific minimum cluster sizes with a peak *P* threshold of 0.005, which correspond to an alpha of at least 0.05, using Monte Carlo simulations with 10,000 iterations. As vmPFC seeded amygdala connectivity failed to reach a significance of $P < 0.05$, we alternatively conducted an amygdala-seeded connectivity analysis; given the well-established importance of the vmPFC-amygdala connectivity in fear conditioning (Phelps et al., 2004; Price, 2007; Hartley et al., 2011; Milad and Quirk, 2012; Roy et al., 2012; Sotres-Bayon et al., 2012), this approach was deemed justified. We used separate masks for the left and right amygdala, based on lateralization of amygdalar responses (Baas et al., 2004). For this analysis, we used the SPM small-volume correction with a 6mm-radius sphere search limit centered on the *a priori* coordinates of the vmPFC (MNI ±4, 40, -20), which was based on group maxima for the F-contrast of effects-of-interest during the fear generalization fMRI task. For scatter plots and post-hoc

correlation analyses, we extracted coefficients in each ROI by applying a 6 mm-radius sphere centered on the peak coordinates.

Structural MRI Analyses: Cortical Thickness.

We performed cortical parcellation and morphometric analyses using Freesurfer (http://surfer.nmr.mgh.harvard.edu/). This automated analysis pipeline includes segmentation, tessellation, and topological correction of the reconstructed surface. After the surface reconstruction, mean vmPFC thickness values were measured in each hemisphere according to the Desikan-Killiany cortical atlas in Freesurfer. An atlas for the medial orbital frontal cortex was used, which was overlapped with the *a priori* coordinate of vmPFC fear generalization gradient.

For a vertex-wise analysis, the individual data were smoothed with 10 mm full width at half-maximum kernel. We used a general linear model to examine the relationship between the thickness and the vmPFC fear generalization gradient, using the mean-centered (by group) vmPFC fear generalization gradients as a covariate, and group as a between-subject factor.

Diffusion Magnetic Resonance Imaging: Probabilistic Tractography and Tract-Based Spatial Statistics.

We used diffusion MRI (dMRI) to evaluate the structural connectivity between the vmPFC and the fear circuit, including the anterior thalamic radiation (ATR), the cingulum cingulate gyrus (CCG) and the uncinate fasciculus (UF). We first stripped the skull in the diffusion-weighted images and performed eddy-current and head motion correction by registering them to reference volumes, which are standard dMRI preprocessing steps as implemented in the FSL package (www.fmrib.ox.ac.uk/fsl). Fractional anisotropy (FA) values were calculated for each voxel by fitting a tensor model in FSL.

We employed a global tractography approach, TRACULA (Yendiki et al., 2011a), to reconstruct the entirety of our *a priori* white matter tracts. This approach has several advantages: (i) it eschews local uncertainty issues due to noise or partial volume effects that may deviate tracts in step-by-step local tractography, (ii) it increases sensitivity and robustness of the results by informing the tractography algorithms of surrounding anatomy of a given tract, and (iii) it minimizes biases caused by the need for manual intervention, as is the case for the local tractography (i.e., drawing ROIs or setting up an arbitrary threshold for angle or length). This approach is particularly suited to the current study in that it provides a useful single variable (i.e., mean FA) per subject and per tract, which

can be used in a multiple regression model with other neural indices. The tractography algorithms are described in detail in the original report (Yendiki et al., 2011a). We performed this global tractography procedure for all participants, and visually inspected the reconstructed tracts. For four participants who showed unsuccessful tracts, we ran the procedure again with new initialization points for the MCMC algorithm for each tract. We then extracted mean FA from the estimated posterior distribution map of the tracts of interest.

To complement this tract-wise approach, we conducted voxel-wise analyses on FA maps using Tract-Based Spatial Statistics (TBSS) as a part of the FSL package. We aligned FA images into a standard MNI space using nonlinear registration in FSL. A mean FA image was created and thinned to create an FA skeleton representing centers of all tracts common to the group. We then projected each aligned FA image onto this skeleton. We determined the effects of group, the vmPFC fear generalization gradient (fear generalization gradient), and the group × fear generalization gradient interaction on FA maps, while including age and total white matter volume as regressors of no interest by means of randomization method (10,000 permutations). We used a combination of threshold-free cluster enhancement and family wise error method to correct for multiple comparisons (corrected $P < 0.05$).

Correlation and Regression.

To evaluate correlations between the fear generalization gradient and the neural features, we conducted Pearson's partial correlation analyses, controlling for effects of group and age. Intracranial volume was included as an additional covariate for the vmPFC thickness analyses. We diagnosed outliers at a threshold of Cook's distance of one. Additionally, we performed robust linear regression analyses: models included fear generalization gradient as the dependent variable, group and each neural feature as the independent variables; and age, intracranial volume (in case of thickness) and whole brain FA (in case of FA) as confounding variables. We examined the impact of clinical anxiety on FA values using a general linear model where group was entered as factor, while age and whole brain FA were entered as covariates. We included depressive symptom scales to account for confounding of depression levels across the entire patient group (Mood and Anxiety Symptom Questionnaire: general distress depression and anhedonic depression; (Clark and Watson, 1991).

For the hierarchical regression model, we extracted the coupling estimates from the resting-state fMRI analyses from all the voxels within a 6 mm-radius sphere centered on group maximum in each ROI. We examined whether this statistically non-independent approach, i.e., selecting a peak voxel in each subject based on the all-subjects group results, causes a bias in the result (Kriegeskorte et

al., 2009). We first re-ran group correlation analyses using a leave-one-out (LOO) method and extracted peak voxel coordinates within the anatomical ROIs iteratively. We then calculated Euclidian distances in each ROI between a peak voxel of the LOO models and the all-subjects model iteratively. As a result, mean distances for the IFG were 2.0 ± 0.37 (SE) mm; the thalamus, 2.5 ± 0.07 mm; the PHG, 1.0 ± 0.05 mm; and the amygdala, 1.7 ± 0.02 mm. Thus, the differences between independent (LOO method) and non-independent approaches were less than one voxel apart. Given a 6 mm FWHM for spatial smoothing, we argue that effects of such a bias in our hierarchical regression model are negligible.

We tested five models with different block entry order. First, we rationalized that the functional coupling may be affected by the two metrics from grey and white matter structures, i.e., the vmPFC thickness and the FA values. Second, the FA values (of the major tracts) reflect a more global feature than the intrinsic functional coupling measures that are based on given two local ROIs. In fact, we observed that a model with the intrinsic coupling entered first showed reduced ΔR^2 of subsequent blocks [IC-FA-CT model: IC ΔR^2, 0.479 ($P < 0.001$); FAΔR^2, 0.071 ($P = 0.107$); CTΔR^2, 0.064 ($P = 0.014$); IC-CT-FA model: CT ΔR^2, 0.038 ($P = 0.074$); FAΔR^2, 0.097 ($P = 0.028$); CT. cortical thickness; FA, fractional anisotropy; IC, intrinsic functional connectivity]. A confirmatory regression analysis without the block terms was performed. This analysis checked

all the possible models and selected a best subset. Neither outliers (Cook's Distances < 0.18) nor multicollinearity (tolerances > 0.70) was observed.

Structural Equation Modeling.

Using structural equation modeling, we tested if the neural correlates of the vmPFC fear generalization have impacts on clinical anxiety. We included all the neural correlates of the vmPFC generalization gradient. We assumed a latent variable to estimate collective effects of FA values (of the tracts) and functional connectivity measures (of the regions). Once an initial model was specified, we modified the model referencing modification indices to improve model fits. This step involved modeling correlations between variables: ATR and vmPFC-PH, ATR and CCG, CCG and vmPFC-PH, vmPFC thickness and vmPFC-IFG, vmPFC-TH and vmPFC-PH, and vmPFC-TH and vmPFC-AM (AM, amygdala; ATR; anterior thalamic radiation; CCG, cingulum cingulate gyrus; IFG, inferior frontal gyrus; PH, parahippocampal gyrus).

Results

Characterization of the vmPFC fear generalization response.

During fear generalization, vmPFC activation showed a significant group difference as a function of perceptual similarity of cues to the conditioned stimulus (CS). Patients with GAD showed a less discriminating vmPFC response during safety vs. threat, compared to healthy individuals (Ref. (Greenberg et al., 2013a) for group difference results). We then identified the contrast for which vmPFC BOLD estimates best predicted clinical anxiety: we conducted a logistic binary regression analysis using group as the dependent variable, and 10 potentially meaningful contrasts among the four conditions. Indeed, we found that the slope of linear fit on all stimuli was the best predictor [Control, -0.33 ± 0.06 (SE); GAD, -0.18 ± 0.06; **Table 4.1**]. Therefore, we used the slope of vmPFC gradient as an index of vmPFC functioning in the following analyses to seek for neural correlates.

Table 4.1. Logistic regression results reveals linear fit of vmPFC activation gradient best predicting group status.

	Model Summary				Variables in the Model				
	-2 Log likelihood	χ^2	$\Delta\chi^2$	Sig.	Variable	B	S.E.	d.f	Sig.
Step1	70.74	7.41		.19	60%-40%	14.59	58526.455	1	1
			-	-	40%-20%	18.92	78035.273	1	1
					20%-CS%	14.33	58526.455	1	1
					60%-Fixation	-.97	1.052	1	.36
					Linear Fit (60 ~CS)	48.54	195088.183	1	1
Step2	71.48	6.68		.15	60%-40%	.30	.519	1	.57
			-.74	.39	20%-CS%	.28	.438	1	.52
					60%-Baseline	-.68	.963	1	.48
					Linear Fit (60 ~CS)	1.85	1.732	1	.29
Step3	71.81	6.35		.09	20%-CS%	.39	.396	1	.32
			-.33	.56	60%-Baseline	-.30	.698	1	.67
					Linear Fit (60~CS)	2.23	1.634	1	.17
Step4	71.99	6.16		.04	20%-CS%	.47	.355	1	.18
			-.18	.66	Linear Fit (60 ~CS)	2.73	1.181	1	.02
Step5	73.88	4.28		.03	Linear Fit (60 ~CS)	1.87	.947	1	.05
			-1.88	.17					

Thickness predicts the vmPFC fear generalization response.

We assessed whether mean thickness of the vmPFC was associated with vmPFC reactivity during fear generalization. We found that a reduction in left vmPFC thickness correlated with a less discriminate vmPFC response (r_{51} = -0.46, P = 0.001, 2-tailed; partial correlation controlling for group, age and intracranial volume) (**Table 4.2**; **Figure 4.2**). No association was observed in the right vmPFC (P > 0.42). We confirmed this with a vertex-based, whole brain surface approach. Peak correlation between cortical thickness and the fear generalization gradient occurred in the left vmPFC (peak vertex: P = 0.0004; MNI -11, 39, -11; size of cluster 45.52 mm^2 at uncorrected P of 0.001). Of note, the peak coordinate is proximal (11mm apart; Euclidean distance) to the coordinate of the peak vmPFC fear generalization gradient effect (MNI -4 , 40, -20; (Greenberg et al., 2013a). Given this strong correlation, a reasonable trajectory would be that patients with GAD would show vmPFC thinning. We thus tested impacts of clinical anxiety on the vmPFC thickness using a general linear model controlling for age, intracranial volume, and self-reported depressive symptoms. We did not find any effects of anxiety on vmPFC thickness (P > 0.44). These results strongly support a positive association between grey matter structural integrity and vmPFC function in generalizing threat.

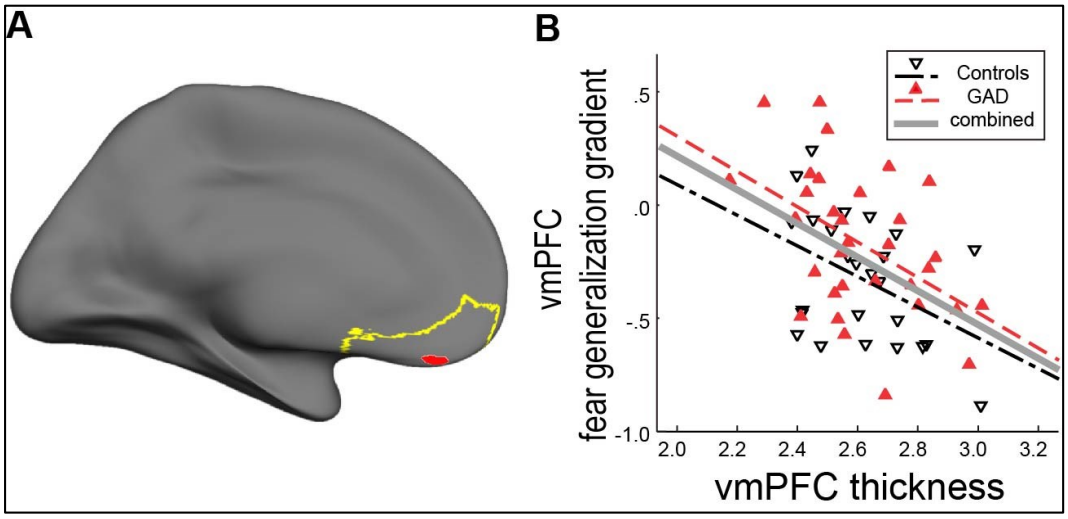

Figure 4.2. VmPFC cortical thickness correlates with the vmPFC fear generalization response. ***A,*** VmPFC ROI for cortical thickness (yellow) and for fear generalization gradient (red) are shown. ***B,*** Scatter plot of vmPFC thickness and fear generalization, i.e., slopes of the linear fit. Participants with a greater vmPFC thickness showed a steeper slope (thus more discriminating) of the fear generalization gradient. See Table 2 for correlation coefficients and significances.

White matter microstructure of prefrontal-subcortical pathway predicts the vmPFC fear generalization response.

We then tested whether vmPFC structural connectivity with other components of the fear circuit would affect the vmPFC fear generalization gradient. To do this, we reconstructed three major white matter pathways converging in the mPFC (including the ventral portion)—the anterior thalamic radiation (ATR), the cingulum-cingulate gyrus (CCG) and the uncinate fasciculus (UF)—using an anatomically informed probabilistic tractography approach (Yendiki et al., 2011a) (**Movie 1**). We used the mean fractional anisotropy (FA) of each tract for correlation analyses. We found that a lower FA significantly correlated with a less discriminate vmPFC response in all the three tracts (left ATR $r_{51} = -0.38$, $P = 0.006$, 2-tailed, partial correlation controlling for group and age; the left CCG, $r_{51} = -0.37$, $P = 0.008$; the left UF, $r_{51} = -0.39$, $P = 0.037$; **Table 4.2**; **Figure 4.3**). FA of the whole brain and posterior tracts did not correlate with the vmPFC generalization gradient (Ps > 0.16) (cf. we observed a correlation at a trend level in the right superior longitudinal fasciculus parietal, $r_{51} = -0.27$, $P = 0.07$). The correlation results were robust to outliers (Ps < 0.026; robust regression). Furthermore, we examined the extents to which clinical anxiety affects FA values. We performed a general linear model using group as a regressor, as well as age, whole brain FA, and depressive symptoms as covariates.

As a result, clinical anxiety had a trend level impact on a decrease in FA of the UF [Wald Chi-Square = 3.21, $P = 0.073$, an estimated mean difference (control - GAD) = 0.26 ± 0.014], but not in the ATR or CCG (Ps > 0.2).

In order to examine the local features of the effects within the tracts-of-interest and neighboring fear circuit components, we then used Tract-Based Spatial Statistics (Smith et al., 2006). We confirmed the above negative correlation between the vmPFC fear generalization gradient and widespread fiber integrity, at whole brain corrected $P < 0.05$ (Figure 4.3). Significant FA foci were found nearby the vmPFC along with the majority of the UF, ATR, and anterior portions of CCG and bordered key fear circuit components, including the accumbens, amygdala, hippocampus, thalamus, and dopaminergic midbrain.

Intrinsic functional connectivity of vmPFC - fear circuit predicts the vmPFC fear generalization response.

We next examined whether the vmPFC fear generalization gradient could be predicted by the extent to which the vmPFC was intrinsically coupled within the fear circuit (i.e., resting-state functional connectivity). Our regions of interest for the intrinsic coupling analyses included the thalamus, amygdala, parahippocampal gyrus (PHG), middle and inferior frontal gyrus.

Table 4.2. Partial correlations of neural metrics and the vmPFC generalization gradient.

	GEN vmPFC					
	Both Groups		Controls		GAD	
	R	*P*	r	*p*	r	*p*
CTlh	-0.46***	5×10^{-4}	-0.45*	0.04	-0.47**	0.008
CTrh	-0.11	0.42	-0.15	0.49	-0.12	0.53
FA AT_{lh}	-0.38**	0.006	-0.48*	0.02	-0.31	0.10
FA AT_{rh}	0.05	0.71	-0.17	0.41	0.05	0.79
FA CG_{lh}	-0.37**	0.008	-0.41*	0.05	-0.34	0.07
FA CG_{rh}	-0.34*	0.01	-0.41*	0.05	-0.30	0.11
FA UF_{lh}	-0.39*	0.04	-0.62**	0.002	-0.05	0.78
FA UF_{rh}	-0.19	0.18	-0.44	0.03	0.01	0.95
IC Am	0.47***	6×10^{-4}	0.54**	0.009	0.41*	0.03
IC Th	-0.50***	2×10^{-4}	-0.24	0.12	-0.60***	2×10^{-4}
IC Ph	0.43**	0.002	0.31	0.16	0.58**	0.002
IC MFG	-0.49***	4×10^{-4}	-0.42*	0.05	-0.55**	0.003
IC INS	0.02	0.91	-0.58**	0.005	0.59**	0.001
IC Am-PH	0.34*	0.02	0.43*	0.04	0.29	0.14

Control variables included group (for "Both Groups") and age (cortical thickness and FA). Am, amygdala; AT, anterior thalamic radiation; CG, cingulum cingulate gyrus; CT, cortical thickness; FA, fractional anisotropy; IC, intrinsic functional coupling; INS, ins.

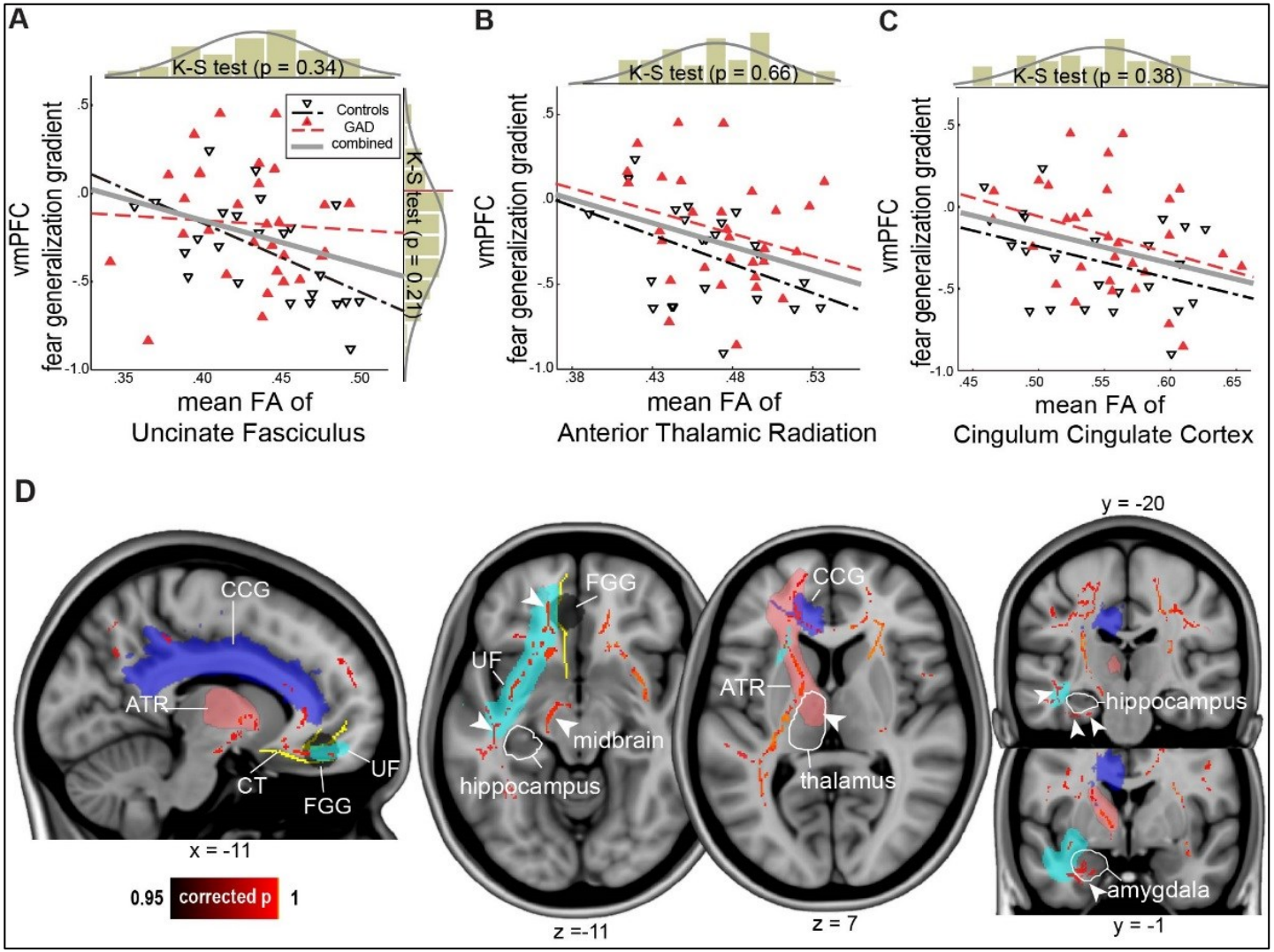
A
K-S test (p = 0.34)
Controls
GAD
combined
vmPFC
fear generalization gradient
K-S test (p = 0.21)
mean FA of
Uncinate Fasciculus
B
K-S test (p = 0.66)
vmPFC
fear generalization gradient
mean FA of
Anterior Thalamic Radiation
C
K-S test (p = 0.38)
vmPFC
fear generalization gradient
mean FA of
Cingulum Cingulate Cortex
D
CCG
ATR
CT
FGG
UF
x = -11
0.95
corrected p
1
FGG
UF
midbrain
hippocampus
z =-11
CCG
ATR
thalamus
z = 7
y = -20
hippocampus
amygdala
y = -1

Figure 4.3. Integrity of the fibers connecting the vmPFC with the fear circuit predict the vmPFC fear generalization response. *A-C,* Scatter plot of the mean FA of the UF (a), the ATR (b) and the CCG (c) vs. vmPFC fear generalization. A reduced FA in each tract predicted a closer-to-zero, thus a more indiscriminating fear generalization. The mean FA of the ATR and the CCG were correlated, $r_{51} = 0.49$, $P = 0.0001$, but other combinations were not(all Ps > 0.11). A histogram of each metric with Kolmogorov-Smirnov test results indicate a continuous distribution. *D*, Tract Based Spatial Statistics revealed the same pattern as the tractography results: less FA values predicted a closer-to-zero vmPFC fear generalization gradient at corrected $P < 0.05$ (whole brain). Three reconstructed major tracts are shown in distinct colors. The vmPFC anatomical ROI (in yellow) and fear generalization (black circle) are also shown (sagittal view in middle). Significant effects were observed along the majority of the UF and the ATR tracts projecting to the ventral and dorsal portions of the fear circuit, respectively (axial view in right). Similarly, the anterior CCG projecting to the dorsal end of the vmPFC showed significant effects. Note that along with the major tracts, local neighboring fibers adjacent to some of the fear circuit showed significant associations: these include the hippocampus, midbrain, thalamus, amygdala and insula (indicated by arrow heads). Tracts that do not directly project to the vicinity of the prefrontal cortex also showed correlations: the putative, cortical spinal tract (around the midbrain region) and the longitudinal fasciculus.

We observed significant associations between the vmPFC fear generalization and vmPFC coupling with the thalamus ($z = 3.38$, peak $P = 3x10^{-4}$, cluster size = 77 voxels; MNI -6, -14, 10), PHG ($z = 3.28$, peak $P = 0.001$,cluster size = 14 voxels; MNI 18, -2, -26), amygdala ($z = 3.30$, peak $P = 4x10^{-4}$, cluster size = 44 voxels; an amygdala-seeded, vmPFC-targeted analysis), and inferior frontal gyrus (IFG) ($z = 3.33$, peak $P = 4 \times 10^{-4}$, cluster size = 40 voxels; MNI -42, 22, 18) at ROI corrected $P < 0.05$ (**Table 4.3**). The effects were robust to controlling for group and age. The peak coordinate in the thalamus occurred within the mediodorsal region showing 65 % structural connectivity probability with the PFC (Thalamic Connectivity Atlas; http://www.fmrib.ox.ac.uk/cgi-bin/thalamus.pl). Post-hoc analyses on extracted coupling estimates revealed that heightened vmPFC-amygdala connectivity ($r_{48} = 0.47$, $P = 6 \times 10^{-4}$, two-sided; partial correlation) and vmPFC-PHG coupling ($r_{48} = 0.43$, $P = 0.002$) predicted more indiscriminate vmPFC fear generalization gradient (**Figure 4.4**). On the other hand, reduced vmPFC-thalamus ($r_{48} = -0.50$, $P = 2 \times 10^{-4}$) and vmPFC-IFG coupling ($r_{48} = 0.49$, $P = 4 \times 10^{-4}$) predicted a more indiscriminate vmPFC fear generalization gradient.

Impact of clinical anxiety on prefrontal and limbic connectivity.

Based on previous literature implicating impaired (dorsal) prefrontal attention and executive system in anxiety (Bishop et al., 2004; Bishop, 2009), we reasoned that abnormal intrinsic connectivity between the dorsal and ventral PFC may be related to clinical anxiety as well. We thus tested impacts of pathological anxiety on vmPFC-frontal gyrus intrinsic coupling. Patients with GAD showed reduced vmPFC-middle frontal gyrus (MFG) functional connectivity compared with controls ($z = 4.49$, peak $P = 3 \times 10^{-6}$, cluster size = 482; MNI -36, 42, 26; **Figure 4.5**).

Table 4.3. VmPFC intrinsic functional connectivity with fear circuit showing correlations with fear generalization or group differences.

Analysis and region	corrected *p**	cluster (voxels)	peak			MNI (mm)		
			F or *t*	z	*p*	x	y	z
vmPFC-seeded connectivity								
Correlation (with fear generalization gradient)								
Thalamus	< 0.001	77	14.69	3.38	$3x10^{-4}$	-6	-14	10
IFG (BA45)	< 0.001	40	14.24	3.33	$4x10^{-4}$	-42	22	18
PHG	< 0.05	14	13.85	3.28	0.001	18	-2	-26
Mean difference (Control > GAD)								
MFG (BA46)	< 0.001	482	5.01†	4.49	$3x10^{-6}$	-36	42	26
Amygdala (Rh)-seeded connectivity								
Correlation (with fear generalization gradient)								
vmPFC	0.024‡	44	14.00	3.30	$4x10^{-4}$	6	42	-20
Mean difference (GAD > Control)								
PHG	< 0.01	26	3.85†	3.59	$2x10^{-4}$	24	-2	-30

*Cluster-extent correction in anatomical ROI (see Methods for details); †t-value; ‡FWE Small Volume Correction (peak value-wise) from *a priori* coordinates due to inaccuracy of 3dClustSim on a small mask.

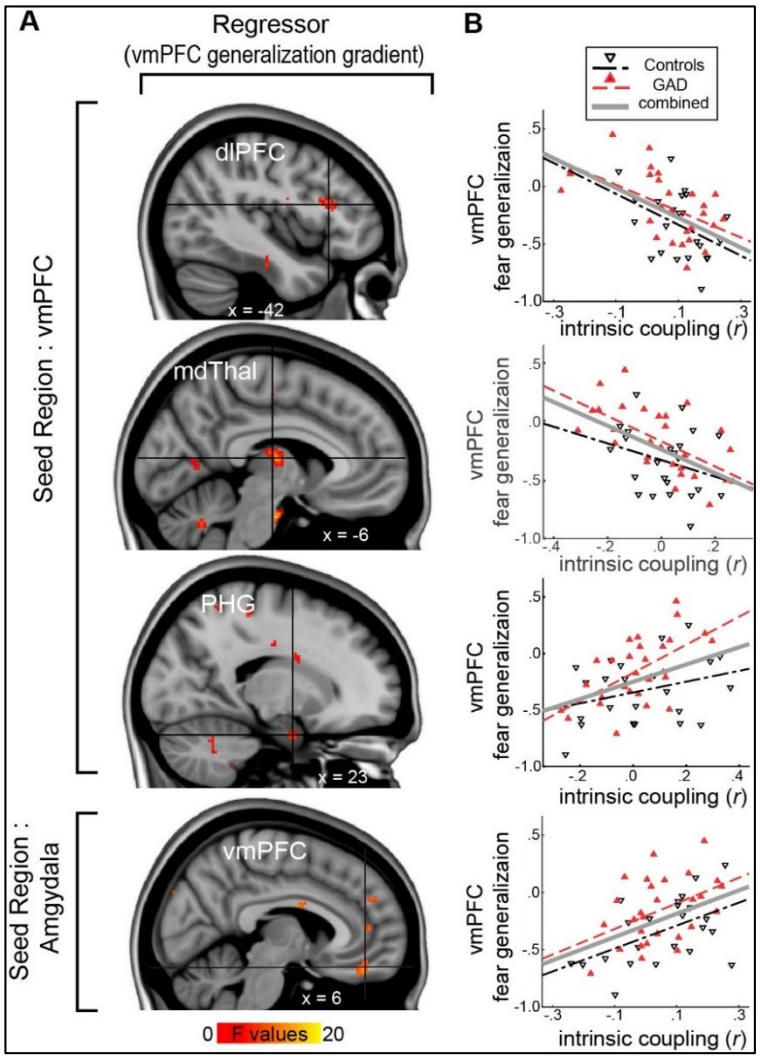

Figure 4.4. VmPFC Resting-state functional connectivity to emotional circuitry predicts the vmPFC fear generalization response. *A,* Whole brain correlation results showing vmPFC intrinsic coupling derived from resting-state fMRI associated with fear generalization. vmPFC coupling with the dlPFC, thalamus and parahippocampal gyrus (vmPFC seeded connectivity), and amygdala (amygdala seeded connectivity) showed significant correlations at corrected $P < 0.05$, controlling for group effects. *B,* Scatter plots of the intrinsic coupling estimates (r) and the vmPFC fear generalization gradient. The vmPFC fear generalization gradient negatively correlated with vmPFC intrinsic coupling to the dlPFC or the thalamus, and positively correlated with the coupling to the PHG and the amygdala. FGG, fear generalization gradient.

Together with literature reporting significant amygdala-PHG connectivity in both emotion processing (Stein et al., 2007) and resting state (Robinson et al., 2010), and based on our results that vmPFC-amygdala and vmPFC-PHG couplings correlated with the fear generalization, we next reasoned that amygdala-PHG coupling would be closely related to vmPFC threat processing or pathophysiology of anxiety. Indeed, amygdala-PHG coupling was significantly correlated with the vmPFC fear generalization gradient, such that a higher coupling predicted a less discriminate vmPFC fear generalization gradient (r_{48} = 0.30, $P < 0.04$, 2-tailed partial correlation controlling for group). Furthermore, a voxel-wise analysis showed that GAD patients demonstrate significantly increased connectivity compared with controls at a corrected $P < 0.01$ (**Table 4.3, Figure 4.5.** Together with the MFG results, these findings suggest a strong association between clinical anxiety and prefrontal (vmPFC-MFG) and limbic (amygdala-PHG) connectivity.

Multiple neural measures predict the vmPFC fear generalization gradient and generalized anxiety disorder: multiple linear regression and structural equation modeling.

We performed multi-block linear regression analyses, taking the vmPFC gradient as the dependent variable and its structural (grey and white matter) and functional

factors as the independent variables, categorized into three blocks: vmPFC thickness, fiber integrity (i.e., FA of each of the three major tracts), and functional connectivity (i.e., vmPFC intrinsic coupling with the amygdala, thalamus, PHG, and IFG respectively; see Materials and Methods for details regarding how coupling estimates were derived). Group and age were initially entered into the model. We found that all three blocks independently accounted for significant portions of the variance in the vmPFC fear generalization gradient (**Table 4.4**). Volumetrics accounted for 15.6 % of variance in the fear generalization ($P < 0.003$), fiber integrity 21.8 % ($P < 0.002$), and functional coupling 19.1 % ($P < 0.001$). The resultant model had an adjusted R^2 of 0.60 ($P < 0.001$). Significant individual predictors included vmPFC cortical thickness ($\beta = -0.28$, $P < 0.01$), FA of anterior thalamic radiation ($\beta = -0.41$, $P < 0.001$), vmPFC-amygdala functional coupling ($\beta = 0.32$, $P < 0.01$), and vmPFC-IFG functional coupling ($\beta = -0.24$, $P < 0.03$), followed by a marginally significant vmPFC-thalamus coupling ($\beta = -0.18$, $P < 0.09$). We investigated relative predictability among the factors by switching block entry order. In all four alternative models, each factor significantly predicted a distinct proportion of the variance in the fear generalization (P's < 0.05). Of note however, the ΔR^2 of each factor dropped when entered last, compared to first (CT, 60.9 %; FA, 31.7 %; IC, 48.2 %).

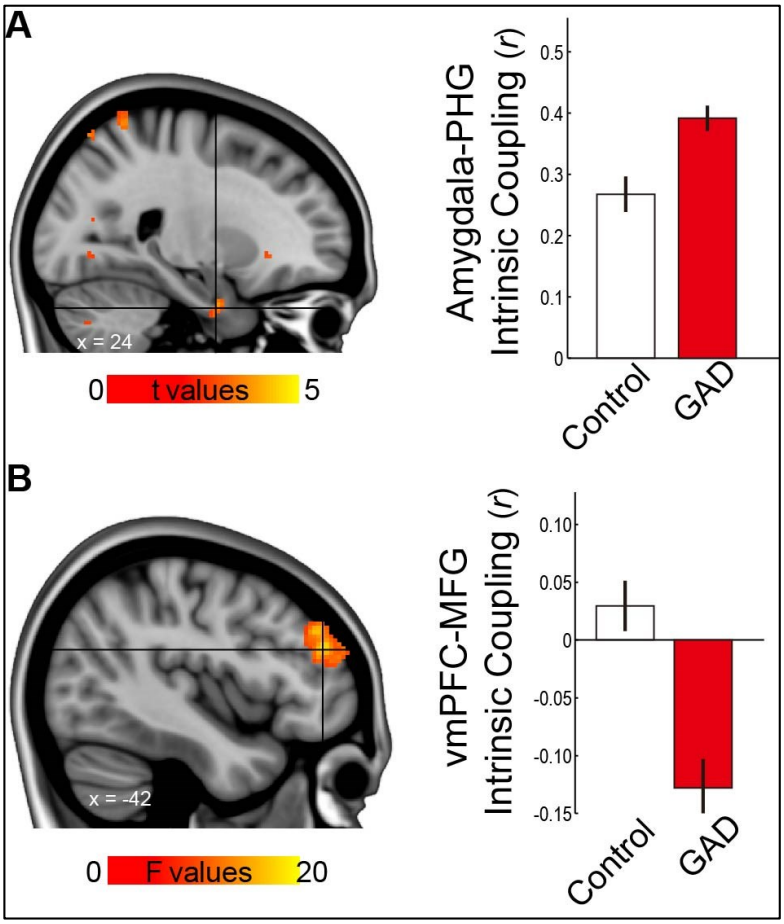

Figure 4.5. Altered intrinsic coupling in GAD. ***A,*** Left; amygdala - parahippocampal gyrus coupling was significantly different between groups. Right; post-hoc analyses revealed that the GAD group showed greater coupling than controls ($t_{50} = 3.58$, $P < 0.001$, two-sample t-test), while both showed mean positive values ($P < 0.001$). ***B,*** Left; voxel-wise analyses showed significant group difference in vmPFC-seeded intrinsic coupling with the dlPFC at corrected $P < 0.001$. Activation maps were thresholded at uncorrected $P < 0.001$, cluster size > 20 voxels. Right, a bar graph from coupling estimates extracted from the peak coordinate (within 6mm radius) revealed reduced and negative vmPFC-dlPFC coupling in GAD.

Table 4.4. Block-wise multiple regression model with vmPFC generalization gradient as the dependent variable and the three categories of neural metrics as the independent variables.

Step	Block	Predictors	Coefficients		Model Summary		
			β	Sig.	R^2	Adj.R^2	$\Delta R^2(p)$
0					0.113	0.075	0.113 (0.060)
	(Initial, fixed terms)	*Group*	*0.283*	*0.045*			
		Age	*0.176*	*0.207*			
1	Cortical Thickness				0.269	0.221	0.156 (0.003)
		CT	*-0.412*	*0.003*			
2					0.269	0.415	0.218 (0.002)
	Fractional Anisotropy	CT	-0.417	0.001			
		FA_{AT}	*-0.310*	*0.020*			
		FA_{CG}	*-0.111*	*0.376*			
		FA_{UF}	*-0.234*	*0.045*			
3					0.678	0.596	0.191 (0.001)
	Intrinsic (Functional) Coupling	CT	-0.277	0.010			
		FA_{AT}	-0.412	0.001			
		FA_{CG}	0.003	0.976			
		FA_{UF}	-0.069	0.500			
		IC_{Am}	*0.317*	*0.011*			
		IC_{Th}	*-0.176*	*0.091*			
		IC_{PHG}	*-0.074*	*0.520*			
		IC_{IFG}	*-0.242*	*0.027*			

Italic denotes newly entered predictors. Am, amygdala; AT, anterior thalamic radiation; CG, cingulum cingulate gyrus; CT, cortical thickness; FA, fractional anisotropy; IC, intrinsic functional coupling; IFG, inferior frontal gyrus, PHG, parahippocampal gyrus; Th, thalamus; UF, uncinate fasciculus.

This indicates association between each factor and indirect effects. Such an observation is indeed intuitive in that all factors in part represent properties of a broad vmPFC network and predict vmPFC fear generalization gradient. A confirmatory regression model without block terms showed similar results: vmPFC thickness, FA of ATR, vmPFC-amygdala, and vmPFC-IFG each significantly (Ps < 0.01) accounted for a portion of the total variance in the vmPFC fear generalization explained (53.9 %).

We then used structural equation modeling to investigate whether each of these correlates of vmPFC fear generalization gradient would be associated with pathological anxiety. Two latent variables were hypothesized to estimate collective impacts of axonal integrity and functional coupling, respectively (See **Methods** for details of model specification). Effects of CCG fiber integrity and vmPFC-PHG coupling were not significant. The model showed that the direct effects of structural and functional neural substrates onto the latent variables, the vmPFC fear generalization gradient, and generalized anxiety disorder were significant. More importantly, the indirect effects of the variables onto pathological anxiety, mediated through the vmPFC fear generalization gradient, were significant (**Figure 4.6**). Together with the multiple regression model, these results suggest that the structural and functional neural features contribute to generalized anxiety disorder via disruption of vmPFC threat processing.

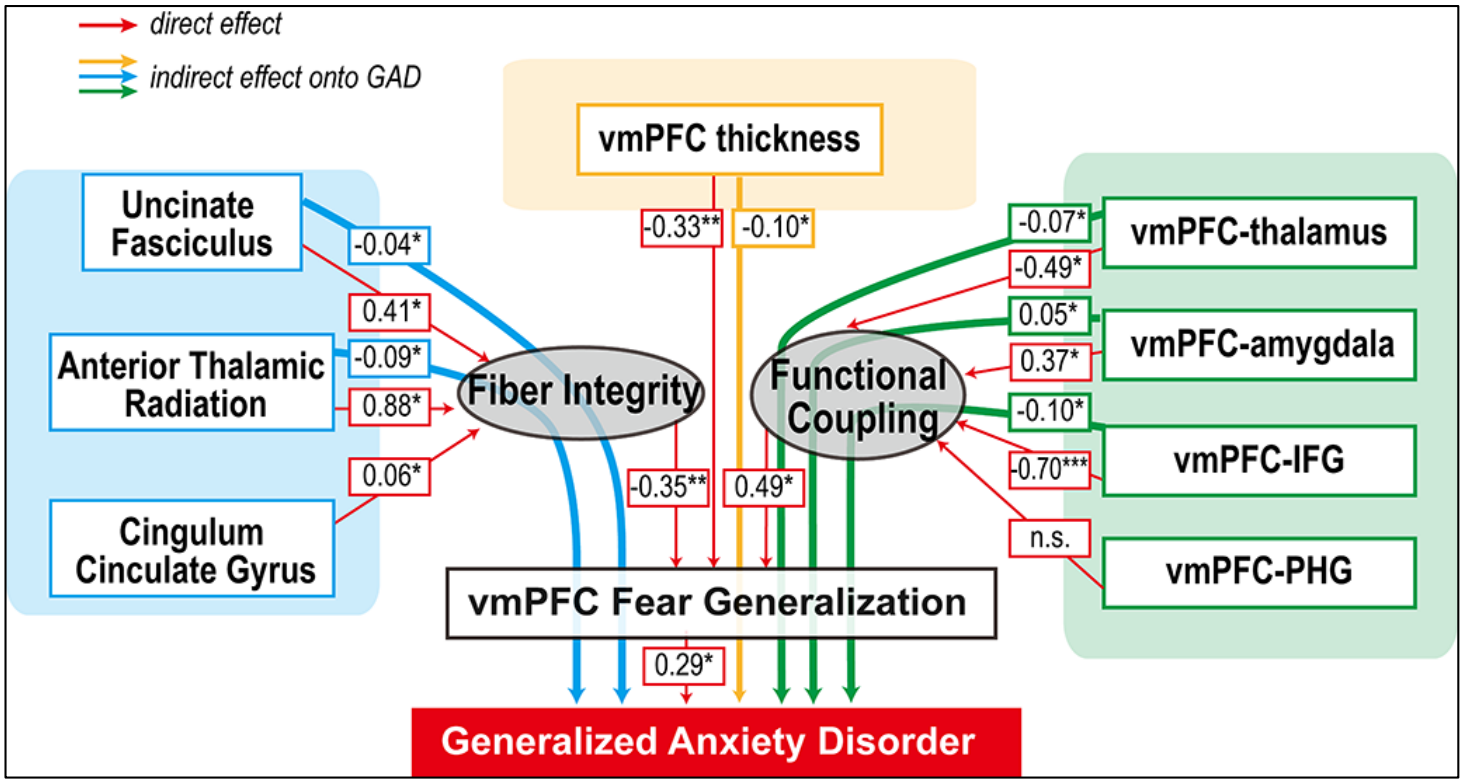

Figure 4.6. Structural equation model shows that individual differences of the circuit-wide neural features are associated with clinical anxiety, an effect appears to be mediated, in part, through vmPFC fear generalization. Indirect effects are depicted as dotted grey lines. The model included the same variables as the multiple regression model. Correlations between some of the variables were modeled, but for brevity, are not shown (see Materials and Methods). This model showed a reasonable fit: *d.f.* = 29; $\chi^2/d.f.$, 1.05; Comparative Fit Index, 0.98; Root Mean Square Error of Approximation, 0.03 (cutoff criteria: CFI > 0.95 & RMSEA < 0.06; Hu and Bentler, 1999). Significance of effects were determined by a bootstrapping sampling method (1000 samples) with Bias-Corrected confidence intervals

Discussion

In the present study, we demonstrate that (i) vmPFC threat processing correlates with variability of grey matter structure and vmPFC connectivity with distributed systems, (ii) this relationship is independent across the neural factors, and (iii) variability in factors may contribute to clinical anxiety by affecting vmPFC function. Our results may therefore lend a support a multivariate model of clinical anxiety. In this model, several individual neural "hits" provide necessary, but insufficient, conditions for psychopathology, leading to disease development only when they are present together.

Our results indicate that individual variability in the vmPFC fear generalization gradient is explained by the vmPFC size, fiber integrity of the white matter tracts converging on it, and intrinsic functional coupling of the corticolimbic fear circuit in an independent manner. These results endorse the notion of the vmPFC's integral role in the corticolimbic system (Roy et al., 2012) and further suggest that impoverished vmPFC recruitment in pathological anxiety, as previously documented by our group (Greenberg et al., 2013a) and others (Milad and Rauch, 2007; Myers-Schulz and Koenigs, 2012), is closely related to parallel system-wide abnormalities between cortical or subcortical nodes in the fear circuit.

We show that individuals with thicker vmPFC display more discriminating vmPFC reactivity during the fear generalization task indicating a direct structure and function relationship. This result is in line with previous research reporting that vmPFC thickness positively correlates with fear extinction, as indexed by skin conductance responses to CS (Milad et al., 2005). It should be noted that, patients with GAD did not show signs of vmPFC thinning. This could be due to relatively young patient samples (mean age of 22.3 ± 4.5 years). Future research may determine the impact of prolonged illness duration on vmPFC thickness.

Our tractography data show that the fiber integrity of all three major pathways that converge upon the prefrontal cortex is correlated with vmPFC fear generalization. Not only do our Tract-Based Spatial Statistics results support this, they also demonstrate that fibers proximal to the hippocampus, the amygdala, the thalamus, and even the midbrain play an important role in contributing to vmPFC function. The pervasive correlation effect throughout the corticolimbic system in the Tract-Based Spatial Statistics analysis is striking, given a conservative whole-brain corrected P combined with a non-parametric permutation method. Thus, these results provide strong support for the role of the vmPFC as a hub of diverse brain regions that collectively contribute to the vmPFC response to affective

stimuli; this notion is also relevant to other domains of vmPFC function, such as cognition, valuation and memory (Price, 2007; Roy et al., 2012).

Regarding the relationship between clinical anxiety and fiber integrity, we found a trend-level effect in the UF. This is in line with previous studies showing attenuation of UF fiber integrity in patients with GAD (Hettema et al., 2012; Tromp et al., 2012a), generalized social anxiety disorder (Phan et al., 2009a) and non-clinical trait-anxious individuals (Kim and Whalen, 2009b). However, it should be noted that the directionality of the relationship between UF fiber integrity and anxiety has produced mixed results (Ayling et al., 2012a; Montag et al., 2012) and certain anxiety-related behaviors such as attentional bias to threat are associated with heightened UF integrity (Carlson et al., 2013b; Carlson et al., 2013a). Nevertheless, it should be noted that here, clinically anxious individuals —without showing an apparent FA reduction—still showed over-generalizing vmPFC functioning to threat vs. safety. This indicates that FA reduction in the UF tract may not be essential for impoverished vmPFC threat processing, and that there may exist parallel pathways for maladaptive vmPFC fear processing.

It is important to note that the directions of correlations between vmPFC coupling and its fear generalization gradient are distinct across different regions. Decreased vmPFC coupling with the mediodorsal thalamus and the IFG correlates with an indiscriminating vmPFC gradient. Indeed, the mediodorsal thalamus-

vmPFC connectivity has been implicated in associative learning in animal studies (Mitchell and Gaffan, 2008; Cross et al., 2012; Parnaudeau et al., 2013). Furthermore, it has been suggested that the mediodorsal thalamus plays a critical role in the modulation of fear extinction (Lee et al., 2012). Our functional connectivity results cannot resolve directionality; nevertheless, they provide support for these previous findings in animals. Similarly, decreased vmPFC-IFG coupling also correlates with indiscriminating vmPFC fear generalization. Furthermore, clinical anxious individuals displayed decreased vmPFC-MFG coupling. These results are well in line with previous reports where vmPFC interaction with prefrontal systems (the MFG and the IFG) has been implicated in emotion regulation (Delgado et al., 2008) and value-based decision making (Hare et al., 2009; Baumgartner et al., 2011). Impoverished functioning in these regions has also been shown to contribute to the development of anxiety (Bishop et al., 2004; Bishop, 2009). Taken together with prior literature, our results suggest that inefficient prefrontal-vmPFC interaction is an important contributor to maladaptive vmPFC threat processing and consequently, in the pathophysiology of anxiety.

In contrast, we found the opposite relationship in vmPFC–limbic system coupling: individuals with greater intrinsic coupling displayed more indiscriminating vmPFC fear generalization gradients. Our results further show

that heightened coupling of the amygdala–PHG is related to clinical anxiety. Thus, maintaining balanced connectivity of the vmPFC–limbic network appears to be critical in precise vmPFC functioning. The idea that a greater vmPFC–limbic coupling is related to attenuated vmPFC threat processing might be controversial. Reduced vmPFC–amygdala intrinsic coupling measured by fMRI is implicated in social anxiety disorder (Hahn et al., 2011), whereas we did not observe group differences here. However, one should consider differences of laterality in these two studies; the result in Hahn et al. is left amygdala seeded connectivity, whereas our result is right amygdala seeded (note that we did not observe a correlation of connectivity and the vmPFC functioning in a left amygdala seeded analysis). Nevertheless, our results may cast a question whether dysregulation in vmPFC–amygdala in anxiety (or in mood disorders more generally) can be merely characterized as a decrease in functional connectivity. In line with this, it is worth noting that an increase in vmPFC-amygdala coupling has been linked to a genetic risk factor of mood disorder, that is, short allele of the serotonin transporter (Heinz et al., 2005), which has been linked to greater amygdala fear reactivity (Hariri et al., 2002) and a greater anxiety-related behaviors (Schinka et al., 2004; Sen et al., 2004; Carlson et al., 2012a). Together, these results provide a more detailed picture of the functional role of vmPFC–limbic connectivity in threat processing than a mere patients–controls comparison,

by linking connection properties to MRI-based cortical functioning that is more objective than diagnostics primarily based on subjective symptom reports.

Our block-wise regression model indicates that vmPFC thickness, fiber integrity, and functional connectivity independently account for variability in vmPFC reactivity during fear generalization. This supports the hypothesis that the altered vmPFC fear response in clinically anxious individuals is associated with parallel neural abnormalities. Pathological anxiety is a heterogeneous construct associated with distinct symptoms or pathologies that may or may not be present in any given individual with anxiety. Complicating issues further, pathological anxiety could be caused by multiple factors, such as prolonged or acute aversive experiences, excessive worry, and/or potential genetic risk factors. Our structural equation modeling supports the notion that clinical anxiety may have multiple parallel pathophysiologies in distributed brain areas, which have significant impacts on vmPFC functioning. This is in accord with recent reports that distinct neural circuits are responsible for different aspects of anxious states in rodent models (Jennings et al., 2013; Kim et al., 2013). Such an accumulative contribution of multiple factors to pathophysiology is similar to that of autism (O'Roak et al., 2011) and cardiac disorders (Spooner, 2009). In conclusion, our findings provide functional and structural support for a multi-hit model for clinical anxiety.

CHAPTER V

(in submission)

Title: Hyper-reactive human ventral tegmental area and mesocortical connectivity in overgeneralization of threat in generalized anxiety disorder

Authors: Jiook Cha[1], Joshua M. Carlson[2,3], Daniel J. DeDora[2], Tsafrir Greenberg[3], Greg Hajcak[3], Lilianne R. Mujica-Parodi[1,2]*

Author Affiliations: 1. Program in Neuroscience; 2. Department of Biomedical Engineering, Stony Brook University, Stony Brook, NY 11794, USA; 3. Department of Psychology, Northern Michigan University, Marquette, MI 49855, USA; 4. Department of Psychology, Stony Brook University, Stony Brook, NY 11794, USA.

*Corresponding author

Abstract

The ventral tegmental area (VTA) has long been associated with reward-motivated behavior and has recently been linked to punishment-motivated behavior. Recent work ties aberrant VTA dopamine signaling to the development and maintenance of anxious behavior in animal models; however, these findings in animal models have yet to be extended to anxiety in humans. Here, we hypothesize that pathological anxiety is linked to dysfunction of the VTA dopaminergic circuit in threat processing; specifically, excessive or uncontrolled activity of the dopaminergic aversion circuit may be etiologically linked to errors in distinguishing cues of threat vs. safety, also known as 'overgeneralization of threat'. To test this, we recruited patients with generalized anxiety disorder (N = 32) and healthy control subjects (N = 25; age-matched, all female). We measured brain activity using functional MRI while subjects underwent a fear generalization task that assessed fear generalization in response to a conditioned stimulus and perceptually similar stimuli. Healthy controls showed a discriminate VTA reactivity pattern, proportional to cue similarity towards threat; in marked contrast, patients with generalized anxiety disorder showed significantly heightened VTA activity to safe cues. This abnormal VTA reactivity was associated with increased mesocortical, and decreased mesohippocampal interactions in response to safe cues. These results provide the first evidence that

aberrant activity in the putative dopaminergic aversion circuit is implicated in generalized anxiety disorder. Thus, therapeutic strategies specifically targeting this mesocorticolimbic circuit may succeed in treating the over generalization of conditioned fear in generalized anxiety disorder.

Introduction

The midbrain ventral tegmental area (VTA) is part of the mesocorticolimbic system containing dopaminergic cell bodies, and has primarily been associated with reward processing. However, recent studies highlight an additional role of the VTA in aversion processing (Pezze and Feldon, 2004; Fairhurst et al., 2007; Joshua et al., 2008; Liu et al., 2008; Fadok et al., 2009; Matsumoto and Hikosaka, 2009; Baliki et al., 2010; Bromberg-Martin et al., 2010; Zweifel et al., 2011; Cohen et al., 2012; Stamatakis and Stuber, 2012; Brooks and Berns, 2013); this role is mediated primarily via the mesocortical projection, which is distinct from the mesolimbic circuit for reward processing in rodent models.

Recently abnormal dopaminergic signaling has been implicated in certain anxiety-based conditions. For example, animal research demonstrates that social-defeat stress can alter VTA dopamine transmission (Anstrom et al., 2009), and that the long-term impact of social defeat is dependent on brain-derived neurotrophic factor (BDNF) expressed in the VTA (Berton et al., 2006). More recent research highlights dopaminoreceptive cortical neurons as the most likely target site of disturbance under chronic stress via glucocorticoid release (Barik et al., 2013) and epigenetic control (Niwa et al., 2013). Furthermore, the increase in dopaminergic neuronal activity and abnormal morphological changes in the VTA

seem to underlie anxiety-related behaviors in a mouse model of bipolar disorder; interestingly, these behaviors are mitigated with lithium treatment, a common medication for mood disorders (Coque et al., 2011a). Such mounting evidence motivates us to question whether abnormal VTA signaling in negative motivation is related to clinical anxiety in humans.

The VTA coordinates mesocorticolimbic circuit activity to encode aversion. In rodents, the VTA receives aversion signals from the lateral habenula and projects to the medial prefrontal cortex (Lammel et al., 2012; Stamatakis and Stuber, 2012). It also projects to the ventral striatum and the thalamus, completing the mesocorticolimbic dopamine circuit (Haber and Knutson, 2010). The hippocampus regulates VTA activity, forming the VTA-hippocampal loop that is crucial in motivational learning and memory (Lisman and Grace, 2005; Lodge and Grace, 2006; Shohamy and Wagner, 2008). The medial and ventromedial prefrontal cortices are also known to regulate VTA dopaminergic activity (Lodge, 2011). VTA aversion signaling is thus dependent on interconnections with the mesocorticolimbic systems.

An important aspect of aversion processing is threat/safety discrimination, which is essential to normative adaptive behavior. Deficits in this have been reported to contribute to overgeneralization of threat (Kheirbek et al., 2012; Greenberg et al., 2013b; Lissek et al., 2013b), which has been suggested as a

pathogenic marker of anxiety disorders, including panic disorder (Lissek et al., 2010), posttraumatic stress disorder (Jovanovic and Ressler, 2010), and generalized anxiety disorder (Greenberg et al., 2013a; Lissek et al., 2013a). In particular, the ventromedial prefrontal cortex (vmPFC) is attenuated during generalization of threat in generalized anxiety disorder (Greenberg et al., 2013a), which has been linked to underlying functional and structural abnormalities in a broader circuit converging upon the vmPFC (Cha et al., in revision). Yet, no studies have linked the midbrain and mesocorticolimbic circuit to fear generalization.

Therefore, the aim of this study was to assess whether the mesocorticolimbic circuit related to overgeneralization of threat in clinical anxiety. We hypothesized that generalized anxiety disorder would be associated with abnormal reactivity in the VTA dopaminergic circuit during threat processing; specifically, excessive activity of the dopaminergic aversion circuit may be etiologically linked to errors in distinguishing cues to threat vs. safety, that is, 'fear generalization'. To test this, we recruited patients with generalized anxiety disorder (N = 32) and healthy control subjects (N = 25; age-matched, all female). We measured brain activity using functional MRI while subjects underwent a modified Pavlovian conditioning task that assessed fear

generalization in response to a conditioned stimulus and perceptually similar stimuli.

Methods

MR data from the same participants have been used in Chapter IV, which provides detailed information regarding participants, study design, and MRI data acquisition parameters.

Pupil size data processing

Pupil size data were processed using in-house MATLAB codes (MathWorks, Natick, MA). First, we excluded periods of eye blinks detected by an on-line parsing system. We used a window of 100 ms prior to onsets of eye blinks and 300 ms following their offset in order to minimize after-blink constriction effects. Missing values were linearly interpolated. Each trial was baseline corrected: a baseline was calculated by averaging 500 data points (500 ms long) preceding stimulus onset. Baseline corrected values were z-scored for cross-subject comparisons and filtered using a low-pass filter (4 Hz cutoff frequency) to reduce measurement noise. After preprocessing, we excluded trials with outliers, exceeding two SD from mean or no pupillary changes in response to luminosity changes of presented stimuli. For statistical analysis, the pupillary

response was defined as the cumulative pupil diameter change (i.e., area under curve) within a 1000 ms window, from one second after stimulus onset. Pupil data were averaged by stimulus type, combining ±conditions to counter-balance confounding of stimulus-specific luminosity.

MRI Data Acquisition

Participants were scanned with a 3T Siemens Trio scanner at the Stony Brook University Social, Cognitive and Affective Neuroscience center. We acquired 440 T2*-weighted echo planar images with an oblique coronal angle and TR = 2100ms, TE = 23ms, flip angle = 83º, matrix = 96 × 96, FOV = 224 × 224 mm, slices = 37, in-plane resolution = 2.33 × 2.33 mm and slice thickness = 3.5 mm. For structural scans, T1-weighted images were acquired with the following parameters: TR = 1900 ms, TE = 2.53, Flip angle = 9°, FOV = 176 × 250 × 250 mm, Matrix = 176 × 256 × 256, and voxel size = 1 × 0.98 × 0.98 mm.

fMRI Analysis: Preprocessing

We performed preprocessing procedures in SPM 8 (www.fil.ion.ucl.ac.uk/spm). This included slice timing correction, motion correction, spatial normalization, and spatial smoothing. For spatial smoothing, a 4 mm of the full-width at half maximum of the Gaussian kernel was used, as this

kernel was reported to be effective in parametric mapping of the VTA BOLD reactivity in previous research (Ballard et al., 2011).

fMRI Analysis: General linear model

For a first-level (subject level) model, we used five regressors-of-interest, i.e., onsets of GS ±60%, GS ±40%, GS ±20%, $CS_{unpaired}$ and CS_{paired}, plus six motion parameters. Serial autocorrelations were modeled using a one-lag auto-correlation [AR(1)] and a canonical HRF was used as a basis function in model estimation. Then, a second level (group level) random effect analysis was carried out on individuals' contrast images for each of the four conditions (i.e., each condition vs. rest), excluding CS_{paired}. The model contained three factors: subject, group, and condition. The significance of group differences in the VTA activation for a given contrast of conditions (e.g., all stimuli vs. rest, etc.) was corrected for multiple comparisons using a small-volume correction method in SPM within a 4mm-radius sphere centered at *a priori* coordinates (MNI, 3 -17 -12) for VTA .

In order to investigate if VTA activity during fear generalization was associated with activity in the dopaminergic aversion circuit, i.e., the mPFC and the hippocampus, we conducted psychophysiological-interaction (PPI) analysis. A seed region in the VTA was defined from the group difference analysis on all stimuli vs. rest. A representative time-series (i.e., first eigenvariate) was extracted

within a 6 mm sphere centered at individual subject peaks ($P < 0.05$) within the group functional VTA mask and deconvolved. This time-series was multiplied by a stimulus condition vs. rest and then convolved with the canonical hemodynamic response function in SPM. This procedure generated one interaction term per condition (i.e., GS ±60%, GS ±40%, GS ±20% and $CS_{unpaired}$), which were entered into a separate model. The model contained three regressors: the VTA time-series by "stimuli vs. rest" interaction, "stimuli vs. rest", and the unmodulated VTA time-series. The primary objective of this analysis was to investigate group differences on mesocorticolimbic interactions modulated by GS vs. rest, on which gave a significant increase in VTA BOLD activation in patients with GAD. For this, we entered individual PPI beta images of the "GS vs. rest" contrast into a random-effect second level model containing subject, group, and condition. On a t-map of either "control - GAD" or "GAD - control," we first applied uncorrected $P < 0.005$ with a cluster extent of 20 voxels. We then corrected the results using a cluster extent method (AFNI's 3dClustSim; 10,000 Monte Carlo simulations) with an alpha of 0.005 for each ROI. Bilateral ROI masks were derived from the AAL atlas (http://www.cyceron.fr/web/aal__anatomical_automatic_labeling.html). These include a broad prefrontal area (i.e., the medial frontal gyrus, the ventromedial PFC and the ACC), the hippocampus, the ventral striatum, and the thalamus.

Results

Pupil dilation

Pupil dilation results were previously reported (Greenberg et al., 2013a). No significant group differences in pupil dilation were observed. The pupil dilation was calculated as a cumulative change (i.e., area under curve) for 1-s window starting from 1000ms after a cue onset (**Figure 5.1.**). This measure was baseline-corrected with an average value of 500-ms data preceding a cue onset in each trial. Effects of condition and group were examined using a mixed linear model.

Considering the apparent group difference in the neural responses and the post-task shock likelihood ratings, this data might not conclude a null effect of pathological anxiety on physiological fear responses. Previous research reports that pupil dilation elicited by affective stimuli reaches at a maximum level at around 2-3 s after onsets of auditory stimuli (Partala and Surakka, 2003). A comparison study reveals the pupil dilation by emotional arousal is slower than skin conductance and heart rate (Bradley et al., 2008). Our study design of 2-s cue presentation thus may not be enough for us to see subtle differences of GAD vs. controls. Furthermore, the fact that luminosity of all screens was not equal could be another confounding.

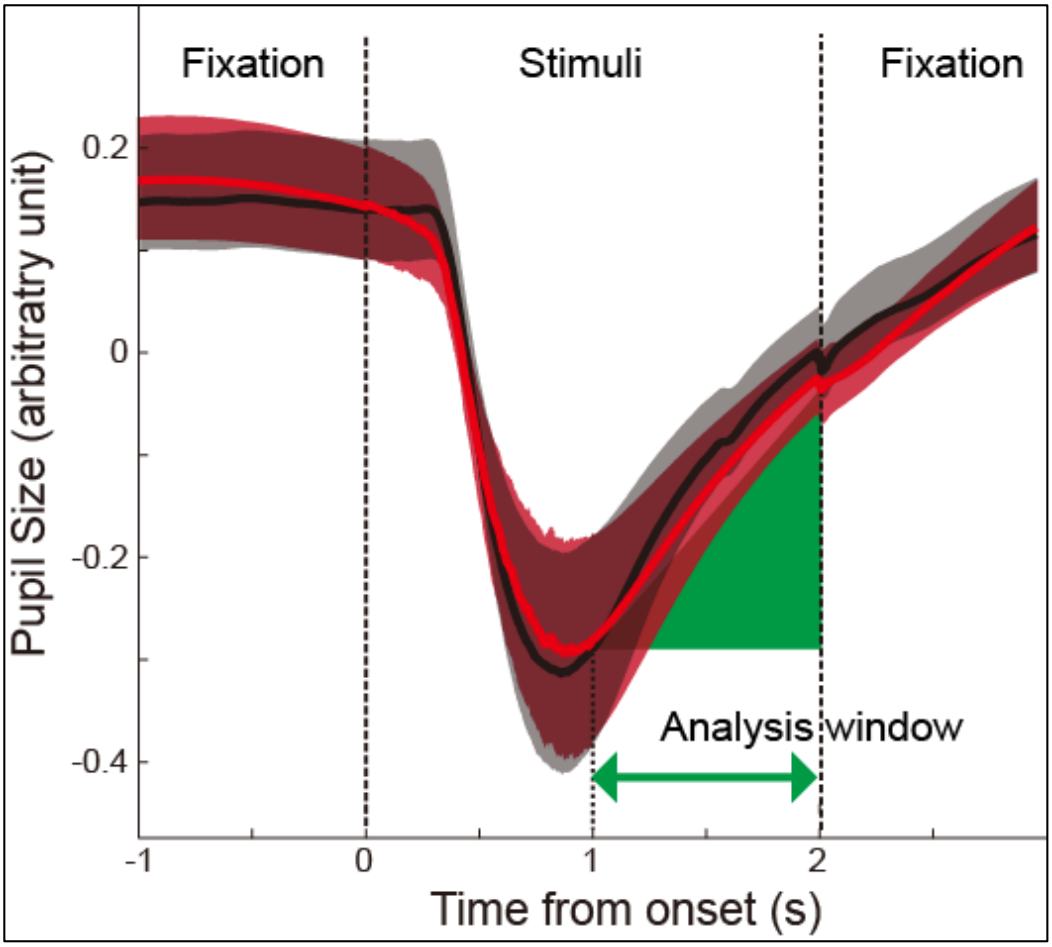

Figure 5.1. Averaged pupil size time course during fear generalization. Following a stimuli onset, a sharp initial pupil constriction occurred, peaked at around one second after the onset. Cumulative pupil size changes (i.e., area under curve; depicted as green shaded are) were measured from 1-2 s after the onset. Red line, GAD; black line, controls. Shaded areas denote one sem.

Functional Magnetic Resonance Imaging

We measured the blood oxygenation level-dependent (BOLD) response to the generalization task on the stimulus vs. rest contrast. The GAD group showed greater VTA activation compared with healthy controls at a corrected $P < 0.05$ (peak z = 3.29, peak $P = 0.0005$; MNI, 2 -18 -14; **Figure 5.2**). Post-hoc analyses on extracted BOLD estimates revealed a differential generalization gradient across groups [group × stimuli interaction, $F(2,178) = 3.31$, $P = 0.04$, repeated-measures ANOVA]: activation of healthy controls' VTA linearly tracked cue similarities to CS (beta = 0.57, $P = 0.01$, a post-hoc linear trend analysis), but not in patients ($P > 0.6$), which resulted from a heightened reactivity to GS ($P = 0.00005$), but not CS ($P > 0.479$). These results suggest that pathological anxiety is associated with elevated and indiscriminative VTA reactivity to GS.

The results of the hyper-reactive VTA in the GAD group raised the question of whether the putative dopaminergic VTA activity would correlate with activity of the mesocorticolimbic dopaminergic circuit (Lisman and Grace, 2005; Lodge and Grace, 2006; Shohamy and Wagner, 2008; Lammel et al., 2012; Stamatakis and Stuber, 2012). To this end, we measured functional connectivity modulated by "CS-Rest" or "GS-Rest" using psychophysiological interaction (PPI) analysis (Fairhurst et al., 2007; Matsumoto and Hikosaka, 2009). We used a functionally defined VTA mask based on the group difference as our seed region,

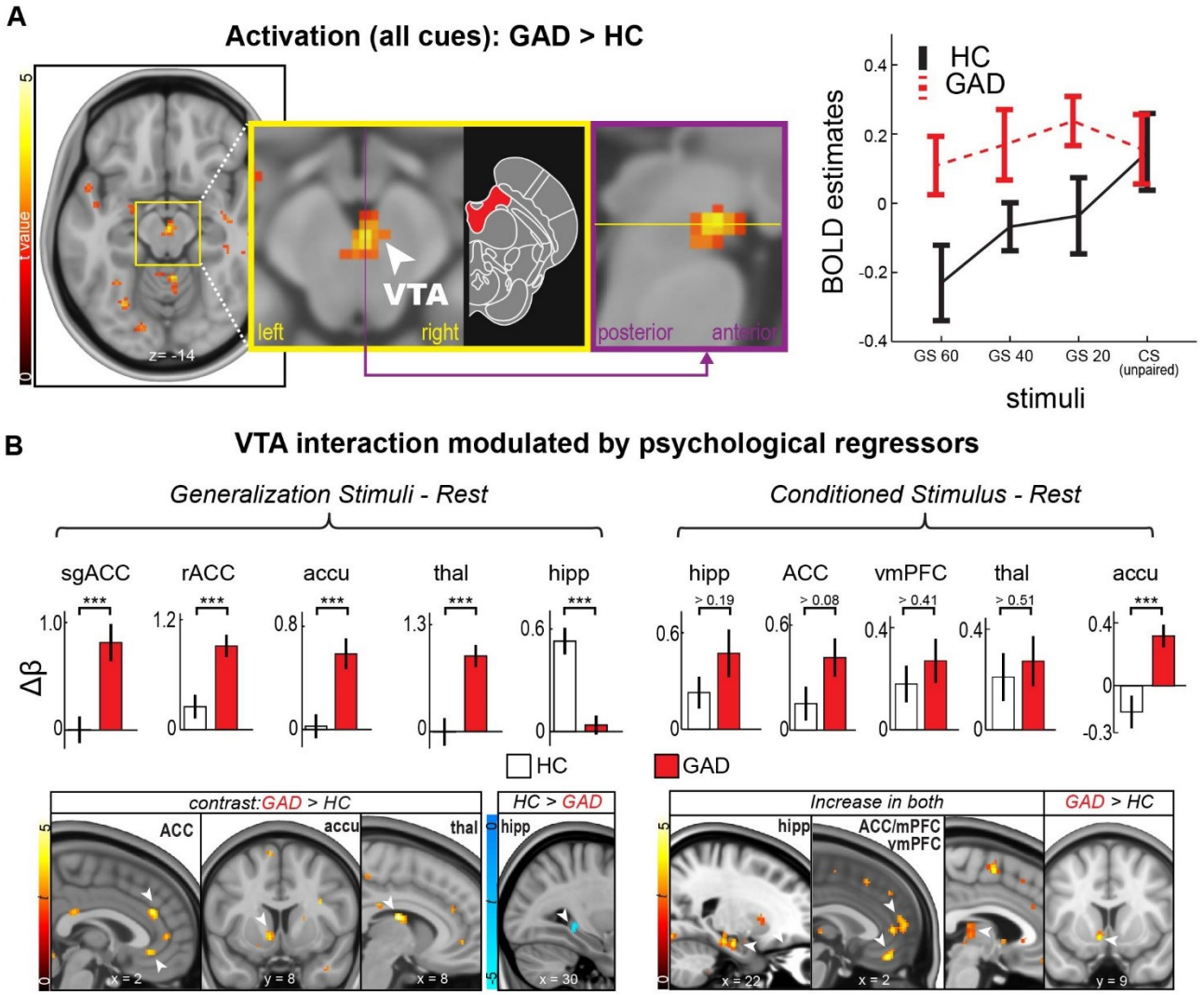
A
Activation (all cues): GAD > HC
t value
z= -14
VTA
left
right
posterior
anterior
HC
GAD
BOLD estimates
GS 60
GS 40
GS 20
CS (unpaired)
stimuli
B
VTA interaction modulated by psychological regressors
Generalization Stimuli - Rest
Conditioned Stimulus - Rest
sgACC
rACC
accu
thal
hipp
ACC
vmPFC
Δβ
HC
GAD
contrast:GAD > HC
HC > GAD
Increase in both
GAD > HC
ACC/mPFC
vmPFC
x = 2
y = 8
x = 8
x = 30
x = 22
y = 9

Figure 5.2. Heightened VTA reactivity and altered mesocorticolimbic interaction in Generalized Anxiety Disorder. *A*, Heightened VTA reactivity in GAD patients, compared with healthy controls, to all stimuli. Magnified views of the medial VTA cluster are shown in a coronal (a yellow panel) and a sagittal view (a purple panel). A schematic depiction of the midbrain with the VTA is shown in red (modified from (Naidich et al., 2009). We found greater VTA activation in GAD to GS ($P = 5\times10^{-5}$), but not CS ($P > 0.48$; one-tailed t-test), compared with controls. *B*, Psychophysiological-interaction analyses were performed to examine the effects of a psychological modulator (i.e., either "GS -Rest" or "CS-Rest") on VTA interaction. The "GS-Rest" contrast increased VTA interactions with the subgenual and rostral ACC, accumbens, and thalamus in patients with GAD and significantly decreased VTA interactions with the hippocampus. The "CS-Rest" contrast, on the other hand, significantly increased VTA interactions with the hippocampus, ACC, vmPFC, and thalamus in both groups, with the exception of interaction with the accumbens, which was not significant in healthy controls but was significant in patients with GAD. The voxel-wise results were significant at ROI-corrected $P < 0.005$. Mean differences of selected voxels were examined by Mann-Whitney U test (significances denoted in the bar graphs). Confidence interval, ± 1 SE. ***, $P < 0.001$. accu, accumbens; hipp, hippocampus; rACC, rostral anterior cingulate cortex; sgACC, subgenual anterior cingulate cortex; thal, thalamus.

and either "CS-Rest" or "GS-Rest" as a psychological regressor. In both groups, "CS-Rest" significantly increased VTA interactions with prefrontal areas (i.e., medial PFC/anterior cingulate cortex & vmPFC), the hippocampus, and the thalamus (ROI corrected $P < 0.005$; **Figure 5.2**; **Table 5.1**); no group differences were found in these regions. However, we observed a group difference in the VTA-accumbens interaction, where GAD patients showed a significant increase in connectivity but healthy controls did not. No significant decreases were observed in either group. These results suggest that activation of mesocorticolimbic dopaminergic circuit may be linked to threat encoding.

In contrast, we expected that the "GS-Rest" contrast would elicit group differences in this circuit based on abnormally heightened VTA BOLD activation in response to GS in GAD patients compared with healthy controls. Indeed, we found a significant increase in VTA interaction with the anterior cingulate cortex (rostral and subgenual), the accumbens, and the thalamus in GAD at ROI corrected $P < 0.005$, but not in healthy controls. On the other hand, the "GS-Rest" significantly increased VTA-hippocampus interaction only in healthy controls, but not in GAD **(Figure 5.2; Table 5.1).** Thus, patients with GAD displayed a unique pattern of heightened VTA-mesocorticolimbic coupling and attenuated VTA-hippocampal coupling in GS.

Table 5.1. VTA interactions modulated by psychological regressors.

Name	cluster size	peak		MNI		
		z	*P*	x	Y	z
Modulator: Generalization Stimuli						
Contrast: GAD > Healthy Controls						
anterior cingulate cortex	61	3.77	7E-5	2	34	26
ventral striatum	36	3.46	3E-4	-8	8	-6
thalamus	84	4.48	3E-6	8	-8	18
accumbens	13	3.27	3.27	-4	0	-4
Contrast: Healthy Controls > GAD						
hippocampus	34	4.78	9E-6	30	-36	-6
Modulator: Conditioned Stimulus						
Contrast: GAD > Healthy Controls						
accumbens	63	3.46	3E-4	-8	10	-8
Contrast: Mean positive effects						
ventromedial PFC	131	4.35	6E-6	2	40	-16
medial PFC	290	4.15	1E-5	-4	56	8
anterior cingulate cortex	-	4.21	5E-5	2	44	6
hippocampus	33	3.81	6E-5	22	-14	-20
thalamus	137	3.25	5E-4	4	-20	6

*alpha of multiple correction in each ROI was set to 0.005.

Table 5.2. Demographics and clinical characteristics across patients and controls.

Variable	GAD Patients (n = 32)		Healthy Control Subject (n=25)		Significance
	Mean	SD	Mean	SD	
Age	22.3	5.14	21.3	4.56	$P > 0.5$
STAI-Trait*	55.1	10.08	37.5	6.52	$P < 0.001$
BDI*	22.3	12.66	4.8	3.54	$P < 0.001$
Anxiety Sensitivity	33.6	12.77	16.7	6.09	$P < 0.001$
Penn State Worry Questionnaire	40.0	19.93	22.5	8.61	$P < 0.001$
Intolerance of Uncertainty Scale	50.5	11.10	31.3	6.73	$P < 0.001$

*Data from (Greenberg et al., 2013a); †Mood and Anxiety Symptom Questionnaire

In relation to our previous reports on vmPFC dysfunction in patients with GAD (Greenberg et al., 2013a), we examined the relationship between the fear generalization gradient in the vmPFC and the VTA. The vmPFC fear generalization gradient, that is, a slope of linear fit on the fear generalization reactivity gradient (as a function of cue similarity to CS) did not show a correlation with the VTA fear generalization gradient either in patients or in healthy controls (Ps > 0.52; nonparametric correlation). Furthermore, we did not find significant correlations with the vmPFC generalization and our PPI measures (Ps > 0.25).

Discussion

In the present study, we demonstrate that in healthy controls, the magnitude of activation in the VTA is proportional to the similarity between potential threats and CS, and the mesocortical connectivity is significantly increased by CS. In pathological anxiety, however, the VTA is hyper-reactive to GS, compared with healthy controls. GS also elicit aberrant VTA connectivity with the prefrontal cortex (increased) and the hippocampus (decreased) in patients, compared with healthy controls. These results suggest that VTA activation and mesocortical connectivity are critical in threat processing, and that abnormalities of the dopaminergic system are implicated in clinical anxiety.

Healthy controls and patients with GAD alike show BOLD activations in the VTA towards the CS. This is in line with previous reports of dopaminergic VTA activation during the perception or anticipation of aversive stimuli (Fairhurst et al., 2007; Matsumoto and Hikosaka, 2009) as well as fear learning (Lammel et al., 2012; Brooks and Berns, 2013). Our results complement and expand these findings by demonstrating that dopaminergic VTA activation linearly tracks the perceived threat level. Furthermore, conditioned threat elicits VTA interaction with the prefrontal systems (e.g., the ACC, the dmPFC and the vmPFC) in both groups. This increase in the mesocortical interaction may represent activation of VTA dopaminergic projection to the prefrontal system during threat processing, as analogous to the animal model of the mesocortical dopaminergic aversion circuit: in this model, the medial VTA dopaminergic neurons that are selectively activated by glutamatergic inputs from the lateral habenula project to dopaminoreceptive medial prefrontal cortex and encode aversion (Lammel et al., 2012). Although our connectivity analysis does not provide directionality, this *a priori* knowledge about the functional circuit may allow us to interpret our finding as VTA aversion signaling to the dopaminoreceptive prefrontal system.

In contrast to healthy controls, patients with GAD show greater VTA activation to GS, but not to CS. This leads to a significant difference in the VTA generalization gradient: that is, a slope of the reactivity gradient to stimuli is

significantly different from zero (positive) in healthy controls, but not in patients with GAD. This effect is well in line with the hypothesis of overgeneralization of fear in pathological anxiety (Jovanovic and Ressler, 2010; Britton et al., 2011; Kheirbek et al., 2012; Greenberg et al., 2013a). It should be noted that, at least in animal models, excessive VTA dopaminergic activity is implicated in anxious behaviors (Coque et al., 2011b). Furthermore, increased VTA dopaminergic activity has been linked to vulnerability to social defeat in animal models (Krishnan et al., 2007). To the best of our knowledge, our results are the first to extend the findings of abnormal VTA signaling in animal models of anxiety to the human brain. Future research may investigate whether this increase in VTA BOLD reactivity is indeed correlated with dopamine activity.

We also found abnormal mesocorticolimbic interactions in GAD. Firstly, patients with GAD showed heightened mesocorticolimbic connectivity elicited by GS, compared with healthy controls. Considering the similar connectivity increase elicited by CS in healthy controls and patients alike, it is possible that this abnormally heightened connectivity indicates an excessive or uncontrolled VTA dopaminergic projection in clinical anxiety. This lends additional support to the abnormal dopamine aversion circuit in anxiety. It is worth noting that abnormalities in VTA dopamine signaling and mesocortical circuit activity are implicated in the pathophysiology of certain stress-related psychiatric diseases.

For example, in mice models, stress response due to repeated aggression mainly results in glucocorticoid release in dopaminoreceptive neurons promoting social aversion, of which expression requires an increase in VTA neuronal firing (Barik et al., 2013). Furthermore, mild isolation stress, in mice models, affects the mesocortical projection of dopaminergic neurons, wherein epigenetic control is elicited, that is, DNA hypermethylation of the tyrosine hydroxylase gene, a key regulator of dopamine synthesis (Niwa et al., 2013).

Secondly, the VTA-hippocampal connectivity elicited by GS is significantly attenuated in patients with GAD, compared with healthy controls. The hippocampus is known to regulate VTA dopaminergic activity, forming a VTA-hippocampal loop that is crucial in motivational learning and memory (Lisman and Grace, 2005; Lodge and Grace, 2006; Shohamy and Wagner, 2008). Our results may suggest that attenuation of this functional loop is associated with impaired threat-safety discrimination in pathological anxiety. This finding is also in line with a recent animal model implicating impaired hippocampal pattern separation—perhaps via restrained neurogenesis under stress—in fear generalization and pathophysiology of anxiety (Kheirbek et al., 2012). Together, our connectivity results thus support the idea that abnormalities of the mesocortical circuit contribute to the pathophysiology of fear overgeneralization in generalized anxiety disorder.

The present results advance the current understanding of the neural underpinnings of fear generalization. Several neuroimaging studies report neural correlates of fear generalization in humans including the cingulate cortex, insula, striatum, and limbic structures (Dunsmoor et al., 2011; Greenberg et al., 2013b; Lissek et al., 2013b). Studies with clinical anxiety document behavioral and/or neural evidence of fear generalization in various forms of anxiety disorder, such as panic disorder (Lissek et al., 2010), posttraumatic stress disorder (Jovanovic and Ressler, 2010), and generalized anxiety disorder (Greenberg et al., 2013a; Lissek et al., 2013a). In particular, we have previously reported the attenuated vmPFC threat processing in GAD; that is, indiscriminating vmPFC BOLD reactivity to the fear generalization stimuli compared with healthy controls (Greenberg et al., 2013a). Admittedly, in the present study, we did not observe a direct link between the vmPFC dysfunction and the abnormal VTA reactivity or connectivity. However, given the extensive literature on the essential role of the two interacting systems (or perhaps mediated by the dorsolateral PFC) in the adaptive behavior (Schoenbaum et al., 2009; Takahashi et al., 2009; Ballard et al., 2011; Takahashi et al., 2011; D'Ardenne et al., 2012), the interaction of the two regions may be still important in fear generalization and perhaps pathophysiology of anxiety. To address this more directly, a combination of fear generalization task and a direct stimulation of the vmPFC while monitoring the midbrain activity would an interesting study (Cf. (D'Ardenne et al., 2012). Altogether, our findings

in the present study contribute to a more complete picture of the pathophysiology of clinical anxiety.

CHAPTER VI

Summary and Concluding Remarks

Summary of Major Findings:

In this dissertation, I investigated neural underpinnings of anxiety and anxiety disorder using human neuroimaging. More specifically, as threat processing involves coordination among various distributed brain systems, circuit-wide abnormalities are likely to play a role in onset or development of maladaptive control of threat. I have used complementary approaches such as multi-modal Magnetic Resonance Imaging (MRI), genotyping, and statistical modeling combined with cognitive paradigms to test this brain connectivity model in anxiety or an anxiety-related behavior. Therefore, the ultimate goal of this dissertation was to map a specific dimension of complex anxiety symptomatology onto observable and objective factors including genetic factor, brain regions and circuits. To that end, I focused on two distinct constructs within the negative valence system that are particularly relevant to onset and development of anxiety disorder, following Research Domain Criteria (Insel et al., 2010; Sanislow et al., 2010); that is, reactivity to imminent threat ("fear") and to distal threat ("anxiety"). First, in Chapter 2 and 3, to elicit behavioral response to imminent threat in healthy individuals, I used a cognitive task to elicit phasic attention

orientation towards negative affect-valence faces, called negative attention bias. I then demonstrated that structural and functional connectivity between the amygdala and the ACC account for individual differences in the behavioral measurement of negative attention bias. Moreover, I found a significant impact of a genetic variability (i.e., BDNF Val66Met polymorphism) on the amygdala-PFC white matter tract microstructure measured by diffusion MRI, which appeared to mediate the negative attention behavior. Second, in Chapter 4, I focused on reactivity to distal and uncertain threat ("anxiety") using a modified Pavlovian conditioning to contextual threat. For this study, we recruited patients with an anxiety spectrum disorder (i.e., generalized anxiety disorder or GAD). Using multi-modal MRI, I demonstrated that attenuation of the vmPFC functioning in patients with GAD, previously reported by our group (Greenberg et al., 2013a), is closely related to multiple neural features ranging from grey matter thickness to vmPFC connectivity with distributed brain regions. Furthermore, I found these neural factors all together significantly account for clinical anxiety, an effect appeared to be mediated by vmPFC fear generalization. This led to a multi-hit model for pathophysiology of anxiety disorder. Last, in Chapter 5, I report novel evidence that the midbrain VTA and its connectivity with the corticolimbic circuit (i.e., the mesocorticolimbic circuit) are involved with fear generalization in anxiety disorder. Patients with GAD showed a significant increase in BOLD reactivity of the VTA and the mesocorticolimbic connectivity during fear

generalization, whereas healthy controls showed a linear increase in the VTA reactivity proportional to threat level (tracking the threat level, in other words) and an increase in the mesocorticolimbic connectivity to CS, but not GS. These suggest, first, the role of dopamine in threat processing in a normal state and, second, the link between its abnormal behavior and clinical anxiety; the brain circuitry of anxiety should thus include this crucial neuromodulatory system.

Final Model of the Amygdala–ACC Network in Negative Attention Bias.

A Number of studies report the perigenual anterior cingulate cortex (pgACC) as a ***controller*** in close relation with anterior midcingulate cortex (Op de Beeck et al., 2008; Orr and Weissman, 2009; Venkatraman et al., 2009; Etkin et al., 2011; Grupe and Nitschke, 2011; Nee et al., 2011). According to this model, the pgACC and aMCC, perhaps along with a functional continuation, implements behavioral control in response to amygdalar inputs (Shackman et al., 2011). This so-called 'adaptive control hypothesis' based on anatomical, functional data and computational models dictates that the aMCC integrate information to control negatively motivated actions.

Studies presented in Chapter II and III may partially lend a support to this model in bottom-up attention bias to threat. The uncinate fasciculus is a prominent anatomical route of the amygdala–ACC (as well as other prefrontal

regions). As an amygdalar input of threat likely transmits via the UF to the ACC –bottom-up way–, dACC or pgACC may first detect this phasic threat information and then perhaps influence dorsally adjacent aMCC to produce a behavioral control, that is, an attention allocation towards fearful face. Alternatively, pgACC might directly involve attentional control without an aMCC recruitment; a previous study reporting coactivation of the amygdala and the pgACC during the negative attention bias supports this interpretation (Carlson et al., 2009b). A non-explicit cognitive demand in our behavioral paradigm may primarily recruit pgACC, which is considered as an affective region –as opposed to cognitive aMCC– to produce rapid attention modulation at preconscious level.

It is worth noting that a positive amygdala–ACC intrinsic functional coupling should not be interpreted as direct evidence of an excitatory connectivity. In fact, the amygdala–ACC network is notorious for diverse connectivity across different ACC subregions and/or in different contexts (Shackman et al., 2011). Furthermore, representation of connectivity is also dependent upon methodology. For example, fMRI-based connectivity is usually a mixture of complex dynamics between excitatory and inhibitory components for a longer period (i.e., typically a few seconds long). Given these, our results should be interpreted as that basal connection properties of this network, regardless of contexts, is closely associated with individual differences in microstructure of the

anatomical substrate and negative attention bias behavior. Our results may thus provide a useful account for future neuroimaging research in anxiety-related behavior in that intrinsic functional connectivity mapping, a convenient and standardizable method, provide a useful measure that correlates with structural connectivity and behavior alike.

Altogether, studies in the Chapter II and III support the model that the bottom-up amygdalar threat information at preconscious or nonconscious level influences the pgACC, which then allocates the spatial attention without apparent cognitive appraisal. A crucial link of this brain–behavior relationship to anxiety is that Met allele in the BDNF Val66Met polymorphism is associated with a greater fiber integrity, which then contributes to a greater negative attention bias. Although causality of these relationships may remain to be validated, this likely gene–brain–behavior mechanism may provide much needed framework for the future research in pathophysiology of anxiety.

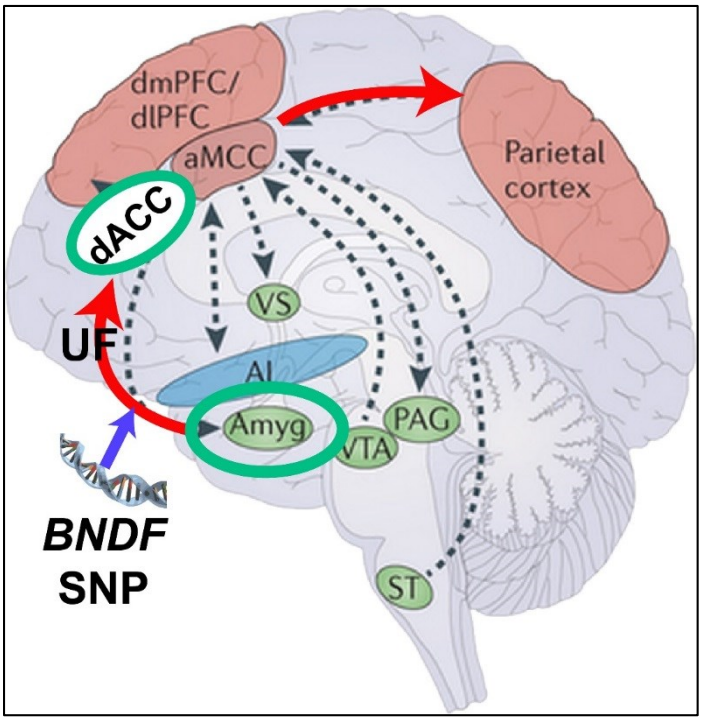

Figure 6.1. Brain circuitry of imminent threat: Final amygdala–ACC connectivity model of negative attention bias. In addition to the ACC-centric anxiety circuitry, our results presented in the Chapter II and III suggest a crucial role of the amygdala–dACC (or perigenual ACC in often cases) connectivity both in structural and functional indices. Together with previous literatures, our results suggest that a bottom-up amygdalar input to the dACC primarily, which then elicits an attentional control to imminent threat stimuli, presumably via an interaction with the adjacent anterior midcingulate cortex and the parietal-visual system. Moreover, the impacts of the BDNF polymorphism onto the structural connectivity of the uncinate fasciculus and the negative attention bias may suggest that abnormalities of this circuitry accounts for potential pathophysiology of anxiety. SNP, single nucleotide polymorphism; UF, uncinate fasciculus. (Modified from Grupe and Nitschke,, 2013).

Integrated Brain Circuit of Fear Generalization

I propose an integrated model for pathophysiology of clinical anxiety based on the results from the fear generalization studies in Chapter 4 and 5. The brain circuit of fear generalization includes the vmPFC-centric corticolimbic circuit and the putative dopaminergic aversion circuit. The two systems are closely related to each other, as I reviewed in Discussion in Chapter 5; the vmPFC integrates various inputs, mediates discrimination of safety vs. threat, and gates subsequent controlling signals to autonomic nervous systems (i.e., sympathetic vs. parasympathetic activation).

Along the acquisition of the clinical anxiety, the mesocorticolimbic dopamine circuit may first go awry most likely through excessive and uncontrollable threat-stress response, that is glucocorticoid signaling. As reviewed in Chapter 1, recent animal studies highlight this; however, this has yet to be translated in humans to my best knowledge.

The aberrant dopamine aversion circuit then may influence the vmPFC, afferents, or efferents to the vmPFC (e.g., ACC to vmPFC). Of note, as our connectivity results show, impacts are most probably multiple and parallel, which perhaps partially explains complex pathophysiology of anxiety disorder. Finally,

integrative effects of the circuit-wide features may be onto the vmPFC, resulting the vmPFC fear generalization.

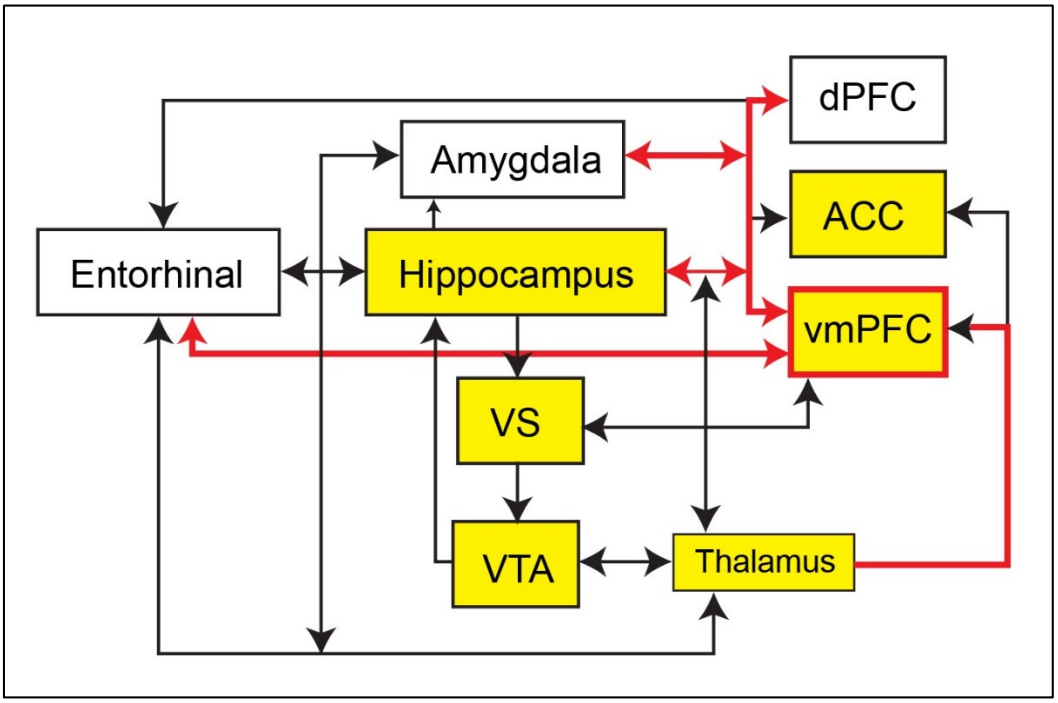

Figure 5.3. Brain circuitry of potential threat: Final connectivity model of overgeneralization of conditioned fear. Dopaminergic circuit is in yellow. Corticolimbic connectivity that may result vmPFC fear generalization is in red arrows.

Significances, Limitations, and Future Directions

Brain Connectivity Model of Imminent Threat

The studies presented in Chapter 2 and 3 demonstrate a more complete picture of neural substrates of negative attention bias, one of the crucial factors of anxiety vulnerability (Fox, 2002; Mathews and MacLeod, 2002; Mogg and Bradley, 2002). First, the gene-brain-behavior relationship well supports the previous literatures on involvement of BDNF SNP in the white matter structure (Chiang et al., 2011; Voineskos et al., 2011; Tost et al., 2013), in affect processing in the limbic regions (Montag et al., 2008), and in mood disorders (Martinowich and Lu, 2008; Lau et al., 2010; Montag et al., 2010b). Moreover, the present results further suggest a likely pathway of this genetic risk factor to development or vulnerability to anxiety. Although a number of studies have already examined impacts of various SNPs on brain connectivity, the present studies illustrate that such attempts can be potentially complemented by robust cognitive paradigms, in order to link variability in the biological factors to psychiatric or psychological processes. Our study thus may provide a useful methodology for future research.

These studies may also contribute to development of a novel biomarker or a treatment strategy for clinical anxiety. For example, in case of individuals with

high negative attention bias, who may already manifest related symptoms, examining their BDNF Val66Met SNP and fiber integrity of the uncinate fasciculus may lead to a more precise and an individualized diagnosis. Moreover, the prefrontal vicinity of the uncinate fasciculus, based on the results from Chapter 3, can be potentially used as a target site for brain stimulation such as transcranial magnetic stimulation to modulate neural activity that is relevant to the non-conscious attention bias to threat [in literature, brain stimulation is often targeted onto the major white matter tracts as in example of pain research (e.g., the corticospinal tract) or deep brain stimulation to treat chronic depression (e.g., the limbic-prefrontal tract)]. Future research may include identification of potential target sites within the uncinate fasciculus and investigation of neural and behavioral impacts of stimulation.

One of the limitations of these studies, as in human neuroimaging research in general, is that we do not provide neurobiological mechanisms of changes in white matter microstructure or diffusion parameters. Studies show that it may depend on a scale of measurement (i.e., voxel-wise or tract-wise). If so, it is indeed a non-trivial task to find neurobiological correlates of a diffusion parameter averaged across an entire major white matter tract, unless one can get a reliable neurobiological measure of an entire white matter tract, such as averaged axonal diameters, numbers of fibers, or degrees of fasciculate. Moreover,

differences between actual and virtual dissection (i.e., probabilistic tractography) have yet to be fully understood. Future research should consider careful comparison studies in non-human primates or human post-mortem brains.

Role of Dopamine in Aversion and Anxiety

The study in Chapter 5 opened the door of dopamine's role in clinical anxiety in humans for the first time. This fear generalization-fMRI study will foster a variety of future research to better understand cellular and neuromodulatory underpinnings of abnormal VTA BOLD reactivity and connectivity in anxiety during fear generalization.

First, dopamine receptor imaging such as PET or SPECT, ideally combined with the fear generalization paradigm and fMRI, would be beneficial. Simultaneous PET/fMRI experiments during the fear generalization in anxious individuals will give a direct account whether dopamine receptor availability is correlated with putative midbrain dopaminergic BOLD (hyper-)activation in anxiety. The generalization fMRI data in Chapter 4 and 5 shows that GAD patients' midbrain VTA is constantly hyper-reactive during all contextual threat cues, which is equivalent to 75 % of entire trials (15 min long). Because of this, PET imaging during fear generalization task may effectively detect changes in dopaminergic receptor availability.

Second, a more indirect approach is computational modeling of fear generalization. Learning algorithms, such as model-based Bayesian modeling, have been applied in human research to model reward prediction error. As fear generalization can be viewed as a maladaptive prediction of punishment, Bayesian learning algorithms can be used to investigate impacts of anxiety in the by comparing data from patients versus controls. Recently proposed Hierarchical Gaussian Filtering (Mathys et al., 2011) would be particularly useful, in that it is more flexible than previously used Bayesian methods, such as Hidden Markov Model, in terms of modeling individual differences or different (hierarchical) levels of representation of adaptive behaviors across brain regions.

Alternatively, the stimulus generalization task can be combined with a pharmacological challenge using L-dopa in healthy individuals. Acute application of L-dopa prior to contextual fear conditioning may induce significant changes in threat/safety discriminability, which may be monitored by startle reflex and/or fMRI. Interestingly, a recent study by the Kalisch group in Germany (Haaker et al., 2013) reports an L-dopa application prior to a safety experience enhance fear extinction. I propose that a dopamine increase with or withdrawal of negative reinforcement (or anticipation of one) may have completely different consequences. In both cases, dopamine may stimulate the on-going process.

Moreover, chronic lithium treatment on mood disorder patients (e.g., anxiety, bipolar or mania) may be linked to normalization of abnormal VTA dopamine firing. A recent study using mice genetic model of mania shows this (Coque et al., 2011a). Thus, it could be possible to use the fear generalization paradigm as a tool to show the effects of lithium on the dopaminergic circuits in particular case of anxiety patients.

A novel direction may be combining these pharmacological challenges with computational modeling. It would be interesting if a learning algorithm can model effects of a dopamine-related drug on stimuli generalization, for it will give us a hint about the underlying neural mechanism.

Third, neural substrates of positive or negative motivation have yet to be fully understood. In humans, this circuit still largely remains unknown. There is an absolute need for 7T fMRI research to investigate the details of this circuit. For example, in relation to our VTA hyper-reactivity in GAD, one of the potential source of VTA dopaminergic firing is the glutamatergic inputs from the lateral habenula. This epithalamic structure is extremely small, so highly susceptible for a partial volume effect in 3T EPI data. Some previous literatures link this structure to motivation in humans based on 3T EPI; however, reliability of such studies is questionable. 7T fMRI has much higher signal-to-noise ratio, which allows single subject analyses. This is extremely advantageous, as no spatial

normalization or warping EPI would be necessary; it will allow identification of anatomical foci with much greater precision. 7T fMRI thus can significantly enhance our understandings on this crucial circuit.

Last, more complete understanding on the link between anxiety and the dopaminergic circuit will lead to development of a new treatment strategy. For example, real-time fMRI with biofeedback of VTA activation level during fear generalization task can effectively normalize VTA activation in anxious individuals. In addition, electric stimulation using transcranial magnetic stimulation or direct current stimulation on the prefrontal cortex that is believed to be part of dopaminergic aversion circuit can affect VTA activation pattern during fear generalization. These intervention studies should be based on the precise mapping of mesocorticolimbic circuit in humans, ideally at a single subject level. Thus, this inevitably requires the ultra-high resolution fMRI (7 Tesla) that has several magnitude-fold better signal-to-noise ratio, compared with 3T fMRI.

REFERENCES

Adler CM, Holland SK, Schmithorst V, Wilke M, Weiss KL, Pan H, Strakowski SM (2004) Abnormal frontal white matter tracts in bipolar disorder: a diffusion tensor imaging study. Bipolar Disorders 6:197-203.

Adolphs R (2004) Emotional vision. Nat Neurosci 7:1167-1168.

Adolphs R, Damasio H, Tranel D, Cooper G, Damasio AR (2000) A role for somatosensory cortices in the visual recognition of emotion as revealed by three-dimensional lesion mapping. Journal of Neuroscience 20:2683-2690.

Adolphs R, Tranel D, Hamann S, Young AW, Calder AJ, Phelps EA, Anderson A, Lee GP, Damasio AR (1999) Recognition of facial emotion in nine individuals with bilateral amygdala damage. Neuropsychologia 37:1111-1117.

Amaral DG, Price JL (1984) Amygdalo-Cortical Projections in the Monkey (Macaca-Fascicularis). J Comp Neurol 230:465-496.

American Psychiatric Association., American Psychiatric Association. Task Force on DSM-IV. (2000) Diagnostic and statistical manual of mental disorders : DSM-IV-TR, 4th Edition. Washington, DC: American Psychiatric Association.

Anstrom KK, Miczek KA, Budygin EA (2009) Increased phasic dopamine signaling in the mesolimbic pathway during social defeat in rats. Neuroscience 161:3-12.

Armony JL, Dolan RJ (2002) Modulation of spatial attention by fear-conditioned stimuli: an event-related fMRI study. Neuropsychologia 40:817-826.

Armony JL, Corbo V, Clement MH, Brunet A (2005) Amygdala response in patients with acute PTSD to masked and unmasked emotional facial expressions. Am J Psychiatry 162:1961-1963.

Ayling E, Aghajani M, Fouche JP, van der Wee N (2012a) Diffusion Tensor Imaging in Anxiety Disorders. Current Psychiatry Reports 14:197-202.

Ayling E, Aghajani M, Fouche JP, van der Wee N (2012b) Diffusion Tensor Imaging in Anxiety Disorders. Curr Psychiatry Rep 14:197-202.

Baas D, Aleman A, Kahn RS (2004) Lateralization of amygdala activation: a systematic review of functional neuroimaging studies. Brain Res Brain Res Rev 45:96-103.

Baliki MN, Geha PY, Fields HL, Apkarian AV (2010) Predicting value of pain and analgesia: nucleus accumbens response to noxious stimuli changes in the presence of chronic pain. Neuron 66:149-160.

Ballard IC, Murty VP, Carter RM, MacInnes JJ, Huettel SA, Adcock RA (2011) Dorsolateral prefrontal cortex drives mesolimbic dopaminergic regions to initiate motivated behavior. J Neurosci 31:10340-10346.

Barik J, Marti F, Morel C, Fernandez SP, Lanteri C, Godeheu G, Tassin JP, Mombereau C, Faure P, Tronche F (2013) Chronic stress triggers social aversion via glucocorticoid receptor in dopaminoceptive neurons. Science 339:332-335.

Barlow DH (2002) Anxiety and its disorders : the nature and treatment of anxiety and panic, 2nd Edition. New York: Guilford Press.

Bassett DS, Bullmore ET (2009) Human brain networks in health and disease. Curr Opin Neurol 22:340-347.

Baumgartner T, Knoch D, Hotz P, Eisenegger C, Fehr E (2011) Dorsolateral and ventromedial prefrontal cortex orchestrate normative choice. Nat Neurosci 14:1468-1474.

Beaver JD, Mogg K, Bradley BP (2005) Emotional conditioning to masked stimuli and modulation of visuospatial attention. Emotion 5:67-79.

Beevers CG, Wells TT, McGeary JE (2009) The BDNF Val66Met Polymorphism Is Associated With Rumination in Healthy Adults. Emotion 9:579-584.

Beevers CG, Gibb BE, McGeary JE, Miller IW (2007) Serotonin transporter genetic variation and biased attention for emotional word stimuli among psychiatric inpatients. J Abnorm Psychol 116:208-212.

Behrens TE, Woolrich MW, Jenkinson M, Johansen-Berg H, Nunes RG, Clare S, Matthews PM, Brady JM, Smith SM (2003) Characterization and propagation of uncertainty in diffusion-weighted MR imaging. Magn Reson Med 50:1077-1088.

Behzadi Y, Restom K, Liau J, Liu TT (2007) A component based noise correction method (CompCor) for BOLD and perfusion based fMRI. Neuroimage 37:90-101.

Berton O, McClung CA, Dileone RJ, Krishnan V, Renthal W, Russo SJ, Graham D, Tsankova NM, Bolanos CA, Rios M, Monteggia LM, Self DW, Nestler EJ (2006) Essential role of BDNF in the mesolimbic dopamine pathway in social defeat stress. Science 311:864-868.

Bishop S, Duncan J, Brett M, Lawrence AD (2004) Prefrontal cortical function and anxiety: controlling attention to threat-related stimuli. Nat Neurosci 7:184-188.

Bishop SJ (2009) Trait anxiety and impoverished prefrontal control of attention. Nat Neurosci 12:92-98.

Boorman ED, Behrens TE, Woolrich MW, Rushworth MF (2009) How green is the grass on the other side? Frontopolar cortex and the evidence in favor of alternative courses of action. Neuron 62:733-743.

Botvinick M, Nystrom LE, Fissell K, Carter CS, Cohen JD (1999) Conflict monitoring versus selection-for-action in anterior cingulate cortex. Nature 402:179-181.

Bradley MM, Miccoli L, Escrig MA, Lang PJ (2008) The pupil as a measure of emotional arousal and autonomic activation. Psychophysiology 45:602-607.

Britton JC, Lissek S, Grillon C, Norcross MA, Pine DS (2011) Development of anxiety: the role of threat appraisal and fear learning. Depress Anxiety 28:5-17.

Bromberg-Martin ES, Matsumoto M, Hikosaka O (2010) Dopamine in motivational control: rewarding, aversive, and alerting. Neuron 68:815-834.

Brooks AM, Berns GS (2013) Aversive stimuli and loss in the mesocorticolimbic dopamine system. Trends Cogn Sci.

Bryant RA, Kemp AH, Felmingham KL, Liddell B, Olivieri G, Peduto A, Gordon E, Williams LM (2008) Enhanced amygdala and medial prefrontal activation during nonconscious processing of fear in posttraumatic stress disorder: An fMRI study. Hum Brain Mapp 29:517-523.

Buckner RL, Krienen FM, Yeo BT (2013) Opportunities and limitations of intrinsic functional connectivity MRI. Nat Neurosci 16:832-837.

Bush G, Luu P, Posner MI (2000) Cognitive and emotional influences in anterior cingulate cortex. Trends Cogn Sci 4:215-222.

Cannistraro PA, Makris N, Howard JD, Wedig MM, Hodge SM, Wilhelm S, Kennedy DN, Rauch SL (2007) A diffusion tensor imaging study of white matter in obsessive–compulsive disorder. Depression and Anxiety 24:440-446.

Carlson JM, Reinke KS (2008) Masked fearful faces modulate the orienting of covert spatial attention. Emotion 8:522-529.

Carlson JM, Reinke KS (2010) Spatial attention-related modulation of the N170 by backward masked fearful faces. Brain Cogn 73:20-27.

Carlson JM, Fee AL, Reinke KS (2009a) Backward Masked Snakes and Guns Modulate Spatial Attention. Evolutionary Psychology 7:527-537.

Carlson JM, Reinke KS, Habib R (2009b) A left amygdala mediated network for rapid orienting to masked fearful faces. Neuropsychologia 47:1386-1389.

Carlson JM, Greenberg T, Mujica-Parodi LR (2010) Blind rage? Heightened anger is associated with altered amygdala responses to masked and unmasked fearful faces. Psychiatry Res 182:281-283.

Carlson JM, Cha J, Mujica-Parodi LR (2013a) Functional and structural amygdala - Anterior cingulate connectivity correlates with attentional bias to masked fearful faces. Cortex 49:2595-2600.

Carlson JM, Reinke KS, LaMontagne PJ, Habib R (2011a) Backward masked fearful faces enhance contralateral occipital cortical activity for visual

targets within the spotlight of attention. Social Cognitive and Affective Neuroscience 6:639-645.

Carlson JM, Reinke KS, LaMontagne PJ, Habib R (2011b) Backward masked fearful faces enhance contralateral occipital cortical activity for visual targets within the spotlight of attention. Soc Cogn Affect Neur 6:639-645.

Carlson JM, Mujica-Parodi LR, Harmon-Jones E, Hajcak G (2012a) The Orienting of Spatial Attention to Backward Masked Fearful Faces Is Associated With Variation in the Serotonin Transporter Gene. Emotion 12:203-207.

Carlson JM, Cha J, Harmon-Jones E, Mujica-Parodi LR, Hajcak G (2013b) Influence of the BDNF Genotype on Amygdalo-Prefrontal White Matter Microstructure is Linked to Nonconscious Attention Bias to Threat. Cereb Cortex.

Carlson JM, Beacher F, Reinke KS, Habib R, Harmon-Jones E, Mujica-Parodi LR, Hajcak G (2012b) Nonconscious attention bias to threat is correlated with anterior cingulate cortex gray matter volume: A voxel-based morphometry result and replication. Neuroimage 59:1713-1718.

Catani M, Howard RJ, Pajevic S, Jones DK (2002) Virtual in vivo interactive dissection of white matter fasciculi in the human brain. Neuroimage 17:77-94.

Cha J, Greenberg T, Carlson JM, Dedora D, Hajcak G, Mujica-Parodi LR (in revision) Circuit-wide Structural and Functional Factors of Ventromedial Prefrontal Fear Response and Contribution to Anxiety Disorder.

Chantarujikapong SI, Scherrer JF, Xian H, Eisen SA, Lyons MJ, Goldberg J, Tsuang M, True WR (2001) A twin study of generalized anxiety disorder symptoms, panic disorder symptoms and post-traumatic stress disorder in men. Psychiatry Res 103:133-145.

Chen ZY, Jing D, Bath KG, Ieraci A, Khan T, Siao CJ, Herrera DG, Toth M, Yang C, McEwen BS, Hempstead BL, Lee FS (2006) Genetic variant BDNF (Val66Met) polymorphism alters anxiety-related behavior. Science 314:140-143.

Chiang MC, Barysheva M, Toga AW, Medland SE, Hansell NK, James MR, McMahon KL, de Zubicaray GI, Martin NG, Wright MJ, Thompson PM (2011) BDNF gene effects on brain circuitry replicated in 455 twins. Neuroimage 55:448-454.

Chib VS, Rangel A, Shimojo S, O'Doherty JP (2009) Evidence for a common representation of decision values for dissimilar goods in human ventromedial prefrontal cortex. J Neurosci 29:12315-12320.

Clark LA, Watson D (1991) Tripartite model of anxiety and depression: psychometric evidence and taxonomic implications. J Abnorm Psychol 100:316-336.

Coelho HF, Cooper PJ, Murray L (2007) A family study of co-morbidity between generalized social phobia and generalized anxiety disorder in a non-clinic sample. J Affect Disord 100:103-113.

Cohen JY, Haesler S, Vong L, Lowell BB, Uchida N (2012) Neuron-type-specific signals for reward and punishment in the ventral tegmental area. Nature 482:85-88.

Collier DA et al. (1996) A novel functional polymorphism within the promoter of the serotonin transporter gene: possible role in susceptibility to affective disorders. Mol Psychiatry 1:453-460.

Coque L et al. (2011a) Specific role of VTA dopamine neuronal firing rates and morphology in the reversal of anxiety-related, but not depression-related behavior in the ClockDelta19 mouse model of mania. Neuropsychopharmacology 36:1478-1488.

Coque L et al. (2011b) Specific role of VTA dopamine neuronal firing rates and morphology in the reversal of anxiety-related, but not depression-related behavior in the ClockDelta19 mouse model of mania. Neuropsychopharmacol 36:1478-1488.

Critchley HD, Nagai Y, Gray MA, Mathias CJ (2011) Dissecting axes of autonomic control in humans: Insights from neuroimaging. Auton Neurosci 161:34-42.

Cross L, Brown MW, Aggleton JP, Warburton EC (2012) The medial dorsal thalamic nucleus and the medial prefrontal cortex of the rat function

together to support associative recognition and recency but not item recognition. Learn Mem 20:41-50.

Cuthbert B, Insel T (2010a) The data of diagnosis: new approaches to psychiatric classification. Psychiatry 73:311-314.

Cuthbert BN, Insel TR (2010b) Toward new approaches to psychotic disorders: the NIMH Research Domain Criteria project. Schizophr Bull 36:1061-1062.

Cuthbert BN, Kozak MJ (2013) Constructing constructs for psychopathology: the NIMH research domain criteria. J Abnorm Psychol 122:928-937.

D'Ardenne K, Eshel N, Luka J, Lenartowicz A, Nystrom LE, Cohen JD (2012) Role of prefrontal cortex and the midbrain dopamine system in working memory updating. Proc Natl Acad Sci U S A 109:19900-19909.

Damoiseaux JS, Greicius MD (2009) Greater than the sum of its parts: a review of studies combining structural connectivity and resting-state functional connectivity. Brain Struct Funct 213:525-533.

Deckersbach T, Dougherty DD, Rauch SL (2006) Functional imaging of mood and anxiety disorders. Journal of Neuroimaging 16:1-10.

Delgado MR, Nearing KI, Ledoux JE, Phelps EA (2008) Neural circuitry underlying the regulation of conditioned fear and its relation to extinction. Neuron 59:829-838.

Diekhof EK, Geier K, Falkai P, Gruber O (2011) Fear is only as deep as the mind allows: a coordinate-based meta-analysis of neuroimaging studies on the regulation of negative affect. Neuroimage 58:275-285.

Dima D, Dietrich DE, Dillo W, Emrich HM (2010) Impaired top-down processes in schizophrenia: a DCM study of ERPs. Neuroimage 52:824-832.

Drevets WC, Ongur D, Price JL (1998) Neuroimaging abnormalities in the subgenual prefrontal cortex: implications for the pathophysiology of familial mood disorders. Mol Psychiatry 3:220-226, 190-221.

Drevets WC, Price JL, Simpson JR, Jr., Todd RD, Reich T, Vannier M, Raichle ME (1997) Subgenual prefrontal cortex abnormalities in mood disorders. Nature 386:824-827.

Dunsmoor JE, Prince SE, Murty VP, Kragel PA, LaBar KS (2011) Neurobehavioral mechanisms of human fear generalization. Neuroimage 55:1878-1888.

Egan MF, Kojima M, Callicott JH, Goldberg TE, Kolachana BS, Bertolino A, Zaitsev E, Gold B, Goldman D, Dean M, Lu B, Weinberger DR (2003) The BDNF val66met polymorphism affects activity-dependent secretion of BDNF and human memory and hippocampal function. Cell 112:257-269.

Elam KK, Carlson JM, DiLalla LF, Reinke KS (2010) Emotional Faces Capture Spatial Attention in 5-Year-Old Children. Evolutionary Psychology 8:754-767.

Etkin A (2010) Functional neuroanatomy of anxiety: a neural circuit perspective. Behavioral Neurobiology of Anxiety and Its Treatment:251-277.

Etkin A, Wager TD (2007) Functional neuroimaging of anxiety: a meta-analysis of emotional processing in PTSD, social anxiety disorder, and specific phobia. Am J Psychiatry 164:1476-1488.

Etkin A, Egner T, Kalisch R (2011) Emotional processing in anterior cingulate and medial prefrontal cortex. Trends Cogn Sci 15:85-93.

Etkin A, Egner T, Peraza DM, Kandel ER, Hirsch J (2006) Resolving emotional conflict: A role for the rostral anterior cingulate cortex in modulating activity in the amygdala (vol 51, pg 871, 2006). Neuron 52:1121-1121.

Etkin A, Klemenhagen KC, Dudman JT, Rogan MT, Hen R, Kandel ER, Hirsch J (2004) Individual differences in trait anxiety predict the response of the basolateral amygdala to unconsciously processed fearful faces. Neuron 44:1043-1055.

Fadok JP, Dickerson TM, Palmiter RD (2009) Dopamine is necessary for cue-dependent fear conditioning. J Neurosci 29:11089-11097.

Fairhurst M, Wiech K, Dunckley P, Tracey I (2007) Anticipatory brainstem activity predicts neural processing of pain in humans. Pain 128:101-110.

Fox E (2002) Processing emotional facial expressions: the role of anxiety and awareness. Cogn Affect Behav Neurosci 2:52-63.

Fox E, Ridgewell A, Ashwin C (2009) Looking on the bright side: biased attention and the human serotonin transporter gene. Proc Biol Sci 276:1747-1751.

Fox E, Cahill S, Zougkou K (2010) Preconscious processing biases predict emotional reactivity to stress. Biol Psychiatry 67:371-377.

Gianaros PJ, Van Der Veen FM, Jennings JR (2004) Regional cerebral blood flow correlates with heart period and high-frequency heart period variability during working-memory tasks: Implications for the cortical and subcortical regulation of cardiac autonomic activity. Psychophysiology 41:521-530.

Goodall C (1983) M-estimators of location: An outline of the theory. In: Understaning Robust and Exploratory Data Analysis (Hoaglin DC, Mosteller F, Tukey JW, eds), pp 339-431. New York: Wiley.

Gray JA, McNaughton N (2000a) The Neuropsychology of Anxiety: An Equiry into the Functions of the Septo-Hippocampal System, 2nd Edition: Oxford.

Gray JA, McNaughton N (2000b) The neuropsychology of anxiety : an enquiry into the functions of the septo-hippocampal system, 2nd Edition. Oxford ; New York: Oxford University Press.

Greenberg T, Carlson JM, Cha J, Hajcak G, Mujica-Parodi LR (2013a) Ventromedial prefrontal cortex reactivity is altered in generalized anxiety disorder during fear generalization. Depress Anxiety 30:242-250.

Greenberg T, Carlson JM, Cha J, Hajcak G, Mujica-Parodi LR (2013b) Neural reactivity tracks fear generalization gradients. Biol Psychol 92:2-8.

Greicius MD, Supekar K, Menon V, Dougherty RF (2009) Resting-State Functional Connectivity Reflects Structural Connectivity in the Default Mode Network. Cerebral Cortex 19:72-78.

Grupe DW, Nitschke JB (2011) Uncertainty is associated with biased expectancies and heightened responses to aversion. Emotion 11:413-424.

Gur RC, Sara R, Hagendoorn M, Marom O, Hughett P, Macy L, Turner T, Bajcsy R, Posner A, Gur RE (2002) A method for obtaining 3-dimensional facial expressions and its standardization for use in neurocognitive studies. J Neurosci Methods 115:137-143.

Haaker J, Gaburro S, Sah A, Gartmann N, Lonsdorf TB, Meier K, Singewald N, Pape HC, Morellini F, Kalisch R (2013) Single dose of L-dopa makes extinction memories context-independent and prevents the return of fear. Proc Natl Acad Sci U S A 110:E2428-2436.

Haber SN, Knutson B (2010) The reward circuit: linking primate anatomy and human imaging. Neuropsychopharmacol 35:4-26.

Hahn A, Stein P, Windischberger C, Weissenbacher A, Spindelegger C, Moser E, Kasper S, Lanzenberger R (2011) Reduced resting-state functional connectivity between amygdala and orbitofrontal cortex in social anxiety disorder. Neuroimage 56:881-889.

Hajcak G, Castille C, Olvet DM, Dunning JP, Roohi J, Hatchwell E (2009) Genetic variation in brain-derived neurotrophic factor and human fear conditioning. Genes Brain Behav 8:80-85.

Hakamata Y, Lissek S, Bar-Haim Y, Britton JC, Fox NA, Leibenluft E, Ernst M, Pine DS (2010) Attention Bias Modification Treatment: A Meta-Analysis Toward the Establishment of Novel Treatment for Anxiety. Biol Psychiat 68:982-990.

Hare TA, Camerer CF, Rangel A (2009) Self-control in decision-making involves modulation of the vmPFC valuation system. Science 324:646.

Hariri AR, Mattay VS, Tessitore A, Kolachana B, Fera F, Goldman D, Egan MF, Weinberger DR (2002) Serotonin transporter genetic variation and the response of the human amygdala. Science 297:400-403.

Hartley CA, Fischl B, Phelps EA (2011) Brain structure correlates of individual differences in the acquisition and inhibition of conditioned fear. Cereb Cortex 21:1954-1962.

Haxby JV, Hoffman EA, Gobbini MI (2000) The distributed human neural system for face perception. Trends in Cognitive Sciences 4:223-233.

Heinz A, Braus DF, Smolka MN, Wrase J, Puls I, Hermann D, Klein S, Grusser SM, Flor H, Schumann G, Mann K, Buchel C (2005) Amygdala-prefrontal coupling depends on a genetic variation of the serotonin transporter. Nat Neurosci 8:20-21.

Hettema JM, Prescott CA, Kendler KS (2001) A population-based twin study of generalized anxiety disorder in men and women. J Nerv Ment Dis 189:413-420.

Hettema JM, Kettenmann B, Ahluwalia V, McCarthy C, Kates WR, Schmitt JE, Silberg JL, Neale MC, Kendler KS, Fatouros P (2012) Pilot multimodal twin imaging study of generalized anxiety disorder. Depress Anxiety 29:202-209.

Hilt LM, Sander LC, Nolen-Hoeksema S, Simen AA (2007) The BDNF Va166Met polymorphism predicts rumination and depression differently in young adolescent girls and their mothers. Neurosci Lett 429:12-16.

Hoffman EA, Haxby JV (2000) Distinct representations of eye gaze and identity in the distributed human neural system for face perception. Nature Neuroscience 3:80-84.

Holland PC, Gallagher M (1999) Amygdala circuitry in attentional and representational processes. Trends Cogn Sci 3:65-73.

Honey CJ, Kotter R, Breakspear M, Sporns O (2007) Network structure of cerebral cortex shapes functional connectivity on multiple time scales. Proceedings of the National Academy of Sciences of the United States of America 104:10240-10245.

Hu LT, Bentler PM (1999) Cutoff Criteria for Fit Indexes in Covariance Structure Analysis: Conventional Criteria Versus New Alternatives. Struct Equ Modeling 6:1-55.

Insel T, Cuthbert B, Garvey M, Heinssen R, Pine DS, Quinn K, Sanislow C, Wang P (2010) Research domain criteria (RDoC): toward a new classification framework for research on mental disorders. Am J Psychiatry 167:748-751.

Insel TR, Cuthbert BN (2009) Endophenotypes: bridging genomic complexity and disorder heterogeneity. Biol Psychiatry 66:988-989.

Jbabdi S, Woolrich MW, Andersson JL, Behrens TE (2007) A Bayesian framework for global tractography. Neuroimage 37:116-129.

Jennings JH, Sparta DR, Stamatakis AM, Ung RL, Pleil KE, Kash TL, Stuber GD (2013) Distinct extended amygdala circuits for divergent motivational states. Nature 496:224-228.

Jiang Y, He S (2006) Cortical responses to invisible faces: Dissociating subsystems for facial-information processing. Current Biology 16:2023-2029.

Joshua M, Adler A, Mitelman R, Vaadia E, Bergman H (2008) Midbrain dopaminergic neurons and striatal cholinergic interneurons encode the difference between reward and aversive events at different epochs of probabilistic classical conditioning trials. J Neurosci 28:11673-11684.

Jovanovic T, Ressler KJ (2010) How the neurocircuitry and genetics of fear inhibition may inform our understanding of PTSD. Am J Psychiatry 167:648-662.

Kalisch R, Korenfeld E, Stephan KE, Weiskopf N, Seymour B, Dolan RJ (2006) Context-dependent human extinction memory is mediated by a ventromedial prefrontal and hippocampal network. J Neurosci 26:9503-9511.

Kemp AH, Felmingham KL, Falconer E, Liddell BJ, Bryant RA, Williams LM (2009) Heterogeneity of non-conscious fear perception in posttraumatic stress disorder as a function of physiological arousal: An fMRI study. Psychiat Res-Neuroim 174:158-161.

Kendler KS, Gardner CO, Gatz M, Pedersen NL (2007) The sources of co-morbidity between major depression and generalized anxiety disorder in a Swedish national twin sample. Psychol Med 37:453-462.

Kessler RC, Berglund P, Demler O, Jin R, Merikangas KR, Walters EE (2005) Lifetime prevalence and age-of-onset distributions of DSM-IV disorders in the National Comorbidity Survey Replication. Arch Gen Psychiatry 62:593-602.

Kheirbek MA, Klemenhagen KC, Sahay A, Hen R (2012) Neurogenesis and generalization: a new approach to stratify and treat anxiety disorders. Nat Neurosci 15:1613-1620.

Kim MJ, Whalen PJ (2009a) The Structural Integrity of an Amygdala-Prefrontal Pathway Predicts Trait Anxiety. Journal of Neuroscience 29:11614-11618.

Kim MJ, Whalen PJ (2009b) The structural integrity of an amygdala-prefrontal pathway predicts trait anxiety. J Neurosci 29:11614-11618.

Kim SY et al. (2013) Diverging neural pathways assemble a behavioural state from separable features in anxiety. Nature 496:219-223.

Kriegeskorte N, Simmons WK, Bellgowan PS, Baker CI (2009) Circular analysis in systems neuroscience: the dangers of double dipping. Nat Neurosci 12:535-540.

Krishnan V et al. (2007) Molecular adaptations underlying susceptibility and resistance to social defeat in brain reward regions. Cell 131:391-404.

Kubarych TS, Aggen SH, Hettema JM, Kendler KS, Neale MC (2008) Assessment of generalized anxiety disorder diagnostic criteria in the National Comorbidity Survey and Virginia Adult Twin Study of Psychiatric and Substance Use Disorders. Psychol Assess 20:206-216.

Kumaran D, Summerfield JJ, Hassabis D, Maguire EA (2009) Tracking the emergence of conceptual knowledge during human decision making. Neuron 63:889-901.

Kwang T, Wells TT, McGeary JE, Swann WB, Jr., Beevers CG (2010) Association of the serotonin transporter promoter region polymorphism with biased attention for negative word stimuli. Depress Anxiety 27:746-751.

Lammel S, Lim BK, Ran C, Huang KW, Betley MJ, Tye KM, Deisseroth K, Malenka RC (2012) Input-specific control of reward and aversion in the ventral tegmental area. Nature 491:212-217.

Lapierre YD, Butter HJ, Oyewumi LK (1983) Benzodiazepine effect on information processing in generalized anxiety disorder. Neuropsychobiology 9:88-93.

Lau JYF, Goldman D, Buzas B, Hodgkinson C, Leibenluft E, Nelson E, Sankin L, Pine DS, Ernst M (2010) BDNF gene polymorphism (Val66Met) predicts amygdala and anterior hippocampus responses to emotional faces in anxious and depressed adolescents. Neuroimage 53:952-961.

Le Bihan D (2003) Looking into the functional architecture of the brain with diffusion MRI. Nature Reviews Neuroscience 4:469-480.

Lee S, Ahmed T, Lee S, Kim H, Choi S, Kim DS, Kim SJ, Cho J, Shin HS (2012) Bidirectional modulation of fear extinction by mediodorsal thalamic firing in mice. Nat Neurosci 15:308-314.

Lehman JF, Greenberg BD, McIntyre CC, Rasmussen SA, Haber SN (2011) Rules ventral prefrontal cortical axons use to reach their targets: implications for diffusion tensor imaging tractography and deep brain stimulation for psychiatric illness. J Neurosci 31:10392-10402.

Lesch KP, Bengel D, Heils A, Sabol SZ, Greenberg BD, Petri S, Benjamin J, Muller CR, Hamer DH, Murphy DL (1996) Association of anxiety-related traits with a polymorphism in the serotonin transporter gene regulatory region. Science 274:1527-1531.

Liddell BJ, Brown KJ, Kemp AH, Barton MJ, Das P, Peduto A, Gordon E, Williams LM (2005) A direct brainstem-amygdala-cortical 'alarm' system for subliminal signals of fear. Neuroimage 24:235-243.

Linhart H, Zucchini W (1986) Model selection. Wiley series in probability and mathematical statistics. Oxford, England: John Wiley & Sons.

Lisman JE, Grace AA (2005) The hippocampal-VTA loop: controlling the entry of information into long-term memory. Neuron 46:703-713.

Lissek S (2012) Toward an account of clinical anxiety predicated on basic, neurally mapped mechanisms of Pavlovian fear-learning: the case for conditioned overgeneralization. Depress Anxiety 29:257-263.

Lissek S, Kaczkurkin AN, Rabin S, Geraci M, Pine DS, Grillon C (2013a) Generalized Anxiety Disorder Is Associated with Overgeneralization of Classically Conditioned Fear. Biol Psychiatry.

Lissek S, Rabin S, Heller RE, Lukenbaugh D, Geraci M, Pine DS, Grillon C (2010) Overgeneralization of conditioned fear as a pathogenic marker of panic disorder. Am J Psychiatry 167:47-55.

Lissek S, Bradford DE, Alvarez RP, Burton P, Espensen-Sturges T, Reynolds RC, Grillon C (2013b) Neural substrates of classically conditioned fear-generalization in humans: a parametric fMRI study. Soc Cogn Affect Neurosci.

Liu ZH, Shin R, Ikemoto S (2008) Dual role of medial A10 dopamine neurons in affective encoding. Neuropsychopharmacol 33:3010-3020.

Lodge DJ (2011) The medial prefrontal and orbitofrontal cortices differentially regulate dopamine system function. Neuropsychopharmacology 36:1227-1236.

Lodge DJ, Grace AA (2006) The hippocampus modulates dopamine neuron responsivity by regulating the intensity of phasic neuron activation. Neuropsychopharmacol 31:1356-1361.

Mackintosh MA, Gatz M, Wetherell JL, Pedersen NL (2006) A twin study of lifetime Generalized Anxiety Disorder (GAD) in older adults: genetic and environmental influences shared by neuroticism and GAD. Twin Res Hum Genet 9:30-37.

MacLeod C, Mathews A (1988) Anxiety and the allocation of attention to threat. Q J Exp Psychol A 40:653-670.

MacLeod C, Rutherford E, Campbell L, Ebsworthy G, Holker L (2002) Selective attention and emotional vulnerability: assessing the causal basis of their association through the experimental manipulation of attentional bias. Journal of Abnormal Psychology 111:107-123.

Margulies DS, Kelly AM, Uddin LQ, Biswal BB, Castellanos FX, Milham MP (2007) Mapping the functional connectivity of anterior cingulate cortex. Neuroimage 37:579-588.

Margulies DS, Vincent JL, Kelly C, Lohmann G, Uddin LQ, Biswal BB, Villringer A, Castellanos FX, Milham MP, Petrides M (2009) Precuneus shares intrinsic functional architecture in humans and monkeys. Proc Natl Acad Sci U S A 106:20069-20074.

Mars RB et al. (2011) Diffusion-weighted imaging tractography-based parcellation of the human parietal cortex and comparison with human and macaque resting-state functional connectivity. J Neurosci 31:4087-4100.

Martinowich K, Lu B (2008) Interaction between BDNF and serotonin: Role in mood disorders. Neuropsychopharmacology 33:73-83.

Mathews A, Mackintosh B (1998) A cognitive model of selective processing in anxiety. Cognitive Therapy and Research 22:539-560.

Mathews A, MacLeod C (2002) Induced processing biases have causal effects on anxiety. Cognition & Emotion 16:331-354.

Mathys C, Daunizeau J, Friston KJ, Stephan KE (2011) A bayesian foundation for individual learning under uncertainty. Front Hum Neurosci 5:39.

Matsumoto M, Hikosaka O (2009) Two types of dopamine neuron distinctly convey positive and negative motivational signals. Nature 459:837-841.

McClure SM, Laibson DI, Loewenstein G, Cohen JD (2004) Separate neural systems value immediate and delayed monetary rewards. Science 306:503-507.

McEwen BS (2013) Neuroscience. Hormones and the social brain. Science 339:279-280.

McIntosh AM, Bastin ME, Luciano M, Munoz Maniega S, del C. Valdes Hernandez M, Royle NA, Hall J, Murray C, Lawrie SM, Starr JM, Wardlaw JM, Deary IJ (2012) Neuroticism, depressive symptoms and whitematter integrity in the Lothian Birth Cohort 1936. Psychological Medicine.

McNaughton N, Gray JA (2000) Anxiolytic action on the behavioural inhibition system implies multiple types of arousal contribute to anxiety. Journal of Affective Disorders 61:161-176.

Meunier D, Lambiotte R, Fornito A, Ersche KD, Bullmore ET (2009) Hierarchical modularity in human brain functional networks. Front Neuroinform 3:37.

Milad MR, Rauch SL (2007) The role of the orbitofrontal cortex in anxiety disorders. Ann N Y Acad Sci 1121:546-561.

Milad MR, Quirk GJ (2012) Fear extinction as a model for translational neuroscience: ten years of progress. Annu Rev Psychol 63:129-151.

Milad MR, Quinn BT, Pitman RK, Orr SP, Fischl B, Rauch SL (2005) Thickness of ventromedial prefrontal cortex in humans is correlated with extinction memory. P Natl Acad Sci USA 102:10706-10711.

Milad MR, Wright CI, Orr SP, Pitman RK, Quirk GJ, Rauch SL (2007a) Recall of fear extinction in humans activates the ventromedial prefrontal cortex and hippocampus in concert. Biol Psychiat 62:446-454.

Milad MR, Wright CI, Orr SP, Pitman RK, Quirk GJ, Rauch SL (2007b) Recall of fear extinction in humans activates the ventromedial prefrontal cortex and hippocampus in concert. Biol Psychiatry 62:446-454.

Milad MR, Pitman RK, Ellis CB, Gold AL, Shin LM, Lasko NB, Zeidan MA, Handwerger K, Orr SP, Rauch SL (2009) Neurobiological basis of failure to recall extinction memory in posttraumatic stress disorder. Biol Psychiatry 66:1075-1082.

Mitchell AS, Gaffan D (2008) The magnocellular mediodorsal thalamus is necessary for memory acquisition, but not retrieval. J Neurosci 28:258-263.

Mogg K, Bradley BP (2002) Selective orienting of attention to masked threat faces in social anxiety. Behav Res Ther 40:1403-1414.

Mohanty A (2007) Neural Mechanisms involved in emotion/attention interactions. In: Department of Pscyhology, p 157. Urbana, Illinois: University of Illinois at Urbana-Champaign.

Mohanty A, Engels AS, Herrington JD, Heller W, Ho MH, Banich MT, Webb AG, Warren SL, Miller GA (2007) Differential engagement of anterior cingulate cortex subdivisions for cognitive and emotional function. Psychophysiology 44:343-351.

Monk CS, Telzer EH, Mogg K, Bradley BP, Mai X, Louro HM, Chen G, McClure-Tone EB, Ernst M, Pine DS (2008) Amygdala and ventrolateral

prefrontal cortex activation to masked angry faces in children and adolescents with generalized anxiety disorder. Arch Gen Psychiatry 65:568-576.

Montag C, Reuter M, Newport B, Elger C, Weber B (2008) The BDNF Val66Met polymorphism affects amygdala activity in response to emotional stimuli: evidence from a genetic imaging study. Neuroimage 42:1554-1559.

Montag C, Schoene-Bake JC, Faber J, Reuter M, Weber B (2010a) Genetic variation on the BDNF gene is not associated with differences in white matter tracts in healthy humans measured by tract-based spatial statistics. Genes Brain and Behavior 9:886-891.

Montag C, Basten U, Stelzel C, Fiebach CJ, Reuter M (2010b) The BDNF Val66Met polymorphism and anxiety: Support for animal knock-in studies from a genetic association study in humans. Psychiatry Research 179:86-90.

Montag C, Reuter M, Weber B, Markett S, Schoene-Bake JC (2012) Individual Differences in Trait Anxiety Are Associated with White Matter Tract Integrity in the Left Temporal Lobe in Healthy Males but Not Females. Neuroscience 217:77-83.

Morris JS, Ohman A, Dolan RJ (1998) Conscious and unconscious emotional learning in the human amygdala. Nature 393:467-470.

Morris JS, Ohman A, Dolan RJ (1999) A subcortical pathway to the right amygdala mediating "unseen" fear. Proc Natl Acad Sci U S A 96:1680-1685.

Morris JS, DeGelder B, Weiskrantz L, Dolan RJ (2001) Differential extrageniculostriate and amygdala responses to presentation of emotional faces in a cortically blind field. Brain 124:1241-1252.

Morris SE, Cuthbert BN (2012) Research Domain Criteria: cognitive systems, neural circuits, and dimensions of behavior. Dialogues Clin Neurosci 14:29-37.

Morris SE, Rumsey JM, Cuthbert BN (2013) Rethinking mental disorders: The role of learning and brain plasticity. Restor Neurol Neurosci.

Myers-Schulz B, Koenigs M (2012) Functional anatomy of ventromedial prefrontal cortex: implications for mood and anxiety disorders. Mol Psychiatr 17:132-141.

Nagai Y, Critchley HD, Featherstone E, Trimble MR, Dolan RJ (2004) Activity in ventromedial prefrontal cortex covaries with sympathetic skin conductance level: a physiological account of a "default mode" of brain function. Neuroimage 22:243-251.

Naidich TP, Duvernoy HM, Delman BN, Sorensen AG, Kollias SS, Haacke EM (2009) Duvernoy's Atlas of the Human Brain Stem and Cerebellum, XII Edition. New York: Springer.

Nee DE, Kastner S, Brown JW (2011) Functional heterogeneity of conflict, error, task-switching, and unexpectedness effects within medial prefrontal cortex. Neuroimage 54:528-540.

Newman SC, Bland RC (2006) A population-based family study of DSM-III generalized anxiety disorder. Psychol Med 36:1275-1281.

Niwa M, Jaaro-Peled H, Tankou S, Seshadri S, Hikida T, Matsumoto Y, Cascella NG, Kano S, Ozaki N, Nabeshima T, Sawa A (2013) Adolescent stress-induced epigenetic control of dopaminergic neurons via glucocorticoids. Science 339:335-339.

Noyes R, Jr., Clarkson C, Crowe RR, Yates WR, McChesney CM (1987) A family study of generalized anxiety disorder. Am J Psychiatry 144:1019-1024.

O'Roak BJ et al. (2011) Exome sequencing in sporadic autism spectrum disorders identifies severe de novo mutations. Nat Genet 43:585-589.

Ohira H, Fukuyama S, Kimura K, Nomura M, Isowa T, Ichikawa N, Matsunaga M, Shinoda J, Yamada J (2009) Regulation of natural killer cell redistribution by prefrontal cortex during stochastic learning. Neuroimage 47:897-907.

Ohman A, Flykt A, Esteves F (2001) Emotion drives attention: detecting the snake in the grass. J Exp Psychol Gen 130:466-478.

Olesen PJ, Nagy Z, Westerberg H, Klingberg T (2003) Combined analysis of DTI and fMRI data reveals a joint maturation of white and grey matter in a fronto-parietal network. Brain Res Cogn Brain Res 18:48-57.

Op de Beeck HP, Haushofer J, Kanwisher NG (2008) Interpreting fMRI data: maps, modules and dimensions. Nat Rev Neurosci 9:123-135.

Orr JM, Weissman DH (2009) Anterior cingulate cortex makes 2 contributions to minimizing distraction. Cereb Cortex 19:703-711.

Osinsky R, Reuter M, Kupper Y, Schmitz A, Kozyra E, Alexander N, Hennig J (2008) Variation in the serotonin transporter gene modulates selective attention to threat. Emotion 8:584-588.

Pacheco J, Beevers CG, Benavides C, McGeary J, Stice E, Schnyer DM (2009a) Frontal-Limbic White Matter Pathway Associations with the Serotonin Transporter Gene Promoter Region (5-HTTLPR) Polymorphism. J Neurosci 29:6229-6233.

Pacheco J, Beevers CG, Benavides C, McGeary J, Stice E, Schnyer DM (2009b) Frontal-Limbic White Matter Pathway Associations with the Serotonin Transporter Gene Promoter Region (5-HTTLPR) Polymorphism. Journal of Neuroscience 29:6229-6233.

Parnaudeau S, O'Neill PK, Bolkan SS, Ward RD, Abbas AI, Roth BL, Balsam PD, Gordon JA, Kellendonk C (2013) Inhibition of mediodorsal thalamus disrupts thalamofrontal connectivity and cognition. Neuron 77:1151-1162.

Partala T, Surakka V (2003) Pupil size variation as an indication of affective processing. Int J Hum-Comput St 59:185-198.

Perez-Edgar K, Bar-Haim Y, McDermott JM, Gorodetsky E, Hodgkinson CA, Goldman D, Ernst M, Pine DS, Fox NA (2010) Variations in the serotonin-transporter gene are associated with attention bias patterns to positive and negative emotion faces. Biol Psychol 83:269-271.

Pezawas L, Verchinski BA, Mattay VS, Callicott JH, Kolachana BS, Straub RE, Egan MF, Meyer-Lindenberg A, Weinberger DR (2004) The brain-derived neurotrophic factor val66met polymorphism and variation in human cortical morphology. J Neurosci 24:10099-10102.

Pezawas L, Meyer-Lindenberg A, Drabant EM, Verchinski BA, Munoz KE, Kolachana BS, Egan MF, Mattay VS, Hariri AR, Weinberger DR (2005) 5-HTTLPR polymorphism impacts human cingulate-amygdala interactions: a genetic susceptibility mechanism for depression. Nat Neurosci 8:828-834.

Pezze MA, Feldon J (2004) Mesolimbic dopaminergic pathways in fear conditioning. Prog Neurobiol 74:301-320.

Pfefferbaum A, Sullivan EV, Hedehus M, Lim KO, Adalsteinsson E, Moseley M (2000) Age-related decline in brain white matter anisotropy measured with spatially corrected echo-planar diffusion tensor imaging. Magnetic Resonance in Medicine 44:259-268.

Phan KL, Orlichenko A, Boyd E, Angstadt M, Coccaro EF, Liberzon I, Arfanakis K (2009a) Preliminary evidence of white matter abnormality in the uncinate fasciculus in generalized social anxiety disorder. Biol Psychiat 66:691-694.

Phan KL, Orlichenko A, Boyd E, Angstadt M, Coccaro EF, Liberzon I, Arfanakis K (2009b) Preliminary evidence of white matter abnormality in the uncinate fasciculus in generalized social anxiety disorder. Biological Psychiatry 66:691-694.

Phan KL, Orlichenko A, Boyd E, Angstadt M, Coccaro EF, Liberzon I, Arfanakis K (2009c) Preliminary evidence of white matter abnormality in the uncinate fasciculus in generalized social anxiety disorder. Biol Psychiatry 66:691-694.

Phelps EA, Delgado MR, Nearing KI, LeDoux JE (2004) Extinction learning in humans: role of the amygdala and vmPFC. Neuron 43:897-905.

Poo MM (2001) Neurotrophins as synaptic modulators. Nature Reviews Neuroscience 2:24-32.

Porrino LJ, Crane AM, Goldmanrakic PS (1981) Direct and Indirect Pathways from the Amygdala to the Frontal-Lobe in Rhesus-Monkeys. J Comp Neurol 198:121-136.

Pourtois G, Grandjean D, Sander D, Vuilleumier P (2004) Electrophysiological correlates of rapid spatial orienting towards fearful faces. Cereb Cortex 14:619-633.

Pourtois G, Schwartz S, Seghier ML, Lazeyras F, Vuilleumier P (2006) Neural systems for orienting attention to the location of threat signals: an event-related fMRI study. Neuroimage 31:920-933.

Price JL (2007) Definition of the orbital cortex in relation to specific connections with limbic and visceral structures and other cortical regions. Ann N Y Acad Sci 1121:54-71.

Puce A, Allison T, Bentin S, Gore JC, McCarthy G (1998) Temporal cortex activation in humans viewing eye and mouth movements. Journal of Neuroscience 18:2188-2199.

Rauch SL, Whalen PJ, Shin LM, McInerney SC, Macklin ML, Lasko NB, Orr SP, Pitman RK (2000) Exaggerated amygdala response to masked facial stimuli in posttraumatic stress disorder: A functional MRI study. Biological Psychiatry 47:769-776.

Rickels K, DeMartinis N, Garcia-Espana F, Greenblatt DJ, Mandos LA, Rynn M (2000) Imipramine and buspirone in treatment of patients with generalized anxiety disorder who are discontinuing long-term benzodiazepine therapy. Am J Psychiatry 157:1973-1979.

Robinson JL, Laird AR, Glahn DC, Lovallo WR, Fox PT (2010) Metaanalytic connectivity modeling: delineating the functional connectivity of the human amygdala. Hum Brain Mapp 31:173-184.

Rodriguez S, Gaunt TR, Day IN (2009) Hardy-Weinberg equilibrium testing of biological ascertainment for Mendelian randomization studies. Am J Epidemiol 169:505-514.

Roy M, Shohamy D, Wager TD (2012) Ventromedial prefrontal-subcortical systems and the generation of affective meaning. Trends Cogn Sci 16:147-156.

Sanislow CA, Pine DS, Quinn KJ, Kozak MJ, Garvey MA, Heinssen RK, Wang PS, Cuthbert BN (2010) Developing constructs for psychopathology research: research domain criteria. J Abnorm Psychol 119:631-639.

Saxe R, Kanwisher N (2003) People thinking about thinking people - The role of the temporo-parietal junction in "theory of mind". Neuroimage 19:1835-1842.

Schinka JA, Busch RM, Robichaux-Keene N (2004) A meta-analysis of the association between the serotonin transporter gene polymorphism (5-HTTLPR) and trait anxiety. Mol Psychiatry 9:197-202.

Schlosser RGM (2010) Fronto-Cingulate Effective Connectivity in Major Depression: A Study with fMRI and Dynamic Causal Modeling. Biological Psychiatry 67:7S-8S.

Schlosser RGM, Wagner G, Koch K, Dahnke R, Reichenbach JR, Sauer H (2008) Fronto-cingulate effective connectivity in major depression: A study with fMRI and dynamic causal modeling. Neuroimage 43:645-655.

Schoenbaum G, Roesch MR, Stalnaker TA, Takahashi YK (2009) A new perspective on the role of the orbitofrontal cortex in adaptive behaviour. Nat Rev Neurosci 10:885-892.

Scholz J, Klein MC, Behrens TEJ, Johansen-Berg H (2009) Training induces changes in white-matter architecture. Nat Neurosci 12:1370-1371.

Sen S, Burmeister M, Ghosh D (2004) Meta-analysis of the association between a serotonin transporter promoter polymorphism (5-HTTLPR) and anxiety-related personality traits. Am J Med Genet B Neuropsychiatr Genet 127B:85-89.

Shackman AJ, Salomons TV, Slagter HA, Fox AS, Winter JJ, Davidson RJ (2011) The integration of negative affect, pain and cognitive control in the cingulate cortex. Nat Rev Neurosci 12:154-167.

Sheline YI, Barch DM, Donnelly JM, Ollinger JM, Snyder AZ, Mintun MA (2001) Increased amygdala response to masked emotional faces in depressed subjects resolves with antidepressant treatment: an fMRI study. Biol Psychiatry 50:651-658.

Shimizu E, Hashimoto K, Iyo M (2004) Ethnic difference of the BDNF 196G/A (val66met) polymorphism frequencies: The possibility to explain ethnic mental traits. American Journal of Medical Genetics Part B-Neuropsychiatric Genetics 126B:122-123.

Shohamy D, Wagner AD (2008) Integrating memories in the human brain: hippocampal-midbrain encoding of overlapping events. Neuron 60:378-389.

Sierra-Mercado D, Padilla-Coreano N, Quirk GJ (2011) Dissociable roles of prelimbic and infralimbic cortices, ventral hippocampus, and basolateral amygdala in the expression and extinction of conditioned fear. Neuropsychopharmacol 36:529-538.

Smith SM, Jenkinson M, Johansen-Berg H, Rueckert D, Nichols TE, Mackay CE, Watkins KE, Ciccarelli O, Cader MZ, Matthews PM, Behrens TEJ (2006) Tract-based spatial statistics: Voxelwise analysis of multi-subject diffusion data. Neuroimage 31:1487-1505.

Song SK, Sun SW, Ju WK, Lin SJ, Cross AH, Neufeld AH (2003) Diffusion tensor imaging detects and differentiates axon and myelin degeneration in mouse optic nerve after retinal ischemia. Neuroimage 20:1714-1722.

Sotres-Bayon F, Sierra-Mercado D, Pardilla-Delgado E, Quirk GJ (2012) Gating of fear in prelimbic cortex by hippocampal and amygdala inputs. Neuron 76:804-812.

Spooner PM (2009) Sudden cardiac death: The larger problem... The larger genome. J Cardiovasc Electrophysiol 20:585-596.

Stamatakis AM, Stuber GD (2012) Activation of lateral habenula inputs to the ventral midbrain promotes behavioral avoidance. Nat Neurosci 15:1105-1107.

Stein JL, Wiedholz LM, Bassett DS, Weinberger DR, Zink CF, Mattay VS, Meyer-Lindenberg A (2007) A validated network of effective amygdala connectivity. Neuroimage 36:736-745.

Stieltjes B, Kaufmann WE, van Zijl PC, Fredericksen K, Pearlson GD, Solaiyappan M, Mori S (2001) Diffusion tensor imaging and axonal tracking in the human brainstem. Neuroimage 14:723-735.

Sylvers P, Lilienfeld SO, LaPrairie JL (2011) Differences between trait fear and trait anxiety: Implications for psychopathology. Clinical Psychology Review 31:122-137.

Takahashi YK, Roesch MR, Wilson RC, Toreson K, O'Donnell P, Niv Y, Schoenbaum G (2011) Expectancy-related changes in firing of dopamine neurons depend on orbitofrontal cortex. Nat Neurosci 14:1590-1597.

Takahashi YK, Roesch MR, Stalnaker TA, Haney RZ, Calu DJ, Taylor AR, Burke KA, Schoenbaum G (2009) The orbitofrontal cortex and ventral tegmental area are necessary for learning from unexpected outcomes. Neuron 62:269-280.

Thayer JF, Ahs F, Fredrikson M, Sollers JJ, 3rd, Wager TD (2012) A meta-analysis of heart rate variability and neuroimaging studies: implications for heart rate variability as a marker of stress and health. Neurosci Biobehav Rev 36:747-756.

Tost H, Alam T, Geramita M, Rebsch C, Kolachana B, Dickinson D, Verchinski BA, Lemaitre H, Barnett AS, Trampush JW, Weinberger DR, Marenco S (2013) Effects of the BDNF val(66)met polymorphism on white matter microstructure in healthy adults. Neuropsychopharmacology 38:525-532.

Tromp DP, Grupe DW, Oathes DJ, McFarlin DR, Hernandez PJ, Kral TR, Lee JE, Adams M, Alexander AL, Nitschke JB (2012a) Reduced structural connectivity of a major frontolimbic pathway in generalized anxiety disorder. Arch Gen Psychiatry 69:925-934.

Tromp DPM, Grupe DW, Oathes DJ, McFarlin DR, Hernandez PJ, Kral TRA, Lee JE, Adams M, Alexander AL, Nitschke JB (2012b) Reduced Structural Connectivity of a Major Frontolimbic Pathway in Generalized Anxiety Disorder. Archives of General Psychiatry 69:925-934.

Turken AU, Whitfield-Gabrieli S, Bammer R, Baldo JV, Dronkers NF, Gabrieli JDE (2008) Cognitive processing speed and the structure of white matter pathways: Convergent evidence from normal variation and lesion studies. Neuroimage 42:1032-1044.

Valentin VV, Dickinson A, O'Doherty JP (2007) Determining the neural substrates of goal-directed learning in the human brain. J Neurosci 27:4019-4026.

Van Dijk KR, Hedden T, Venkataraman A, Evans KC, Lazar SW, Buckner RL (2010) Intrinsic functional connectivity as a tool for human connectomics: theory, properties, and optimization. J Neurophysiol 103:297-321.

Vasile RG, Bruce SE, Goisman RM, Pagano M, Keller MB (2005) Results of a naturalistic longitudinal study of benzodiazepine and SSRI use in the treatment of generalized anxiety disorder and social phobia. Depress Anxiety 22:59-67.

Venkatraman V, Rosati AG, Taren AA, Huettel SA (2009) Resolving response, decision, and strategic control: evidence for a functional topography in dorsomedial prefrontal cortex. J Neurosci 29:13158-13164.

Verhagen M, van der Meij A, van Deurzen PAM, Janzing JGE, Arias-Vasquez A, Buitelaar JK, Franke B (2010) Meta-analysis of the BDNF Val66Met polymorphism in major depressive disorder: effects of gender and ethnicity. Molecular Psychiatry 15:260-271.

Vincent JL, Patel GH, Fox MD, Snyder AZ, Baker JT, Van Essen DC, Zempel JM, Snyder LH, Corbetta M, Raichle ME (2007) Intrinsic functional architecture in the anaesthetized monkey brain. Nature 447:83-86.

Voineskos AN, Lerch JP, Felsky D, Shaikh S, Rajji TK, Miranda D, Lobaugh NJ, Mulsant BH, Pollock BG, Kennedy JL (2011) The brain-derived neurotrophic factor Val66Met polymorphism and prediction of neural risk for Alzheimer disease. Arch Gen Psychiatry 68:198-206.

Vuilleumier P, Richardson MP, Armony JL, Driver J, Dolan RJ (2004) Distant influences of amygdala lesion on visual cortical activation during emotional face processing. Nat Neurosci 7:1271-1278.

Wager TD, van Ast VA, Hughes BL, Davidson ML, Lindquist MA, Ochsner KN (2009) Brain mediators of cardiovascular responses to social threat, part II: Prefrontal-subcortical pathways and relationship with anxiety. Neuroimage 47:836-851.

Whalen PJ, Rauch SL, Etcoff NL, McInerney SC, Lee MB, Jenike MA (1998) Masked presentations of emotional facial expressions modulate amygdala activity without explicit knowledge. J Neurosci 18:411-418.

Whitfield-Gabrieli S, Moran JM, Nieto-Castanon A, Triantafyllou C, Saxe R, Gabrieli JD (2011) Associations and dissociations between default and self-reference networks in the human brain. Neuroimage 55:225-232.

Wiens S (2006) Current concerns in visual masking. Emotion 6:675-680.

Williams LM, Das P, Liddell BJ, Kemp AH, Rennie CJ, Gordon E (2006a) Mode of functional connectivity in amygdala pathways dissociates level of awareness for signals of fear. J Neurosci 26:9264-9271.

Williams LM, Liddell BJ, Kemp AH, Bryant RA, Meares RA, Peduto AS, Gordon E (2006b) Amygdala-prefrontal dissociation of subliminal and supraliminal fear. Hum Brain Mapp 27:652-661.

Yendiki A, Panneck P, Srinivasan P, Stevens A, Zöllei L, Augustinack J, Wang R, Salat D, Ehrlich S, Behrens T, Jbabdi S, Gollub R, Fischl B (2011a) Automated probabilistic reconstruction of white-matter pathways in health and disease using an atlas of the underlying anatomy. Front Neuroinform 5:23.

Yendiki A, Panneck P, Srinivasan P, Stevens A, Zöllei L, Augustinack J, Wang R, Salat D, Ehrlich S, Behrens T, Jbabdi S, Gollub R, Fischl B (2011b) Automated probabilistic reconstruction of white-matter pathways in health and disease using an atlas of the underlying anatomy. Frontiers in Neuroinformatics 5.

Zweifel LS, Fadok JP, Argilli E, Garelick MG, Jones GL, Dickerson TM, Allen JM, Mizumori SJ, Bonci A, Palmiter RD (2011) Activation of dopamine neurons is critical for aversive conditioning and prevention of generalized anxiety. Nat Neurosci 14:620-626.